Modeling of Polarization Insensitive Phase Sensitive Amplifier for Phase Regeneration

Dushani Rasoja Munasinghe

(188033P)

Thesis submitted in partial fulfillment of the requirements for the degree
Master of Philosophy

Department of Electronic and Telecommunication Engineering

University of Moratuwa
Sri Lanka

October 2021

Declaration

I declare that this is my own work, and this thesis does not incorporate without acknowledgement any material previously submitted for a degree or diploma in any other university or institute of higher learning, and to the best of my knowledge and belief it does not contain any material previously published or written by another person except where the acknowledgement is made in the text.

Also, I hereby grant to University of Moratuwa the non-exclusive right to reproduce and distribute my thesis, in whole or in part, in print, electronic, or any other medium. I retain the right to use this content in whole or part in future works (such as articles or books).

Signature: Date:

The candidate, whose signature appears above, carried out research for the Msc dissertation under my supervision.

Name of the supervisor:

Signature: Date:

Abstract

This thesis describes a novel configuration which implements a polarization insensitive phase sensitive fiber optic parametric amplifier for phase regeneration. The proposed design can be used to address the inherent gain degradation issue in a polarization insensitive phase sensitive amplifier when polarization diversity loop is incorporated. This research investigates the possibilities for a significant gain enhancement when the polarization diversity loop is implemented.

At first, a baseline for a phase sensitive amplifier scheme is developed by taking different parameters into consideration. In this case, an extensive characterization is carried out to identify the variations of phase sensitive fiber amplifier gain associated with the parameter changes. Once the baseline is developed, the polarization diversity loop is implemented in the phase sensitive amplifier in order to make the phase sensitive fiber amplifier insensitive to polarization state variations of the input signals. Moreover, the existing issues in the polarization diversity loop are identified.

Finally, a strategic design is developed to overcome one of the major issues that persists in the existing polarization diversity loop configurations. It is the degradation of maximum achievable gain due to not being able to utilize the total pump power for parametric amplification process as only half of the pump power is available after polarization splitting at the input of the loop. The proposed design includes the concatenation of fiber pieces together to explore the possibility of gain enhancement of the diversity loop. To assess the performance of the proposed design, an extensive analysis is carried out. The gain enhancement introduced to the existing system is presented and suggestions are made for further improvements in the future.

Index terms— FOPA, PSA, FWM, polarization diversity, cascaded fiber

Acknowledgements

I extent my utmost gratitude towards Prof. L.W.P. Ruwan Udayanga of Department of Electronic and Telecommunication Engineering for his excellent guidance and supervision that I received throughout this research study. I am so grateful for his continuous support and understanding despite of the difficult times, for being a mentor and a role model and most importantly, for having faith on my capabilities to make this work a success.

I am thankful to Dr. Chamira Edussooriya and Dr. Mevan Gunawardena at the Department of Electronic and Telecommunication Engineering who evaluated the progress of this research during progress reviews for their invaluable comments and follow ups which greatly enhanced the quality of this research work.

I would also like to thank the entire academic staff at the Department of Electronic and Telecommunication Engineering for their insightful guidance and support in numerous ways.

I appreciate the continuous support and encouragement provided by my colleagues at the Department of Electronic and Telecommunication Engineering at University of Moratuwa. The knowledge and wisdom I have gained from them is immense. Moreover, I express my gratitute towards all the non-academic staff at the Department of Electronic and Telecommunication Engineering for their support throughout.

Finally, I am grateful to my parents, sister, teachers and everyone who gave me strength and courage to move forward in life and achieve milestones along the way.

D.R.Munasinghe

Contents

List of Figures

List of Tables

List of Abbreviations

Abbreviation	Description
WDM	Wavelength Division Multiplexing
DFA	Doped Fiber Amplifier
EDFA	Erbium Doped Fiber Amplifier
SOA	Semiconductor Optical Amplifier
OEO	Optical-to-Electrical-to-Optical
ASE	Amplified Spontaneous Emission
SNR	Signal to Noise Ratio
SRS	Stimulated Raman Scattering
FOPA	Fiber Optic Parametric Amplifier
FWM	Four Wave Mixing
HNLF	Highly Nonlinear Fiber
PI-FOPA	Phase Insensitive Fiber Optical Parametric Amplifier
PS-FOPA	Phase Sensitive Fiber Optical Parametric Amplifier
PIA	Phase Insensitive Amplifier
PSA	Phase Sensitive Amplifier
M-QAM	M-ary Quadrature Amplitude Modulation
M-PSK	M-ary Phase Shift Keying
NF	Noise Figure
SOP	State of Polarozation
PMD	Polarization Mode Dispersion
PDM	Polarization Dependent Modulation
PDL	Polarization Dependent Loss
PDG	Polarization Dependent Gain
BER	Bit Error Rate
SBS	Stimulated Brillouin Scattering
SPM	Self Phase Modulation
XPM	Cross Phase Modulation

CME	Coupled Mode Equation
NLSE	Nonlinear Shrödinger Equation
GVD	Group Velocity Dispersion
ZDF	Zero Dispersion Frequency
ZDW	Zero Dispersion Wavelength
NOLM	Nonlinear Optical Loop Mirror
PM-HNLF	Polarization Maintaining Highly Nonlinear Fiber
PBS	Polarization Beam Splitter
PBC	Polarization Beam Combiner
DSF	Dispersion Shifted Fiber
PC	Polarization Controller
PRBS	Pseudo Random Bit Sequence
QPM	Quasi-Phase Matching
PS-FBG	Phase Shifted-Fiber Bragg Grating
GER	Gain Extinction Ratio
SSFM	Split Step Fourier Method
DCF	Dispersion Compensating Fiber
HPL	Half Passed Loop
OSNR	Optical Signal to Noise Ratio
OSA	Optical spectrum analyzer
OBSF	Optical Band Stop Filter
OBPF	Optical Band Pass Filter
FSK	Frequency Shift Keying
BPSK	Binary Phase Shift Keying
QPSK	Quadrature Phase Shift Keying
MI	Modulational Instability
FPU	Fermi-Pasta-Ulam recurrence

Chapter 1

INTRODUCTION

In today's world, with the drastic growth of the number of communication devices, the existing obsolete communication technologies based on electrical wiring has become incapable of providing the services for the exponential growth of the demand. Hence, optical fiber communication where data transmission is enabled through the propagation of light along a glass fiber has become the most viable telecommunication solution for the data-centric communication during the past decade. It is not unfair to state that the global optical fiber network is the driving element of the present day's telecommunication infrastructure. Its capability to serve capacity requirement, high speed, low latency, high bandwidth while preserving the reliability and the efficiency of the communication system enables the long-distance transmission. With the exponential growth of popularity and applicability of optical fiber technology, efficient phase modulation formats took the lead in data transmission. The capacity requirement is met by using advanced modulation techniques which uses both amplitude and phase modulation, polarization division multiplexing as well as by wavelength division multiplexed (WDM) transmission. The reliability is ensured by the regeneration capability and the noiseless performance of the mid link components during the transmission. The susceptibility of optical fibers towards electrical interference is also another aspect which increases the reliability of the transmission system. Another important reason that stands for the popularity of optical fibers is the very low loss $i.e. \approx 0.15 - 0.2dB/km$ exhibited by them in $1.55\mu m$ wavelength region which is the most relevant wavelength region in telecommunication applications. Even though the loss exhibited by optical fibers is very less compared to other wireline technologies, aggregation of losses and distortion of the optical signals become significant in long haul transmission fiber spans. On the other hand, the high data rate requirement is increasing at a much higher pace demanding for Giga bits per second (Gbps) or even Tera bits per second (Tbps) transmission rates [2].

1.1 Background to the Research Topic

Eventhough optical fibers demonstrate very low losses compared to other wireline technologies, in long haul transmission, the signal power degradation becomes more significant with distance if amplifiers are not deployed in required spacings. To realize long haul transmission, one approach is to increase the power of the signal at the input of the optical fiber. When doing so, fiber's response gradually become nonlinear in nature which has become the major phenomena behind the origin of phase noise. Not only the phase but the amplitude of the signal may degrade as well during the transmission. Therefore, regeneration of the phase and the amplitude at the receiver end becomes a necessity. Hence, optical amplification which boost the signal power to their original levels while preserving the transmission parameters has become the major interest in the minds of researchers all around the world. The performance of a fiber link is usually evaluated by the capacity-distance product which can be improved by the use of optical amplifiers. As depicted in figure 1.1, optical amplifiers consist of a gain medium which is energized by an external pump source which is usually a high power laser diode. The interaction in the gain medium subjects the input signal to be amplified to a higher power level. Two major categories of optical amplifiers currently in use are solid state amplifiers and fiber amplifiers.

Semiconductor optical amplifiers (SOAs) are solid state amplifiers which use semiconducting materials made from group III-V elements as gain media. They provide gains upto 30 dB [3]. There are several disadvantages of using SOAs over other existing types because of their high noise figure, high coupling loss, polarization dependence, relatively lower gain and low output power compared to other existing types and the effect of adverse nonlinearities. The second category, fiber amplifiers, can be divided into two main types as doped fiber amplifiers (DFAs) and parametric processes based fiber amplifiers. Discovery of DFAs in 1980's is a stepping stone in the history of optical fiber communication because it made all-optical amplification a reality instead of the amplification took place by optical-to-electrical-to-optical (OEO) conversion. All-optical amplification did not require conversion between electrical and optical domains which reduced the system complexity while improving the accuracy. DFAs use doped fiber as gain media. The medium is doped by using rare-earth Lanthenide elements such as Erbium, Yitterbium, Thulium, Neodymium etc. which are triply ionized [4]. Amplification is achieved by the stimulated emission of photons from the excited

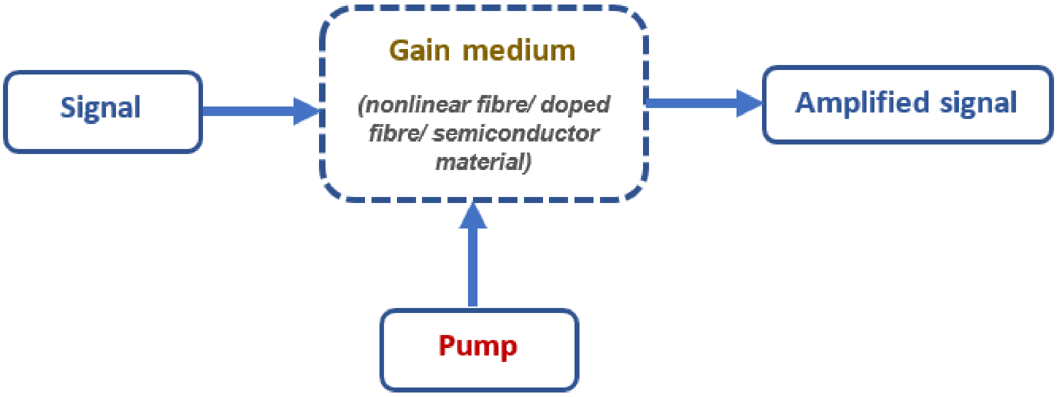

Figure 1.1: The schematic of an optical amplifier.

ions in the medium. It provides gain over a wider wavelength range and provide relatively higher gains such as 30 dB or above compared to SOAs [5]. The most popular type is Erbium Doped fiber amplifier (EDFA) which is widely used in many fiber based telecommunication systems. But the noise generated in EDFAs, amplified spontaneous emission (ASE) noise, becomes much significant when EDFAs are deployed in long haul systems. Also, EDFAs do not provide any remedy for the phase distortions of the phase modulated signals. In EDFAs, the noise figure which is defined as the input to output signal to noise ratio (SNR) is limited to the quantum limit which is 3 dB and cannot be reduced beyond that.

It is important to introduce the phenomenon behind the origin of optical nonlinearities before analyzing the second type of fiber amplifiers which is the parametric process based amplifiers. Optical nonlinearities occur due to the modifications of the optical properties of the dielectric material in the optical fiber when the input optical intensities are relatively high (in the order of $1GW/cm^2$). As a result, the refractive index of the fiber is no longer a constant rather it becomes intensity dependent which is the major cause for fiber nonlinearity. This phenomenon is known as *Kerr effect* which was founded by John Kerr in 1875 [6]. The optical Kerr effect creates optical nonlinearities arise from higher order optical susceptibilities where susceptibility is a dimensionless proportionality constant which indicates the degree of polarization induced by an applied electric field. When the susceptibility is greater, the material is able to polarize in response to the applied field. Most popular are second (χ^2) and third (χ^3) order susceptibilities which create second and third order nonlinearities respectively. χ^2 nonlinear responses are proportional to the square of the applied electric field while χ^3 are proportional to the cube of the applied electric field. In glass fibers, because of the molecular symmetry, χ^2 susceptibilities can be ignored [7]. Another important categorization of fiber amplifiers is based on the energy transfer between the interacting waves and the medium. The processes which conserve energy and momentum of the signals which do not incur an exchange of energy between interacting signals and the optical medium are known as parametric processes. The opposite stands for non- parametric processes. These parametric and non-parametric processes can be linear or non-linear depending on their responses to the input signals.

A popular category of fiber amplifiers which is commercially available at present which is based on such a nonlinear non-parametric process is the Raman amplifier. A weak signal participates in scattering a stronger pump wave to a higher frequency by the stimulated Raman scattering (SRS) when operating in the non-linear regime [8]. As a consequence of this scattering process, one additional signal photon is created which amplifies the signal. This phenomenon is termed as inelastic as well as non-parametric because it does not conserve the energy of the interacting waves or in other words, some of the energy is absorbed by the medium. Maximum gain could be obtained when the frequency difference between pump and signal waves is approximately $10 - 15THz$. Although Raman amplifiers can be operated in different wavelength regions, they require higher pump powers to obtain higher gains. They also require fibers with a much higher lengths when used as lumped elements but usually in commercial applications, the gain medium is considered as the transmission fiber itself by providing a distributed amplification because of this requirement. This is possible because the gain medium does not require special dopants like was the case in EDFAs. Apart from this requirement for longer fiber lengths, as another disadvantage, the coupling of pump noise to the signal is much significant in Raman amplifiers. Also the gain is polarization dependent which is unfavorable for maintaining an exact amplifier response.

The topic of interest in this thesis, Fiber optic parametric amplifiers (FOPAs) which makes use of χ^3 susceptibility based optical nonlinearity process called four wave mixing (FWM) has become the most interesting research area on fiber amplifiers in past few years [9], [10]. The FWM is a parametric process where interaction between two or three signals at different wavelengths create waves at new wavelengths when travelling through a nonlinear medium. Since FWM is a nonlinear effect, a special type of fiber which triggers such nonlinearity has to be used in practical implementations. In other words, a fiber with a higher nonlinear index hence a higher nonlinear coefficient (γ) which is greater than $10W^{-1}km^{-1}$ should be used. In that case, the most popular fiber type is the highly nonlinear fiber (HNLF) which is used over and over in many research works in order to demonstrate and utilize fiber nonlinearities for different applications.

It is worth assessing why the interest towards FOPA over other existing types of fiber amplifiers such as Raman and EDFAs has been grown drastically in recent years. The reason is due to several attractive features that can be offered by FOPAs which can be very favorable for long haul transmission systems. Since FWM is a highly efficient nonlinear process, FOPAs are capable of providing comparatively high gains. In certain experiments, researchers have been able to achieve gains upto as high as $70dB$ [11]. They are also capable of demonstrating gain bandwidths of around $100nm$. In [12], they have obtained a gain bandwidth of $400nm$ with an on-off gain of $65dB$ which is outstanding compared to EDFAs as EDFAs demonstrate a gain bandwidth of around $32nm$ in the conventional band. Apart from that, FOPAs are capable of mid span spectral inversion which can be used to compensate for fiber dispersion and adverse nonlinear effects [13]. FOPAs are also used in other applications such as optical signal sampling, optical time division multiplexing and wavelength conversion [1]. The performance of FOPAs can be largely improved by the invention of high power pump lasers, fiber designs which demonstrate higher nonlinear indices and careful wavelength allocation of interacting signals. Along with above mentioned attractive features depicted by FOPAs, a categorization can be carried out as phase insensitive PI-FOPAs or in other words, phase insensitive amplifiers (PIAs) and phase sensitive PS-FOPAs or in other words, phase sensitive amplifiers (PSAs) depending on the dependency of FOPA gain on the relative input phase of the interacting signals. Based on this categorization, application of FOPA on PI or PS mode can be decided depending on the requirement for noise performance of the system. Current research is focused on the development of PSA schemes to resist different impairments, to resist polarization variations, to be compatible with higher modulation formats like M-PSK and M-QAM while gaining higher spectral efficiencies, capacities and gains [14], [15], [16].

In present day, the commercially available amplifiers such as Raman amplifiers and EDFAs not only amplify the in-phase signal components but also the out-of-phase components which means that they also amplify the noise components. Accordingly, the signal will most likely become distorted along the transmission line so that separate regenerative repeaters have to be added in the mid link in order to regenerate the signal back to its original form. Therefore, when deploying long haul transmission systems, there occurred a need for a type of an optical amplifier which can perform amplification and regeneration at the same time. The invention of low noise optical amplifiers became the most viable solution for this issue. They are capable of amplifying weak optical signals along with suppressing noise components. They can also suppress noise in the sub-quantum limit i.e. NF performance of less than $3dB$, which could never be achieved using EDFAs.

Low noise amplifiers are not only being used to fulfil the demands in telecommunication but also in optical sensing, imaging, metrology and so on [17]. In recent years, such optical amplifiers which yield higher gains along with sub-quantum limit amplification which leads to noiseless amplification and regeneration has become the most attractive topic among the researchers. Currently available low noise optical amplifiers are fiber based amplifiers which make use of the nonlinearity of the optical fiber [18], [19]. Aforementioned PSAs, which is a category of FOPAs, act as low noise amplifiers by amplifying signal components whilst suppressing noise components which leads to noise figure performances below the quantum limit of $3dB$.

As mentioned earlier, the demand for the increase of system capacity is the main concern for any communication network in the present day. The meaning behind increasing the capacity of a transmission system is the increase of throughput, not the increase in the upper limit of Shannon's capacity which is not possible without modifying the system parameters [2]. Throughput can be increased by improving the SNR of the system. Hence, the noise performance of the system plays a critical role in deciding the maximum system capacity. SNR of the system can be greatly improved by deploying PSAs as optical amplifiers instead of Raman amplifiers and EDFAs because of their impressive noise figure performances below $3dB$ quantum limit. PSAs are also capable of amplifying and regenerating phase modulated signals as well as signals with advanced modulated formats whilst suppressing amplitude and phase noise by using different strategic approaches. Alongside the excellent noise performance, PSAs are capable of providing very high gains and demonstrate gain throughout the gain bandwidth exhibited by PI-

FOPAs. Therefore, PSAs are considered as low noise optical amplifiers which can be a feasible solution in long haul transmission systems due to their contribution towards the improvement of system capacity and regeneration capability.

The state of polarization (SOP) which is the indication of direction of oscillation of electric field of a transmission signal is an important parameter to be considered in telecommunication systems because of its influence on the performance of system components. Hence, random rotation of the SOPs of the signals during transmission may adversely affect the telecommunication systems. This is usually caused by birefringence induced by the thermal and mechanical stress experienced by the fiber core as well as the irregularities of the fiber core. The induced birefringence is also subjected to random variations with the temperature, pressure and other environmental conditions. Therefore, the predictability of the SOP of the propagating signals at the end of the fiber is highly violated and variation of SOP becomes time dependent hence leading to a random variation of SOPs. At the end of the fiber, it usually is in an elliptical polarization state with varying degrees of ellipticity which has no information about the initial SOP of the input signals. This random variation of SOP gives rise to polarization dependent impairments like polarization mode dispersion (PMD), polarization dependent loss (PDL), polarization dependent modulation (PDM) and polarization dependent gain (PDG) [20].

The gain of a PSA is highly dependent on the relative polarization between the interacting waves. In realistic scenarios, due to aforementioned causes, the relative SOP varies randomly with time. Polarization sensitivity of PSA is in such a way that for certain polarization angles, gain is maximum while for certain others, gain is minimum [16]. There have been many strategies that have been introduced to mitigate the polarization sensitivity of FOPAs in general. Thus they are also applicable for PSAs. By opting a suitable strategy to mitigate polarization dependency of PSA gain, not only the maximum possible gain can be obtained for any random polarization rotation of the signal but also the amplification of dual polarization modulated signals can also be achieved.

There are two strategic approaches to mitigate polarization sensitivity of PSAs. One is the vector scheme and the other is the polarization diversity loop [16], [21]. The vector scheme which is used to mitigate the polarization sensitivity needs two pump waves with orthogonal SOPs for its implementation. Since FOPAs and

PSAs can be implemented using a single pump or dual pumps, vector scheme is most suitable for a dual pump PSA scheme. This research work is focused on single pump PSAs because of the advantages of using single pump over dual pump configuration such as, the simplicity of the configuration, WDM compatibility and the ability to amplify advanced modulation formats [19]. Therefore, the second strategy, which is the polarization diversity loop is the most suitable for a single pump PSA scheme. In the diversity loop, the input SOPs of the incoming signals are split into two orthogonal polarization components and sent through a HNLF in which FWM takes place. The propagation of these waves are in opposite directions. At the end of the fiber, the signals are reconstructed back to their initial SOPs. In that way, gain is experienced by the weak signal from FWM process despite of its input SOP. It is the basic principle behind polarization diversity loop.

Several implementations of diversity loop based phase insensitive FOPAs or PIAs have been carried out and tested recently [20], [22], [23], [24], [25]. In these experiments, different pump powers have been used and the polarization insensitivity of the PIA has been evaluated by considering the signal gain variation for different input relative SOPs. Many experiments demonstrate that the gain variation is minute against the variation of input relative SOPs when diversity loop is implemented. When frequency or phase modulated signals are transmitted, the system performance is evaluated by using bit error rate (BER) performance at the receiver. Power penalty of the received signal power has been illustrated by considering the BER curves obtained with and without polarization diversity loop. Also, the eye diagrams have been used to evaluate the system performance with and without diversity loop. The experiments have confirmed that there is a significant performance improvement when diversity loop is deployed. In the contrary, there are several issues that can arise in the diversity loop. In this technique, orthogonally polarized waves are counter-propagating in opposite directions. With this counter- propagation, an adverse scattering effect called stimulated Brillouin scattering (SBS) can arise in the deployed setup. It is a phenomenon which can arise when input signal powers are relatively high. Due to this scattering, counter-propagating waves/sidebands with new frequencies can be formed. These sidebands can interact with other counter-propagating waves in a diversity loop setup which can adversely affect the expected performance. Therefore, several research works have been done in order to analyze the effect of SBS, mitigation methods and their success when used in a polarization diversity loop. Another major issue is the significant gain reduction in diversity loop based architecture due to the unavailability of total pump power at the input of PSA.

Therefore, the motivation of this thesis is to address the performance limitations of diversity loop implementations of PSAs by incorporating a design modification to the polarization diversity loop and to assess its performance improvement in terms of polarization sensitivity and gain compared to the conventional diversity loop technique.

1.2 Objectives and Scope of the Thesis

- Development of a baseline of a PSA scheme which demonstrates optimum performance
- Improvement of the developed PSA scheme with polarization diversity to achieve polarization independence
- Identifying the optimization of gain and phase parameters for developed PSA scheme with polarization Independence
- Characterization of polarization diverse PSA scheme for different impairments.

1.3 Structure of the Thesis

- Chapter 1: Introduction
  This chapter describes the background and the motivations that led to carryout this work. The research problem has been elaborated briefly.

- Chapter 2: Theoretical Background
  The concept of fiber optic parametric amplification has and an extensive theoretical analysis has been carried out about fiber nonlinearities, four wave mixing process based parametric amplification and phase sensitive amplification along with a thorough literature survey. Characterizations have been carried out on parametric amplification and gain performance of phase sensitive amplifier on quadratic gain regimes has been introduced.

- Chapter 3: Polarization Diversity Loop
  This concept of polarization diversity loop has been introduced and an extensive literature survey has been carried out to explore the performance aspects of polarization diversity loop.

- Chapter 4: Modified Polarization Diversity Loop for PSA
  The concept of cascaded fiber architecture has been introduced and polarization diversity loop based PSA has been characterized for cascaded fiber configuration.

- Chapter 5: Conclusion and Future Work
  The work has been concluded based on the results obtained from the previous sections and prospective future improvements have been discussed.

Chapter 2

THEORETICAL BACKGROUND

2.1 Introduction

This chapter introduces the theoretical aspects of the propagation of an electromagnetic light wave through an optical fiber both in linear and nonlinear regimes followed by introducing the concept of fiber optic parametric amplification which utilizes a fiber nonlinearity as the parametric process. An extensive study will be carried out to analyze the gain achieved by the parametric process through a thorough literature survey and the concepts have been further validated by numerical characterizations. Later on, the concept of phase sensitive amplification which is the basis of the discussion in this thesis will be introduced by utilizing the theory of parametric amplification and further analysis will be carried out using numerical characterizations. Furthermore, the gain performance of the phase sensitive amplifier in the quadratic gain regime will be introduced for the first time to the best of our knowledge. Finally, the dependence of the phase sensitive amplification process on the SOP is discussed and theory behind important scattering phenomenon called SBS will be introduced as well. The discussion in this thesis is limited to single mode Silica fibers where fiber loss and dispersion is present.

2.2 Wave Propagation in Optical Fiber

An optical fiber can be viewed as a dielectric wave guide by which optical signals are propagated. They propagate under linear and nonlinear regimes decided by the different parameters of fiber being used. The time varying electric field of an optical wave propagating along the z direction can be represented as,

$$\overrightarrow{E}(r) = \frac{1}{2}\hat{x}\big[E(r)exp\big[i(\beta z - \omega t)\big] + c.c\big] \tag{2.1}$$

where $\overrightarrow{E}(r)$ represent the space dependent electric field vector, $\hat{x}$ the polarization unit vector along x direction, $E(r)$ the electric field intensity, β the propagation constant which is frequency dependent, ω the signal frequency and $c.c$ the complex conjugate of the electric field [7].

The linear effects on optical pulse propagation are signal attenuation, chromatic dispersion and PMD which act on each frequency component independently. Signal attenuation determines the effective length (L_{eff}) of the fiber which is different from the physical length of the fiber L by incorporating the attenuation coefficient α which can be expressed as, [26].

$$L_{eff} = \frac{1}{\alpha}(1 - exp(-\alpha L)) \tag{2.2}$$

Fiber Loss is a frequency dependent factor and commonly used Silica fibers exhibit approximately a $0.2dB/km$ loss near $1.55\mu m$ wavelength region. Chromatic dispersion is the other linear effect which occurs due to the wavelength dependence of the refractive index of the fiber. It gives rise to the wavelength dependent nature of the propagation constant $\beta(\omega)$. Lastly, PMD is a linear effect which results in a polarization state dependence of the refractive index of the fiber in which the orthogonal polarization components of the signal travel in different velocities. The polarization dependence of the refractive index is termed as birefringence.

In contrast to linear effects, fiber nonlinearities occur when the refractive index of the fiber becomes optical intensity dependent. As a result, waves at different frequencies can interact with each other to give rise to different nonlinear phenomena. Since this thesis is centred around fiber nonlinearities, it will be discussed in a broader sense in the following sections.

2.3 Fiber Nonlinearities

Fiber nonlinearity is a result of induced polarization of an optical material by the effect of nonlinear response of bound electrons of the material to an electromagnetic field. This causes the refractive index of the material to be dependent on the intensity of the electromagnetic waves. Hence, the overall refractive index of the fiber when it exhibits nonlinearity can be expressed as the sum of its frequency dependent linear refractive index which causes dispersive effects and intensity dependent nonlinear counterpart which causes fiber nonlinearities as,

$$n = n_0 + n_2 I \tag{2.3}$$

where n_0 and n_2 are linear and nonlinear refractive indices respective while I is the intensity (irradiance) of the optical wave [27]. Usually in Silica fibers, n_0 is 1.5 and n_2 is in the order of $10^{-20}m^2$/W by which the requirement of higher optical intensities for the nonlinear effects to become significant can be understood. Based on the nonlinear refractive index, the fiber nonlinearity coefficient γ can be expressed as [7],

$$\gamma = \frac{\omega n_2}{cA_{eff}} = \frac{2\pi n_2}{A_{eff}\lambda} \tag{2.4}$$

where c, A_{eff} and λ are the speed of light in vacuum, the effective area of the fiber and the wavelength of the optical signal respectively. The nonlinear coefficient is a convenient quantity to determine the nonlinearity of an optical fiber.

Due to the intensity dependent modification of refractive index of the fiber, the dielectric polarization responds non-linearly to the electric field of the electromagnetic wave as,

$$P_{NL} = e_0(\chi^{(1)}.E + \chi^{(2)} : EE + \chi^{(3)}\vdots EEE + ...) \tag{2.5}$$

where P_{NL} is the induced nonlinear polarization, e_0 is the permittivity in vacuum and $\chi^{(j)}$ is the j^{th} order susceptibility tensor. Susceptibility is a dimensionless proportionality constant which indicates the degree of polarization induced by an applied electric field. When the susceptibility is higher, the material is able to polarize in response to the applied electric field. $\chi^{(1)}$ is the linear susceptibility which contributes to the dielectric constant of the fiber, $\chi^{(2)}$ is responsible for second order nonlinear effects such as sum frequency generation, second harmonic generation [28] and so on but in case of Silica fibers, because of the symmetric nature of the molecules, second order nonlinearity is inhibited and instead, $\chi^{(1)}$, the third order susceptibility contributes to the nonlinear effects such as SPM, XPM and FWM also termed as Kerr nonlinearity [7].

2.3.1 Self Phase Modulation (SPM)

SPM is the phenomenon in which the phase of the optical pulse modifies due to the intensity of the pulse itself. The phase shift introduced by SPM is the nonlinear phase shift and the maximum phase shift occurs at the center of the pulse. For example, when a high intensity Gaussian pulse is propagating inside the nonlinear fiber or media, SPM introduces a spectral broadening of the pulse having a maximum phase shift at the center.The nonlinear phase shift induced by SPM can be written as,

$$\phi_{SPM} = \gamma P L_{eff} \tag{2.6}$$

where, P is the optical power of the pulse. An initially unchirped optical pulse acquires a chirp (time varying instantaneous frequency variations) by the effect of SPM. Spectral compression occurs if the initial pulse is a chirped pulse. The optical spectrum is affected by SPM. SPM is responsible for important occurrences like soliton generation and spectral broadening of ultrashort optical pulses [29].

2.3.2 Cross Phase Modulation (XPM)

When two or more waves are co-propagating in a nonlinear optical fiber or media, XPM occurs when the phase of one wave gets modified due to the influence of intensity of another thereby spectrally broadening the signal. The phase shift is proportional to the intensity of the second wave. This can also be viewed as a crosstalk occurring between co-propagating waves. XPM can be utilized in optical switching and multiplexing technologies [30].

2.3.3 Four Wave Mixing (FWM)

FWM is a nonlinear process based on $\chi^{(3)}$ nonlinearity when four waves at distinct frequencies interact with each other. It is a flow of photons between different frequencies in a momentum and energy conserving manner. It can take place in any medium (like KTP crystals) which has nonlinear properties but in this thesis, our focus is on parametric amplification by FWM taking place in Silica fibers. The occurrence of FWM process can be described as follows. If two waves at frequencies ω_1 and ω_2 propagate through a fiber exhibiting nonlinearity, preferably a HNLF, a beating occurs at $\omega_2 - \omega_1$ which modulates the nonlinear index of the medium. If a third wave is introduced at ω_3, it will get phase modulated due to the modified refractive index and as a result, ω_3 scatters to form two sidebands at $\omega_3 \pm (\omega_2 - \omega_1)$. Similarly, due to the beating of ω_3 with ω_1, ω_2 scatters to form sidebands at $\omega_2 \pm (\omega_3 - \omega_1)$ and beating between ω_3 with ω_2 creates sidebands at $\omega_1 \pm (\omega_3 - \omega_2)$. Likewise, new sidebands will be created at $\omega_{jkl} = \omega_j \pm \omega_k \pm \omega_l$. If the initial phases of the interacting signals are ϕ_j, ϕ_k and ϕ_l, the sidebands created by FWM have a phase relationship with each other as, $\phi_{jkl} = \phi_j \pm \phi_k \pm \phi_l$. Some of these sidebands will overlap with each other or with originally input waves and these newly generated frequency

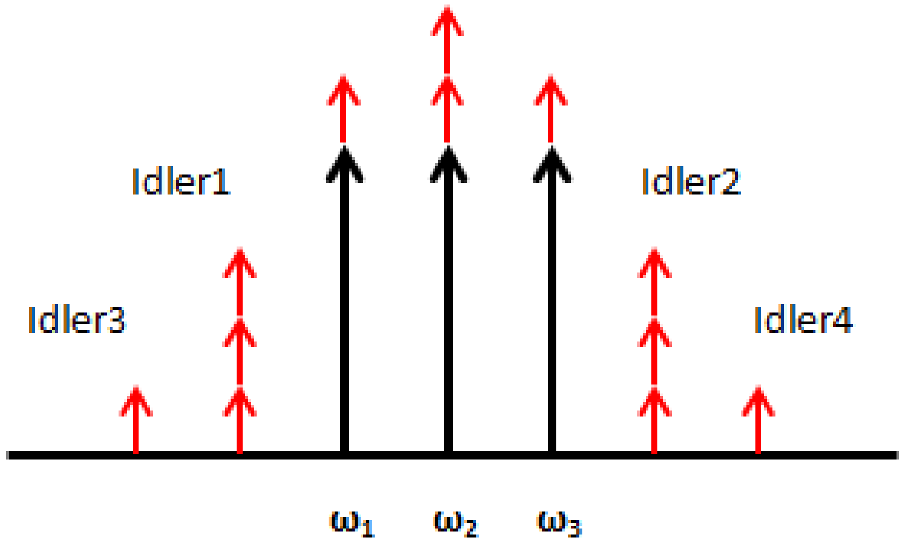

Figure 2.1: Generated FWM idlers for three input waves with equal frequency spacings [1]

components with strong amplitudes are usually considered as idlers while weak ones are neglected. Therefore, only frequency components with $\omega_{jkl} = \omega_j + \omega_k - \omega_l$ and $\phi_{jkl} = \phi_j + \phi_k - \phi_l$ are considered. The idlers which overlap with original signals provides a gain to the original signals [26], [31], [32],

As a special case, if frequency spacings, $\omega_2 - \omega_1$ is as same as $\omega_3 - \omega_2$, the idler generation by the FWM process is represented in figure 2.1. In this case, four idler frequencies are distinct while in the case where frequency spacings between original waves is not similar, nine such idlers will be generated at distinct frequencies from each other as well as from original waves. Since FWM process is capable of providing a gain to the original waves, it can be utilized as a way of amplifying a weaker signal. If a weak signal is input to a HNLF along with two strong waves, i.e., pumps and if they are separated by same frequency spacings, the annihilation of pump photons will lead to the creation of idler photons which overlap with the signal frequency. If their phases match with each other, the signal will be subjected to parametric amplification.

The FWM processes can be categorized as degenerate or non-degenerate based on whether the involved frequencies differ from each other or not. If the frequencies overlap, it is termed as a degenerate process and of they are distinct, it is a non-degenerate process. For example, in a dual pump configuration, if

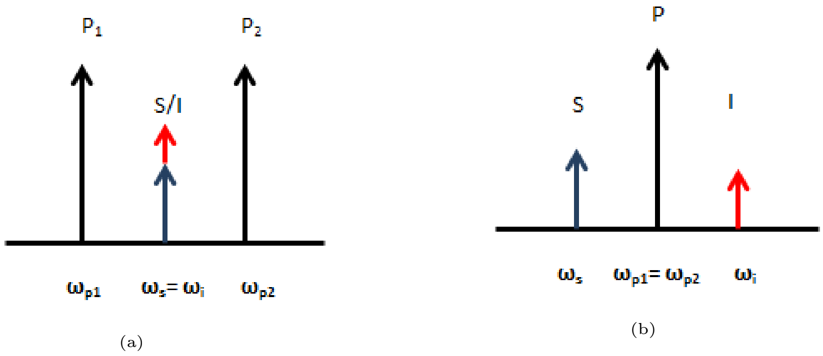

Figure 2.2: (a) Dual pump degenerate FWM (one-mode) (b) Single pump non-degenerate FWM (two-mode)

the signal and idler frequencies overlap with each other, it is a pump frequency non-degenerate and a signal-idler frequency degenerate process. But in short, it is usually termed as a dual-pump degenerate process. Another important fact is, if signal and idler frequencies are degenerate, it is said to be a one-mode process. Likewise, if signal-idler frequencies are non-degenerate i.e. which are distinct and do not overlap, it is a two-mode process [19]. Figure 2.2 illustrates the two processes by considering pump waves P_1 and P_2 at frequencies ω_{p1}, ω_{p2} and signal (S) and idler (I) at frequencies ω_s, ω_i respectively. The idler generated by process (a) has a frequency and phase relationship to the pumps and signal waves as $\omega_i = \omega_{p1} + \omega_{p2} - \omega_s$ and $\phi_i = \phi_{p1} + \phi_{p2} - \phi_s$ where, pumps, signal and idler phases are ϕ_{p1}, ϕ_{p2}, ϕ_s and ϕ_i respectively whereas, the idler of process (b) has a frequency relationship with pump and signal waves as $\omega_i = 2\omega_p - \omega_s$ and a phase relationship as $\phi_i = 2\phi_p - \phi_s$ where, $\omega_{p1} = \omega_{p2} = \omega_p$.

Although FWM is utilized in parametric amplification, it is an undesirable effect in WDM applications because it generates unnecessary frequency components by the nonlinear interaction of multiple frequencies. But since FWM is a fast and an instantaneous process, it can be utilized in ultrafast signal processing applications which is outside the scope in this thesis [33].

2.3.3.1 Coupled Mode Equations (CMEs)

Coupled amplitude equations which are derived by substituting electric field intensity of a wave in the well known nonlinear Shrödinger equation (NLSE) [7]. CMEs represent the evolution of the wave envelops of the co-propagating waves in the fiber core along the direction of fiber length (z-direction) when fiber attenuation, higher order dispersion, wavelength dependence of γ and Raman effect are neglected [7], [27]. For example, when the propagation of the pump is considered,

$$\frac{dA_p}{dz} = i\gamma\{[\underbrace{|A_p|^2}_{\text{SPM}} + \underbrace{2(|A_s|^2 + |A_i|^2)}_{\text{XPM}}]A_p + \underbrace{2A_sA_iA_p{}^*exp(i\Delta\beta z)}_{\text{FWM}}\} \tag{2.7}$$

where, A_p, A_s, A_i are the slowly varying amplitudes of the pump, signal and idler waves respectively, γ is the nonlinear coefficient of the fiber, z is the direction of wave propagation along the fiber and $\Delta\beta$ is the wavelength dependent propagation constant mismatch of the waves which is given by,

$$\Delta\beta = 2\beta_p - \beta_s - \beta_i \tag{2.8}$$

where, β_p, β_s and β_i are the propagation constants of the pump, signal and idler waves respectively. In R.H.S. of the equation 2.7, the first term represents the effect of SPM on the pump wave where nonlinear phase shift is gained due to its own intensity, the second term represents the nonlinear phase shift gained by pump wave due to the effect of XPM and the third term represents the FWM of the pump wave with the interaction between signal and idler waves along the propagation direction of the fiber. In a similar manner, the CMEs for the slowly varying amplitudes of the signal and idler waves can be written as [7],

$$\frac{dA_s}{dz} = i\gamma\{[|A_s|^2 + 2(|A_p|^2 + |A_i|^2)]A_s + 2A_pA_iA_s{}^*exp(i\Delta\beta z)\} \tag{2.9}$$

$$\frac{dA_i}{dz} = i\gamma\{[|A_i|^2 + 2(|A_p|^2 + |A_s|^2)]A_i + 2A_pA_sA_i{}^*exp(i\Delta\beta z)\} \tag{2.10}$$

Slowly varying amplitudes, A_p, A_s and A_i can be written in terms of optical power P and the absolute phase of the wave, θ, as,

$$A = \sqrt{P}exp(i\theta) \tag{2.11}$$

Using equation 2.11, the CMEs for the pump, signal and idler waves can be re-written in terms of change of optical power in the z-direction of propagation as,

$$\frac{dP_p}{dz} = -4\gamma({P_p}^2 P_s P_i)^{\frac{1}{2}} sin(\theta_{rel}) \tag{2.12}$$

$$\frac{dP_s}{dz} = \frac{dP_i}{dz} = 2\gamma({P_p}^2 P_s P_i)^{\frac{1}{2}} sin(\theta_{rel}) \tag{2.13}$$

where, P_p, P_s, P_i are the optical powers of pump, signal and idler waves respectively and θ_{rel} is the relative phase of the waves which is varied along the propagation length, can be expressed as,

$$\theta_{rel}(z) = 2\phi_p(z) - \phi_s(z) - \phi_i(z) \tag{2.14}$$

where, $\phi_p(z)$, $\phi_s(z)$, $\phi_i(z)$ represent the absolute phases of pump, signal and idler respectively. The variation of θ_{rel} along fiber length can be expressed as [34],

$$\begin{aligned} \frac{d\theta_{rel}}{dz} =& \Delta\beta + \gamma\{(2P_p - P_s - P_i) \\ &+ [(P_p^2 P_s/P_i)^{(\frac{1}{2})} + (P_p^2 P_i/P_s)^{(\frac{1}{2})} - 4(P_s P_i)^{(\frac{1}{2})}]cos(\theta_{rel})\} \end{aligned} \tag{2.15}$$

In the power flow equations, 2.12 and 2.13, it is clear that the parametric amplification of the signal can be achieved at a positive θ_{rel} value and maximum power flow (amplification) is obtained when $\theta_{rel} = +\pi/2$ where pump photons disintegrate at a maximum rate in order to generate signal and idler photons which is the favorable case. Similarly, parametric attenuation can be witnessed when θ_{rel} is a negative value and power transfer is in the opposite direction where signal and idler photons disintegrate to generate pump photons. Maximum signal attenuation can be seen when $\theta_{rel} = -\pi/2$. Therefore, θ_{rel} value plays a major role in the process of parametric amplification. It is also to be noted that, when power flow equations are considered, only FWM process is taken into account while other third order nonlinear processes such as, SPM and XPM are neglected. It has been assumed that the power flow is not affected by fiber attenuation along the fiber length. Otherwise, mathematical analysis has to be carried out by simply replacing the physical fiber length by effective length (L_{eff}) given by equation, 2.2 where attenuation has been taken into account [26], [32].

2.3.3.2 Conditions for Phase Matching

It is clear from the CMEs in equations, 2.7, 2.9, 2.10 as well as from power flow equations, 2.12, 2.13 that, the magnitude and the direction of power flow due to FWM depends on the relative phase, θ_{rel}, of the interacting waves which leads to the concept of phase matching. It also shows that the total power in the system is conserved because two pump photons are annihilated to create a signal and an idler photon. In the process of phase matching, θ_{rel} should be maintained throughout the propagation distance. In order to do so, the linear and nonlinear phase shifts introduced during propagation should be cancelled out to maintain the original phase relation at a constant value. When properly phase matched, the generated idler and amplified signal will show an exponential growth during the interaction.

Linear Phase Mismatch

One of the two terms which contribute for the variation of θ_{rel} value of the waves during propagation is the linear phase shift acquired by the waves due to the frequency dependence of propagation constant, β. It is the cause for the effect known as, *chromatic dispersion*. The propagation constant can be expanded around centre angular frequency (ω_c) of the pulse spectrum in a Taylor series expansion as [7],

$$\beta(\omega) = \beta_0 + \beta_1(\omega - \omega_c) + \frac{1}{2}\beta_2(\omega - \omega_c)^2 + ... \tag{2.16}$$

where, $\beta_m, m = 0, 1, 2, ...$ are the wavelength dependent coefficients (higher order derivatives of the propagation constant) which contribute for the chromatic dispersion. Coefficient β_1, is related to the group velocity which determines the speed at which the envelop of the wave propagates while β_2, which is also known as the group velocity dispersion (GVD) parameter, can be expressed in terms of dispersion parameter (D) as,

$$D = -\frac{2\pi c}{\lambda^2}\beta_2 \tag{2.17}$$

where, λ is the wavelength of the signal and c is the speed of light. The measuring unit of dispersion parameter is $ps/nm.km$. GVD parameter becomes zero at *zero dispersion frequency (ZDF)/wavelength (ZDW)* of the fiber. Based on the sign of the GVD parameter, the effect of fiber nonlinearity on the propagating waves can be varied and can be explained in two dispersion regimes. For signal wavelengths which are smaller than ZDW where, $D < 0$ i.e. $\beta_2 > 0$, the fiber operates in the *normal dispersion regime* where, higher frequency components of an optical pulse are travelling at lower speeds than lower frequency components. For signal wavelengths which are higher than ZDW, $D > 0$ and $\beta_2 < 0$ in which the fiber operates in the *anomalous dispersion regime* where, higher frequency components of the optical pulse travel faster in the fiber. From the two dispersion regimes, fiber operating at anomalous dispersion regime is important when phase matching of FWM process is considered. In addition, another frequently used quantity, *dispersion slope*, which is derived from the dispersion parameter can be defined as,

$$Dispersion\ Slope = \frac{dD}{d\lambda} \tag{2.18}$$

Dispersion slope is related to β_3 when operating near ZDW and it is frequently used in fiber characterization and related calculations.

Propagation constant mismatch, $\Delta\beta$ given in equation 2.8 which is responsible for the linear phase shift acquired by the wave propagation in fiber, can be re-written by using the Taylor series expansion of β in equation 2.16 around ZDF, ω_0, as [1],

$$\Delta\beta = \{\beta_3(\omega_p - \omega_0) + \frac{\beta_4}{2}[(\omega_p - \omega_0)^2 + \frac{1}{6}(\omega_p - \omega_s)^2]\}(\omega_p - \omega_s)^2 \tag{2.19}$$

Since β_4 is in the order of 10^{-4}, the effect of β_4 can be neglected. Therefore, $\Delta\beta$ can be expressed using dispersion slope given in equation 2.18 and substituting wavelengths instead of angular frequencies in equation 2.19 as follows.

$$\Delta\beta = \frac{-2\pi c}{{\lambda_0}^2}\frac{dD}{d\lambda}(\lambda_p - \lambda_0)(\lambda_p - \lambda_s)^2 \tag{2.20}$$

where, c is the speed of light, λ_0 is the zero dispersion wavelength of the fiber, λ_p is the pump wavelength, λ_s is the signal wavelength and $\frac{dD}{dz}$ is the dispersion slope of the fiber at zero dispersion wavelength. Equation 2.20 uses the approximation that, $\omega_i - \omega_j = c/2\pi\lambda_0^2(\lambda_j - \lambda_i)$, which is valid for the bandwidths where, $\lambda_p - \lambda_s << \lambda_p$ [1]. In anomalous gain regime, $\Delta\beta$ given in equation 2.20 is a negative value which is important in the process of phase matching which will be discussed in the upcoming sections.

Nonlinear Phase Mismatch

When a signal with optical power P is propagated for a distance L along a fiber having a nonlinearity γ, the nonlinear phase shift acquired by the signal due to SPM can be expressed as γPL similarly as in equation 2.6. The nonlinear phase shift induced by XPM on signal wave due to the optical power of pump wave can be expressed as $2\gamma P_p$ in a similar manner. When the undepleted pump is assumed where $P_p >> P_s$, the overall nonlinear phase shift acquired by the signal wave during propagation along the fiber can be approximated as $2\gamma P_p$.

Net Phase Mismatch

As stated before, normally at the beginning of the fiber, if there is no pre-generated idler input to the fiber along with pump and signal waves, the FWM process sets the initial θ_{rel} value to be $\pi/2$ for maximum efficiency. Therefore, by considering equation 2.15, it can be noted that, the variation of θ_{rel} along the propagation distance depends on first and second terms where, the effect of third term can be neglected as initial θ_{rel} is $\pi/2$. Hence, the condition for phase matching can be expressed as,

$$k = \Delta\beta + \gamma(2P_p - P_s - P_i) \tag{2.21}$$

If the pump power is much higher compared to signal and idler powers, i.e., $P_p >> P_s, P_i$, equation 2.16 can be re-written as,

$$k = \Delta\beta + 2\gamma P_p \tag{2.22}$$

where, k is the net phase mismatch. In anomalous dispersion regime, $\Delta\beta$ can be used to compensate for the accumulated nonlinear phase mismatch thereby reinstating the initial value of θ_{rel}. The peak FWM efficiency can be observed when $k = 0$ where, $2\gamma P_p = -\Delta\beta$. This is known as the perfectly phase matched case which yields an exponential gain from FWM. From equation 2.20, it can be observed that the perfect phase matching can be attained at a certain λ_s value away from λ_p with a positive detuning i.e. $\lambda_p - \lambda_s = +\delta\lambda_s$ where, $\lambda_p > \lambda_s$, or a negative detuning from the pump wavelength i.e. $\lambda_p - \lambda_s = -\delta\lambda_s$ where, $\lambda_p < \lambda_s$. Hence, two signal wavelengths, λ_{s1} and λ_{s2} will exhibit the perfectly phase matched case with an equal spacing from pump wavelength to either sides of the positioning of λ_p in the spectrum, which results in a gain spectrum with two symmetric lobes containing two maximum gain points. According to equation 2.20, when λ_s is closer to λ_p, $\Delta\beta \to 0$ which gives the net phase mismatch to be $k = 2\gamma P_p$, which in turn gives a local minimum in the gain spectrum. Therefore, it can be seen that, the value of k which is obtained for different values of $\Delta\beta$ and $2\gamma P_p$ define different conditions for phase matching in the FWM process. It is also to be noted that unlike FWM, other third order nonlinearities like SPM and XPM effects do not require a phase matching because they only depend on the intensities of the interacting waves.

2.4 Fiber Optic Parametric Amplification

The first FWM based parametric amplification was reported by R.H. Stolen in 1975 where higher gain and broader amplification bandwidth had been observed compared to the popular Raman gain based amplifiers [35]. In this work, the emphasis on phase matching to achieve higher gains is noteworthy. Developments and analyses carried out on FOPAs in later years have opened up a new arena of parametric amplification where phase sensitive noiseless amplification and regeneration along with modulation format independence are possible with outstanding performances compared to Raman amplifiers and EDFAs. Hence, it can be predicted that the next generation of optical amplifiers will be hugely impacted by FOPAs.

FOPA uses the parametric process, four wave mixing taking place in an optical fiber where a weak signal wave is amplified and an idler is generated in the presence of a strong pump wave [32], [26]. This process is energy conserved which means that there is no energy transfer between the medium and the interacting waves. The gain medium is a HNLF where, the nonlinear coefficient (γ) is comparatively high. FOPAs can be implemented in both single pump and dual pump configurations. In dual pump configuration, the idler is generated at a frequency where, $\omega_i = 2\omega_c - \omega_s$ in which ω_c stands for the center frequency of two pump waves which can be expressed in terms of pump1 and pump2 frequencies as, $\omega_c = (\omega_{p1} + \omega_{p2})/2$. In single pump case, since $\omega_{p1} = \omega_{p2} = \omega_p$, the idler has a frequency relationship with signal and pump as, $\omega_i = 2\omega_p - \omega_s$. In both configurations, the idler wave is the phase conjugated form of the signal wave.

Based on whether the idler frequency overlaps with the signal frequency, the FOPAs are categorized as signal-idler degenerate FOPAs and signal-idler non-degenerate FOPAs. These configurations are corresponding to the illustration in figure 2.2 where a dual pump degenerate and a single pump non-degenerate processes have been represented. Figure 2.3 shows the basic configuration of a FOPA where a single pump or dual pumps are combined with a weak signal to form an idler after passing through the HNLF where parametric amplification takes place. The pump(s) is/are usually phase modulated using several RF tones

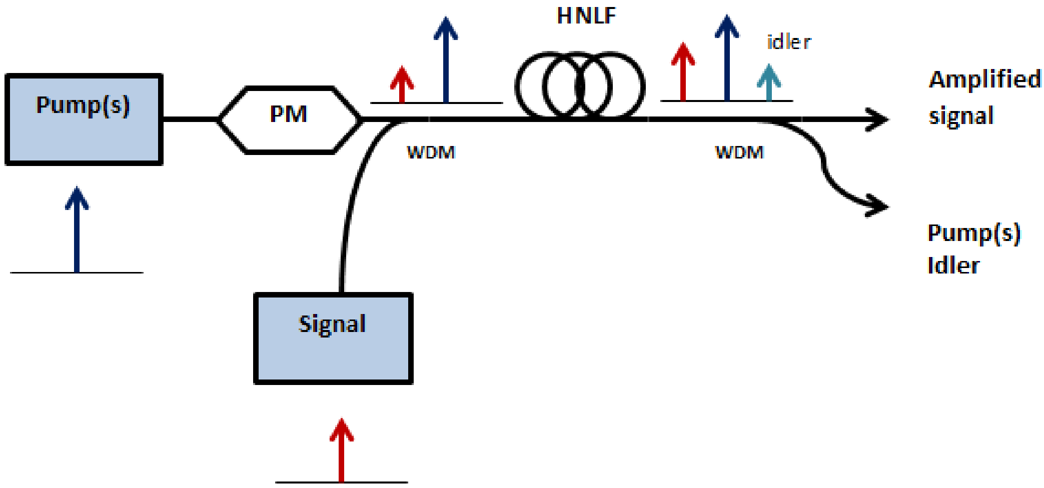

Figure 2.3: Basic design of FOPA where PM: Phase modulation of pump(s), WDM: wavelength division multiplexing coupler, HNLF: highly nonlinear fiber.

in order to make the system susceptible to SBS which affects the gain of FOPA adversely [36].

2.4.1 Phase Insensitive (PI) and Phase Sensitive (PS) FOPA

Phase sensitivity of an amplifier can be defined as the alteration of the amplification factor/amplifier gain depending on the variation of phase of the input waves due to the accumulated linear and non-linear phase noise during propagation. The phase sensitivity and insensitivity of fiber optic parametric amplification can be explained in the perspective of FWM based wave propagation as follows.

In a FOPA where there are only two waves namely, signal and pump input to the HNLF, an idler wave will be generated immediately after propagating for an infinitesimal distance of δz along the fiber which later on will lead towards the further building up of the idler, amplification of the signal and depletion of the pump wave as the wave propagation continues. As stated in section 2.3.3, the generated idler has a phase and frequency relationship to the original signal and pump waves. The generated idler takes a phase such that the FWM efficiency is maximum i.e., θ_{rel} is $\pi/2$ and this idler tracks the variations of absolute phase of the signal wave during propagation and changes its own phase such that initial θ_{rel} is maintained at the desired value [37]. For example, if the signal phase changes by $+\theta$, the idler phase is rotated by $-\theta$ so that the field contribution that is

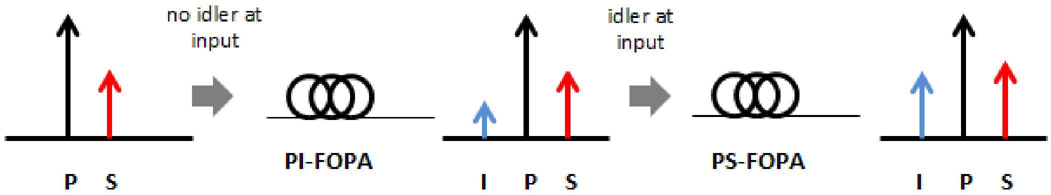

Figure 2.4: PI-FOPA without pre-generated idler at the input and PS-FOPA with pre-generated idler at the input, P: pump, S: Signal, I: idler

being added to the signal for the amplification process due to the disintegration of pump wave also rotates by $+\theta$, leading to constructive interference and hence amplification of the signal despite of its phase variations at any given time of propagation. Therefore, when a pre-generated idler is not present at the input of the HNLF along with the signal and pump waves, the internally generated idler tends to track the phase variations of the propagating signal wave which leads to a signal gain which is insensitive to signal phase. It leads to the phase insensitive fiber optic parametric amplification.

In a scenario where a phase and frequency correlated pre-generated idler is present along with the signal and pump waves at the input of the HNLF, since idler is not generated internally by the parametric process, it is unable to track the phase variations of the input signal. Therefore, field contributions added to the signal due to FWM process becomes sensitive to the variations of the relative phase of the propagating waves. This leads to the interference between field contributions from FWM process and the existing field of the signal to be constructive or destructive based on the phase matching conditions which results in a PS-FOPA. Since the focus of this thesis is on phase sensitive amplification of a single-pump based parametric process, the presence of a pre-generated FWM based idler being present at the input of the HNLF is a vital requirement which is contrast to the case of dual-pump based phase sensitive amplification.
Figure 2.4 illustrates the PI-FOPA when only pump and signal waves are present at the input of HNLF and PS-FOPA when generated idler from the PI-FOPA stage is input to the second HNLF along with pump and signal waves. This is demonstrated for single pump non-degenerate configuration where signal, pump and idler waves are located at distinct frequencies.

2.4.2 PI-FOPA Gain

In a quantum mechanical point of view, fiber optic parametric amplification based on FWM can be expressed as a process which involves in the creation of a signal and an idler photon after annihilating two pump photons where no energy is transferred to or from the medium in the form of heat energy, vibrational energy etc. A gain is acquired by the signal wave due to the creation of a new signal photon and by which the signal gets amplified. The signal gain for PI-FOPA can be obtained by solving the differential equation 2.13 by assuming that the pump depletion during the parametric interaction is negligible (undepleted pump regime).

$$Gs = \frac{P_s(L)}{P_s(0)} = 1 + \left[\frac{\gamma P_p}{g}\sinh(gL)\right]^2 \tag{2.23}$$

where, $P_s(L)$ and $P_s(0)$ are the signal power at the output of the fiber of length L and the signal power at the input of the fiber respectively, G_s is the signal gain, γ is the nonlinear coefficient of the HNLF, P_p is the pump power and g is the parametric gain coefficient. Taylor series expansion can be applied to equation 2.23 to re-write the signal gain as [32],

$$Gs = 1 + (\gamma P_p L)^2 + \left[1 + \frac{(gL)^2}{6} + \frac{(gL)^4}{120} + ...\right] \tag{2.24}$$

The parametric gain coefficient, g, can further be expressed as,

$$g = \sqrt{(\gamma P_p)^2 - (k/2)^2} = -\Delta\beta\left(\frac{\Delta\beta}{4} + \gamma P_p\right) \tag{2.25}$$

where k is the net phase mismatch and $\Delta\beta$ is the propagation constant mismatch which contributes for the linear phase shift which is expressed by equations 2.19 and 2.20.

2.4.3 Characterization

Characterization of FOPA gain spectrum has been carried out in order to analyze the operating gain regimes of FOPA and the effect of variations different system parameters on the FOPA gain spectrum. The ultimate goal of any amplifier used in communication systems is to obtain a nearly maximum gain over a large bandwidth. In optical communication systems, the FOPA gain is affected by the interplay between fiber dispersion and nonlinear contribution of the fiber

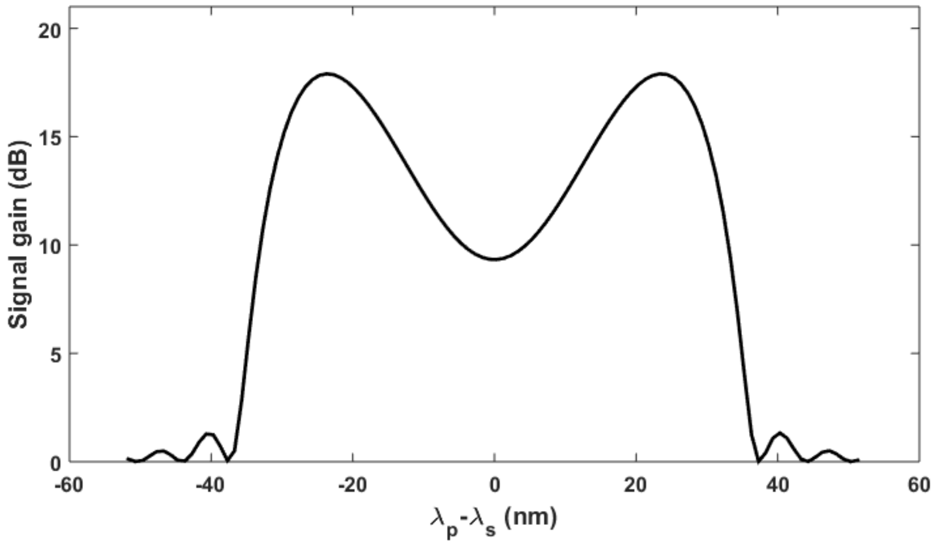

Figure 2.5: PI-FOPA gain for different signal wavelength (λ_s) detunings from pump wavelength (λ_p) for single pump FOPA.

for different relative signal wavelength positionings from pump wavelength. Figure 2.5 represents the PI-FOPA gain spectrum where signal gain is a function of phase matching conditions provided by equation 2.22. The gain spectrum has been obtained by considering a $250m$ long HNLF with nonlinear coefficient, γ, of $11W^{-1}km^{-1}$, a ZDW of $1559nm$ and a dispersion slope of $0.03ps/nm^2km$. The pump wave input to the fiber is at $1560.7nm$ with an input power of $1W$. The signal wavelength has been varied relative to pump wavelength in a span of $100nm$. Two symmetric gain lobes can be observed at either sides where $\lambda_s > \lambda_p$ and $\lambda_s < \lambda_p$. A gain peak can be observed for each gain lobe at a specific signal wavelength detuning from pump wavelength. A local minimum is observed for the signal wavelengths which reside in the vicinity of pump wavelength where, $(\lambda_p - \lambda_s) \to 0$. In the gain spectrum, the PI-FOPA gain spectrum for single pump case is not uniform throughout the operating bandwidth and hence the gain is not flat but in the two-pump PI-FOPA, approximately flat gain spectrum can be obtained in the span of signal wavelength [38].

Analyzing the gain spectrum of PI-FOPA is the initial step to identify the gain characteristics of the PS-FOPA or the PSA which is the main scope of this thesis. It can be achieved as follows.

- The signal wavelengths at which the gain is maximum/minimum can be identified by analyzing the PI-FOPA gain spectrum. Then, PSA can be implemented in that particular signal wavelength at which the desired gain exist for the PSA to be operated. It is worthwhile to note that at any particular signal wavelength, the PI-FOPA gain value does not give the maximum obtainable PSA gain for that particular signal wavelength. The relationship between PI-FOPA gain at a certain signal wavelength and the corresponding maximum PSA gain will be introduced later on.

- For a fiber with known parameters such as ZDW, fiber length, dispersion etc., and considering the output power of the chosen pump, PI-FOPA gain spectrum shows the bandwidth of signal wavelengths over which the gain exists. Therefore, by utilizing the knowledge of span of signal wavelengths over which the gain exists, suitable values for signal and pump wavelengths can be obtained to achieve the required PSA gain.

- Once the PI-FOPA gain is fully characterized based on the parameters like gain bandwidth, maximum and minimum gain points, gain flatness, shape of the spectrum etc., the PI-FOPA gain spectrum can be altered to change these parameter values in order to obtain the desired PSA gain performance.

2.4.3.1 Operating Gain Regimes of PI-FOPA

Two operating gain regimes can be identified by analyzing the PI-FOPA gain spectrum which in turn decides the operating gain regimes of PSA based on the dispersion regimes introduced in section 2.3.3.2 which is briefly mentioned below.

- Normal dispersion regime where, $\lambda_p < \lambda_0$, thus $\Delta\beta > 0$

- Anomalous dispersion regime where, $\lambda_p > \lambda_0$, thus $\Delta\beta < 0$

where, λ_p, λ_0 and $\Delta\beta$ are pump wavelength, ZDW and propagation constant mismatch. As mentioned in section 2.3.3.2, by operating the PI-FOPA in the anomalous dispersion regime, it makes it possible to compensate the linear phase mismatch for the nonlinear phase mismatch and achieve the phase matching without the aid of fiber bireringence unlike in the case for normal dispersion regime [1]. When the PI-FOPA is operating in the anomalous dispersion regime, the two gain regimes of PI-FOPA are,

- Quadratic gain regime where, λ_s close to λ_p, $\Delta\beta \approx 0$,

$$G_s \approx (\gamma P_p L)^2 \tag{2.26}$$

- Exponential gain regime (maximum gain) where, $k = 0$ and $\gamma P_p L >> 1$,

$$G_s \approx \frac{1}{4} exp(2\gamma P_p L) \tag{2.27}$$

where, λ_s, γ, L, k and G_s are the signal wavelength, fiber nonlinearity coefficient, fiber length, net phase mismatch given by equation 2.22 and signal gain. In the gain spectrum given in figure 2.5, the two highest peaks in the symmetric gain lobes around zero signal detuning wavelength correspond to the exponential gain regime given in equation 2.27 where perfect phase matching is contained. In the exponential gain regime, equation 2.20 can be re-written as,

$$2\gamma P_p = -\Delta\beta \propto (\lambda_p - \lambda_0)(\lambda_p - \lambda_s)^2 \tag{2.28}$$

The local minimum at zero signal detuning frequency corresponds to the quadratic gain regime given in equation 2.26 where higher order terms containing parametric gain coefficient, g, in equation 2.24 can be neglected as $g \to 0$ when signal wavelengths are closer to the pump wavelength. In the quadratic gain regime, signal gain depends on the nonlinear phase mismatch.

2.4.3.2 Effect of Pump Power on Gain Spectrum

Characterization of the effect of pump power on PI-FOPA gain spectrum is carried out based on the equations from 2.23 to 2.25. In the figure 2.6, the signal gain increases with pump power but the gain increasing factor is different for different signal wavelengths. The gain spectra for different pump power values have been obtained by varying pump powers from $0.25W$ to $1.75W$ in the steps of $0.25W$. The gain spectra have been obtained for the same parameter values used in figure 2.6 except for the fiber length which is $500m$. From figure 2.6, following observations can be made.

- Separation between gain peaks increases with pump power.
- Bandwidth over which the gain exists increases with pump power.
- Flatness of the spectrum reduces with pump power.

Increase in the separation of the gain peak and bandwidth can be explained by equation 2.28. According to the equation, as the pump power increases, $\Delta\beta$ has to be increased as well so that for fixed pump and zero dispersion wavelengths, the value of $(\lambda_p - \lambda_s)$ will be increased which explains the reason for the shifting

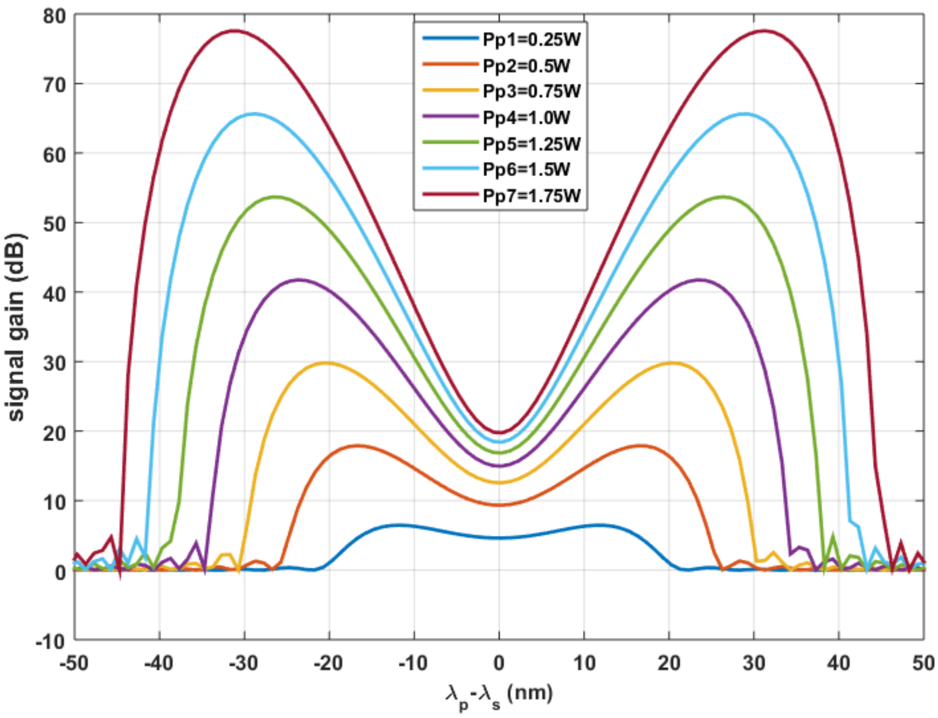

Figure 2.6: Effect of pump power on PI-FOPA gain spectrum for different signal wavelength (λ_s) detunings from pump wavelength (λ_p) for single pump FOPA.

of gain peaks farther apart from the pump wavelength. This leads to the increase in the gain bandwidth as well.

In conclusion, higher pump powers lead to high gains in PI-FOPA. It is to be noted that, the signal wavelength corresponding to the gain peaks change with pump power. The higher the pump power is, the greater the bandwidth over which the PI-FOPA gain exists.

2.4.3.3 Effect of Fiber Length on Gain Spectrum

According to the equations 2.23 and 2.24, fiber length i.e., HNLF length, is another parameter which determines the PI-FOPA gain. By varying the length of HNLF from 350m to 600m, the effect of fiber length on the PI-FOPA gain spectrum was characterized. In figure 2.7, it can be observed that the gain of the PI-FOPA increases with fiber length but the separation between gain peaks is not affected. Thus, the signal wavelength span over which the gain exists, i.e., the gain bandwidth, does not change. By referring to equation 2.28, it can be seen that the fiber length does not affect the gain bandwidth.

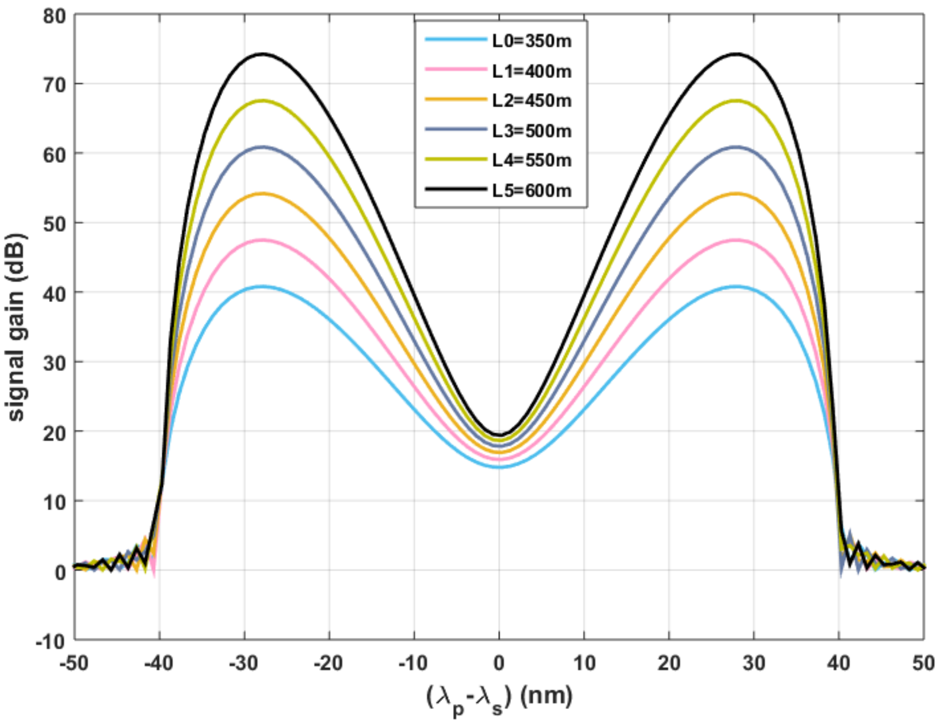

Figure 2.7: Effect of fiber length on PI-FOPA gain spectrum for different signal wavelength (λ_s) detunings from pump wavelength (λ_p) for single pump FOPA.

Effect of fiber length on gain bandwidth for fixed gain

Usually, the gain bandwidth of a PI-FOPA is known as the width of each gain lobe surrounding the pump wavelength. The width is taken at $3dB$ below the peak power. Generally, non-parametric amplifiers such as EDFAs operate with a bandwidth of around $35nm$ [4]. In contrast, FOPAs are capable of having bandwidths upto $300nm$ [1]. The bandwidth of FOPAs depend on the pump power, fiber nonlinearity and fiber dispersion properties.

In the figure 2.7, the PI-FOPA gain has been increased with fiber length but the gain bandwidth is not affected. But analysis can be carried out using a different approach in order to determine the effect of fiber length on gain bandwidth for a fixed gain value. It can be seen from equation 2.24 that the $\gamma P_p L$ is the determining factor of the PI-FOPA gain. The PI-FOPA gain can be kept constant by increasing or decreasing the fiber length but simultaneously, the value of γP_p should be decreased or increased. For example, for a fixed pump power and for a shorter fiber length, gain can be kept fixed by choosing a HNLF with higher nonlinear coefficient. For a fixed gain value, as the fiber length decreases, the value

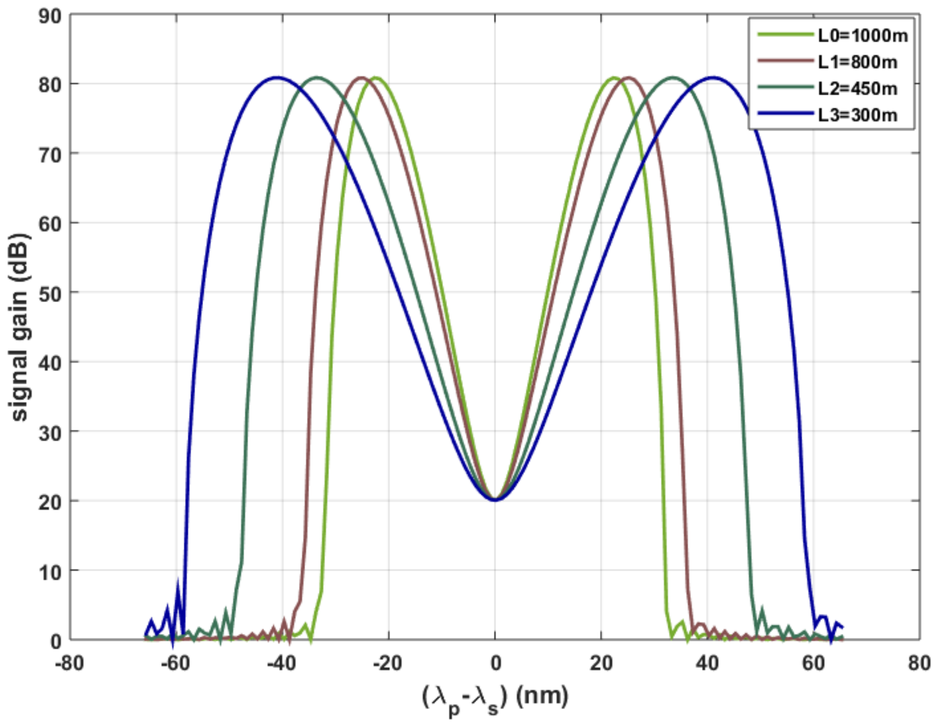

Figure 2.8: Effect of fiber length on PI-FOPA gain for a fixed gain value.

of γP_p is increased by choosing proper parameter values and thus the value of $\Delta\beta$ has to be increased according to the equations 2.24 and 2.25. For a fiber with pre-determined parameter values for ZDW (λ_0) and dispersion slope ($dD/d\lambda$), by considering equation 2.20, the $\Delta\beta$ is increased by increasing the signal bandwidth over which the gain exists, i.e, ($\lambda_p - \lambda_s$). Since the availability of higher pump powers is always a limiting factor in FOPA implementations, HNLFs with higher nonlinear indices can be used along with shorter fiber lengths to realize higher signal bandwidths without affecting the overall gain of the FOPA, i.e, for fixed FOPA gain. Figure 2.8 represents the expansion of signal bandwidth for decreasing fiber lengths from $1000m$ to $300m$ for a fixed gain value of $80.83dB$. Pump power has been varied from $0.83W$ to $1W$ which is within the practically achievable range using available high power pump sources while the nonlinear coefficient of the fiber has been varied from $10W^{-1}km^{-1}$ to $40W^{-1}km^{-1}$. The gain bandwidth has been improved more than twice as the initial bandwidth which was available for $1km$ long fiber for the fixed gain value. Therefore, in practical scenarios, shorter fiber lengths can be used along with fibers with higher nonlinear indices so that a satisfactory bandwidth can be achieved without affecting the overall maximum achievable PI-FOPA gain.

2.4.3.4 Effect of ZDW on Gain Spectrum

The positioning of pump wavelength with respect to the ZDW of the fiber is a determining factor that affects the PI-FOPA gain and bandwidth. It is important to analyze its effect in detail because although the ZDW of a fiber is a pre-determined fixed value and is inherent to the fiber during the manufacturing, ZDW tends to fluctuate along the fiber length due to external environmental factors [39].

In the figure 2.9, characterization has been carried out for the same parameter values that have been used previously. The ZDW detuning from pump wavelength has been varied as $1.7nm, 0.8nm, 0.4nm$ for $\lambda_0 < \lambda_p$ and $-0.4nm$ and $-1.6nm$ for $\lambda_0 > \lambda_p$. It can be seen that for negative detuning values of ZDW, the PI-FOPA gain has been reduced drastically and the shape of the gain spectrum is affected as well. This region of operation corresponds to a positive $\Delta\beta$ which represents the normal dispersion regime. Positive detuning values of ZDW represent the anomalous dispersion regime where $\Delta\beta$ is negative. When anomalous dispersion region is considered, the gain bandwidth has increased for the ZDW values which are closer to pump wavelength. But the maximum gain of PI-FOPA is not affected. When normal dispersion regime is considered, the maximum achievable gain has been dropped is constricted around the quadratic gain regime of the PI-FOPA. Moreover, the overall gain bandwidth has been affected and for higher negative detuning values, the gain bandwidth is lower. The difference in the PI-FOPA gain spectrum in the anomalous and normal dispersion regimes can be understood by referring to the $+0.4nm$ and $-0.4nm$ ZDW detunings respectively. In conclusion, for a better PI-FOPA performance, it has to be operated in the anomalous dispersion regime and close monitoring has to be done to ensure that the ZDW fluctuations and the choosing of pump wavelength have to be in such a way that PI-FOPA is operating in the anomalous dispersion regime.

2.5 Phase Sensitive Amplifier (PSA)

Phase sensitive amplification is realized by the parametric FWM process that has been discussed in section 2.3.3 but with a pre-generated idler present at the input of the HNLF. The popularity of PSAs in fiber optic communication systems has increased in recent years because of the superior noise performance exhibited by them. State-of-the-art implementations suggest that the PSAs are capable of achieving noise figures as low as $0dB$ which is well beyond the quantum limited

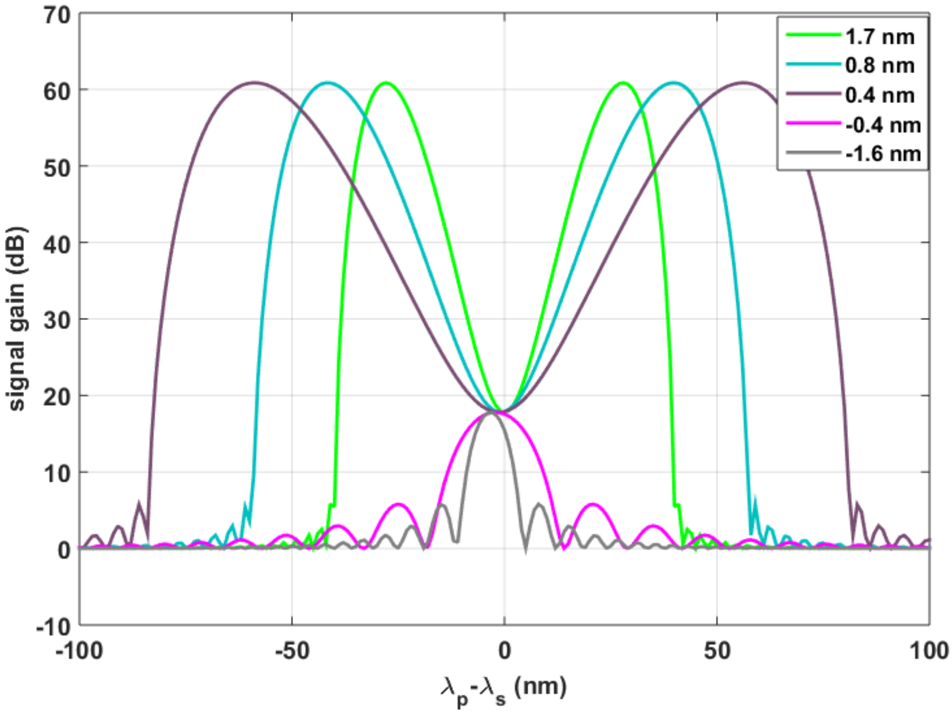

Figure 2.9: Effect of ZDW wavelength fluctuations for PI-FOPA gain spectrum

noise figure of $3dB$ [19]. Michael E. Marhic demonstrated the phase sensitive amplification in fiber optic communication systems using a Sagnac interferometer in 1991 for the first time [40]. Afterwards, with the development of the technology, a reported noise figure of $1.8dB$ with a $16dB$ gain was achieved in 1999 and several new discoveries in the history of PSAs have been invented in the past decade [14]. PSAs exist in interferometric as well as in non-interferometric configurations. Interferometric PSAs have been implemented using nonlinear optical loop mirrors (NOLMs) while non-interferometric PSAs are based on the parametric FWM process which is the basis of this thesis [14], [17].

In the present day's scenario, optical fiber communication systems use advanced modulation formats, essentially M-PSK, to transmit data because of their high resilience to noise [17]. In order to increase the spectral efficiency, the carrier is suppressed during the transmission. So, at the receiver end (in this context, the receiver is an optical amplifier), the carrier has to be recovered by a suitable carrier recovery scheme [41]. Along with carrier recovery, phase synchronization is essential to ensure that the carrier information is successfully recovered at the receiver. To do so, after recovering the carrier,the signal, pump and idler are phase synchronized using an optical injection locking scheme [42] or an optical phase locked loop [43]. This thesis assumes that these prior stages of optical carrier recovery as well as phase synchronization has been performed beforehand to utilize the pump, signal and idler waves for phase sensitive amplification.

Phase regeneration capability of PSA

When phase modulated signals are transmitted through a communication system, regenerative repeaters have to be placed in the mid-link in order to regenerate the distorted signals back to their original forms. In optical communication systems, regeneration is of two-folds as amplitude regeneration and phase regeneration. The significant difference between the amplifiers and regenerators is such that, the amplifiers only increase the power level of the signal while regenerators perform re-shaping and re-timing of the signals along with re-amplification [9]. Optical amplifiers are also able to perform one or a few regenerative functions. For example, EDFA is capable of amplitude regeneration when operated in the gain satuarated mode. PSA is an amplifier which is capable of phase regeneration due to its inherent phase squeezing capability associated with it [19], [14]. Therefore, PSAs are capable of exhibiting superior noise performances which surpasses the sub-quantum noise figure limit of $3dB$ [19].

The electric field of an optical signal has a stochastic indeterminacy inherent with it. This is termed as the quantum noise which is the error of the description of any physical system within the classical theory. The concept of squeezing can be utilized to minimize the quantum noise associated with a system either by amplitude squeezing or phase squeezing [44]. They do not commute with each other and therefore, we can reduce noise in either phase or amplitude in one instance with the expense of increase in the other. Figure 2.10 illustrates phase space representation of a coherent state with same amount of noise present in the in-phase and quadrature phase components of a signal. For a coherent state, the variances of quadrature operators are equal. By the aid of PSA, this coherent state with equal uncertainties in both quadratures is transformed to a coherent squeezed state with reduced variance in phase with an increased variance in the amplitude. Hence, PSAs are capable of phase regeneration and amplitude regeneration as well when operated in gain saturation [17].

2.5.1 Phase Sensitive Gain

Phase sensitive amplification is capable of amplifying signals along with the reduction of phase noise associated with it. It requires a pre-generated idler wave

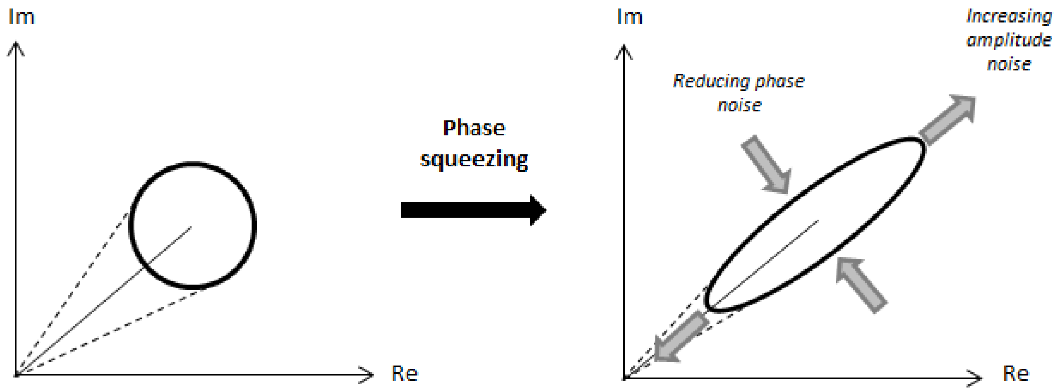

Figure 2.10: Conversion of coherent state of light with equal variances in both quadratures into coherent state with unequal variances in both quadratures (squeezed light) by phase sensitive amplification.

to be present at the input of the PSA along with the pump and the signal to be amplified.

Input-output transfer matrix

Mathematical interpretation of phase sensitive amplification can be presented with the transfer matrix associated with the input and output fields which is also known as the squeezing transformation [19]. The transformation can be one or two mode based on the signal and idler degeneracy. But first, two mode squeezing transformation is taken into account as the general case.

$$\begin{pmatrix} A_{s,out} \\ A^*{}_{i,out} \end{pmatrix} = \begin{pmatrix} \mu & v \\ v^* & \mu^* \end{pmatrix} \begin{pmatrix} A_{s,in} \\ A^*{}_{i,in} \end{pmatrix} \tag{2.29}$$

where, $A_{s,in}$ and $A_{i,in}$ are input signal and idler complex amplitudes while $A_{s,out}$ and $A_{i,out}$ are output signal and idler complex amplitudes. Equation 2.29 represents the transfer matrix with complex coefficients μ and v. The complex conjugate of the respective amplitude fields is represented by the '*' [15]. Therefore, output amplitudes can be expressed as,

$$A_{s,out} = \mu A_{s,in} + vA^*{}_{i,in} \tag{2.30a}$$

$$A_{i,out} = vA^*{}_{s,in} + \mu A_{i,in} \tag{2.30b}$$

Equations 2.30 mathematically represent the phase sensitive interaction of the signal and idler fields with the idler being present at the input because, the output fields can be viewed as the linear superposition of scaled original input signals and the conjugates which can be constructive or destructive based on the relative phase between μ, v and $A_{s,i}$ [19]. It is to be noted that, in the case of phase insensitive amplification discussed in section 2.4.2, when idler is not present at the fiber input, i.e., $A_{i,in} = 0$, the output signal field can be written as, $A_{s,out} = \mu A_{s,in}$. In equation 2.30, the coefficients μ and v can be expressed as,

$$\mu = cosh(gL) + \frac{ik}{2g} sinh(gL) \tag{2.31}$$

$$v = \frac{i\gamma P_p}{g} sinh(gL) \tag{2.32}$$

where, g is the parametric gain coefficient, k is the net phase mismatch, L is the length of the fiber, P_p is the pump power and γ is the nonlinear coefficient. The complex coefficients given by equations 2.31 and 2.32 depend on the pump power, phase matching conditions, nonlinear interaction strength and the states of polarization of the signals.

Phase sensitive gain

By using equations 2.30, phase sensitive gain can be written as,

$$G_{PSA} = \frac{\mid \mu A_s + v A_i{}^* \mid^2}{\mid A_s \mid^2} \tag{2.33}$$

Equation 2.33 can be re-written for equal input signal and idler powers as,

$$G_{PSA} = \mid \mu \mid^2 + \mid v \mid^2 + 2\mid \mu \mid\mid v \mid \cos(\theta_{rel}) \tag{2.34}$$

where, $\theta_{rel} = \theta_\mu - \theta_v + \theta_s + \theta_i$. From equation 2.34, by substituting the expressions for complex coefficients given in equations 2.31 and 2.32, the signal gain can be further simplified as [45],

$$\begin{aligned} G_s = 1 + 2\left(\frac{\gamma P_p}{g}\right)^2 sinh^2(gL) + 2\frac{(\gamma P_p)}{g} sinh(gL)\Bigg[\frac{k}{2g} sinh(gL) cos(2\theta_{s,in}) \\ + cosh(gL) sin(2\theta_{s,in})\Bigg] \end{aligned} \tag{2.35}$$

The ideal phase sensitive conditions have been assumed in the equation 2.35, i.e., $P_{s,in} = P_{i,in}$ and $\theta_{s,in} = \theta_{i,in}$.

2.5.1.1 Operating Gain Regimes of PSA

Similar to the PI-FOPA, operating gain regimes of PSA can be obtained based on the phase matching conditions given in section 2.3.3.2.

PSA gain in exponential gain regime

In case of perfect phase matching in the exponential gain regime, the net phase mismatch parameter, k, is zero. Therefore, according to equation 2.25, the parametric gain coefficient, g, equals to the product, γP_p. Since $k = 0$, the coefficients μ and v given by equations 2.30 can be expressed as, $\mu = cosh(gL)$ and $v = isinh(gL)$. Therefore, PSA gain in the exponential gain regime can be expressed as,

$$G_s = 1 + 2sinh^2(gL) + sinh(2gL)sin(2\theta_{s,in}) \tag{2.36}$$

When hyperbolic sine term in equation 2.36 is written in the exponential form as, $sinh(gL) = \{\exp(gL) - \exp(-gL)\}/2$, the maximum and minimum phase sensitive gains obtainable in the exponential gain regime can be written as,

$$G_{max,min} = \exp(\pm 2gL) \tag{2.37}$$

By considering equations 2.27 and 2.37, it can be seen that, in the exponential gain regime, maximum PSA gain is greater than the maximum PI-FOPA gain by $6dB$ when decibel scale values are considered.

PSA gain in quadratic gain regime

In quadratic gain regime, the net phase mismatch, k, is equal to the nonlinear phase shift which is, $2\gamma P_p$ and the gain coefficient, g, is zero. Hence, by considering equation 2.35, the PSA gain in quadratic gain regime can be re-written as,

$$G_s = 1 + 2(\gamma P_p L)^2 \left\{ 1 + \sqrt{1 + (\gamma P_p L)^2} sin\left[2\theta_{s,in} + arctan(\gamma P_p L)\right] \right\} \tag{2.38}$$

where, $\theta_{s,in}$ is the input signal phase in equations 2.37 and 2.38.

2.5.2 Characterization

In order to identify the dependence of PSA gain on different parameters, the characterization of PSA gain with respect to relative input signal phase has been

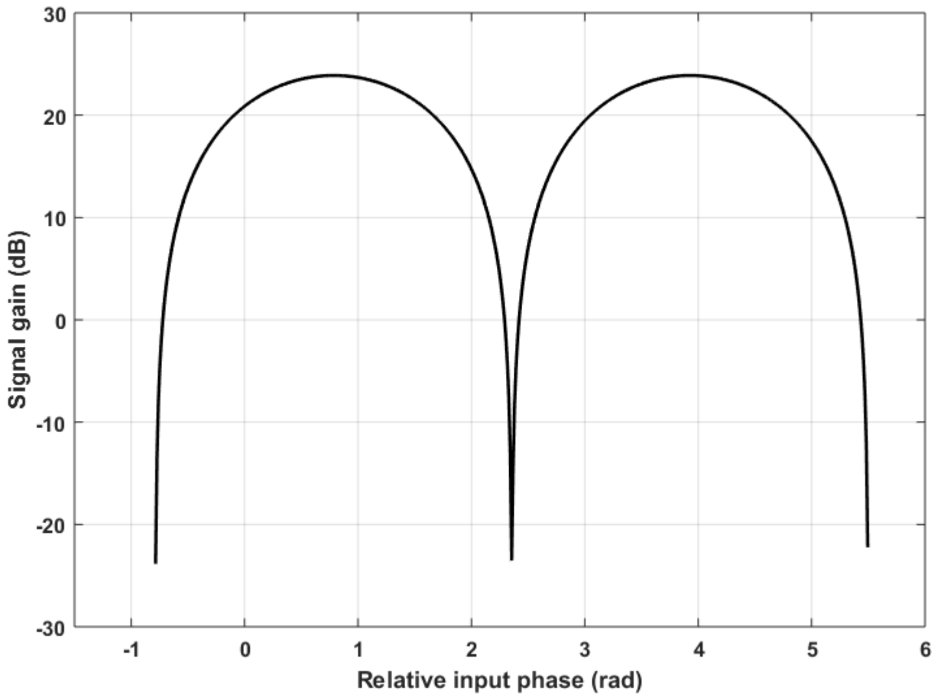

Figure 2.11: Phase sensitive amplifier gain with relative signal input phase

carried out. The PSA gain plot can be derived from the PO-FOPA gain spectrum. For example, for PSA to operate in the exponential gain regime, the signal wavelength is chosen such that it belongs to the maximum gain point in the PI-FOPA gain spectrum.

Figure 2.11 is the illustration of the input relative phase dependence of the PSA gain. It can be seen that for certain relative input phase angles, the gain is maximum while for certain others, the gain is minimum. The ratio between maximum and minimum possible gains that can be achieved in a PSA is known as the *phase sensitive swing* which is also the difference between maximum and minimum gains in decibel scale. It is a fact that the amplifier performance is improved for higher phase sensitive swings because the suppression of out-of-phase components is high for higher phase sensitive swings [14]. The characterization has been carried out by considering a $250m$ long HNLF with a nonlinear coefficient of $11W^{-1}km^{-1}$ as the gain medium. The ZDW of thw HNLF is $1559nm$ and the pump is at $1560.7nm$ with an output power of $1W$. Since the pump wavelength is greater than ZDW, the PSA is operating in the anomalous dispersion regime. The maximum phase sensitive gain that has been obtained for these parameters is $23.89dB$. The signal attains a maximum gain when the relative input phase is

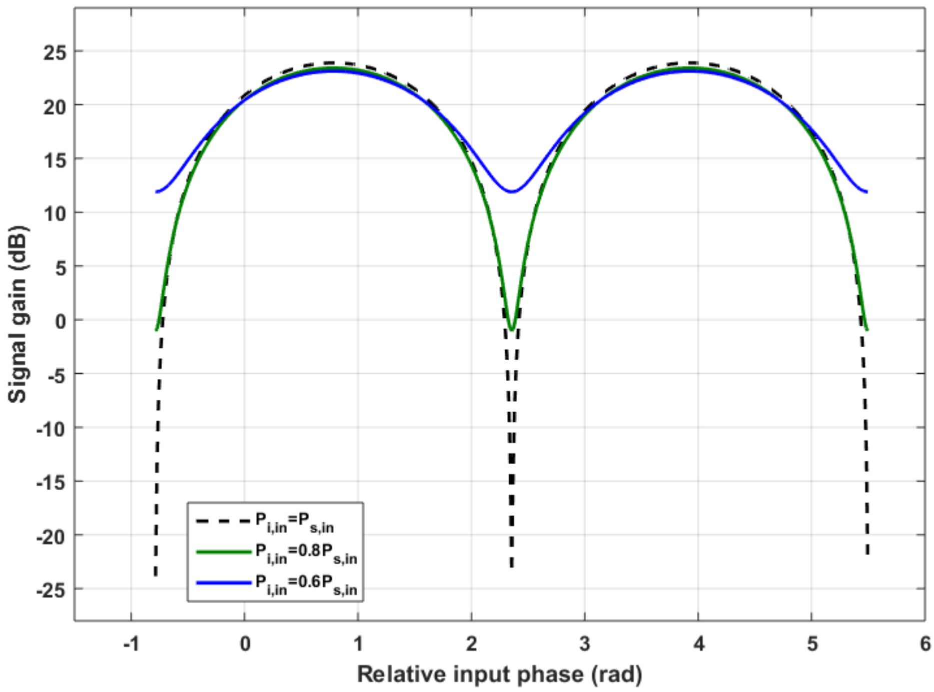

Figure 2.12: Variations in phase sensitive swing with same input signal, idler powers (ideal case) and with different input signal and idler powers (non-ideal case)

an odd multiples of $\frac{\pi}{4}$ radians and minimum gain is achieved for even multiples of $\frac{\pi}{4}$ radians. This is in the large gain limit of the exponential gain region where, $gL >> 1$. It can also be observed that a strict phase stabilization is required to achieve the minimum gain because of the very narrow and sharp dips that represent the maximum attenuation points. Also, since maximum absolute gain is equal to the minimum absolute gain, the phase sensitive swing that can be obtained in this PSA design is twice the maxim gain i.e., $47.77dB$. In non-ideal phase sensitive amplifier conditions, the phase sensitive swing is affected by the input signal and idler power values.

In figure 2.12, the input signal and idler power dependence of phase sensitive swing of the PSA is illustrated. It can be seen that, a full phase sensitive swing can be obtained when input signal and idler powers are same. It can also be seen that the variation of input signal and idler powers has not affected the maximum phase sensitive amplifier gain but it affects the ability of out-of-phase noise suppression of the PSA. For example when input idler power is approximately half of the input signal power, the in-phase signal components experience a maximum gain of around $24dB$ but the quadrature phase noise components are not attenuated by the same amount. Therefore, superior noise performance of the PSA cannot to achieved.

2.5.2.1 Effect of Pump Power, Fiber Length and Fiber Nonlinearity on PSA Gain

According to the equation 2.35, PSA gain increases with the input pump power, fiber nonlinearity as well as fiber length. Therefore, PSA gain is a function of $\gamma P_p L$ product. As special cases, it is worthwhile to analyze the effect of $\gamma P_p L$ product for both exponential and quadratic gain regimes of PSA.

Effect of $\gamma P_p L$ on the exponential gain regime of PSA

According to equation 2.36 where gain coefficient, g, can be expressed in terms of pump power and fiber nonlinearity as in equation 2.25, phase sensitive gain with respect to input relative phase is a function of $\gamma P_p L$ product. Figure 2.13 shows the phase sensitive gain of the signal for $\gamma P_p L$ values of $0.5, 2.042$ and 2.75. It can be observed that for higher values, the PSA gain is high and the shape of the gain curve has not been affected for different $\gamma P_p L$ values. It should be noted that the characterization has been carried out for the exponential gain regime where perfect phase matching is realized. In the exponential gain regime, along with the PSA gain increase, the sharpness of the dips corresponding to maximum attenuation has been increased as well. This suggests that, more phase stabilization of gain can be obtained when PSA is operating for higher $\gamma P_p L$ values in exponential gain regime.

Effect of $\gamma P_p L$ on the quadratic gain regime of PSA

The characterization has been carried out for the signal gain with $\gamma P_p L$ when PSA is operating in the quadratic gain regime where, $\Delta\beta = 0$. In the figure 2.14, the PSA gain for $\gamma P_p L$ values of $0.5, 2.042, 2.75$ has been obtained for quadratic gain regime. It can be seen that, unlike in the case of exponential regime, the quadratic gain regime exhibits a phase instability of gain for different values of $\gamma P_p L$. For example, the relative phase value for different $\gamma P_p L$ values. This can affect the stability of phase regeneration performed by PSA when it is operating near the quadratic gain regime.

2.5.2.2 Phase stabilization of PSA gain in the Quadratic Gain Regime

For the first time to the best of our knowledge, an analysis has been carried out to identify the strategies by which the phase stabilization of PSA gain can be

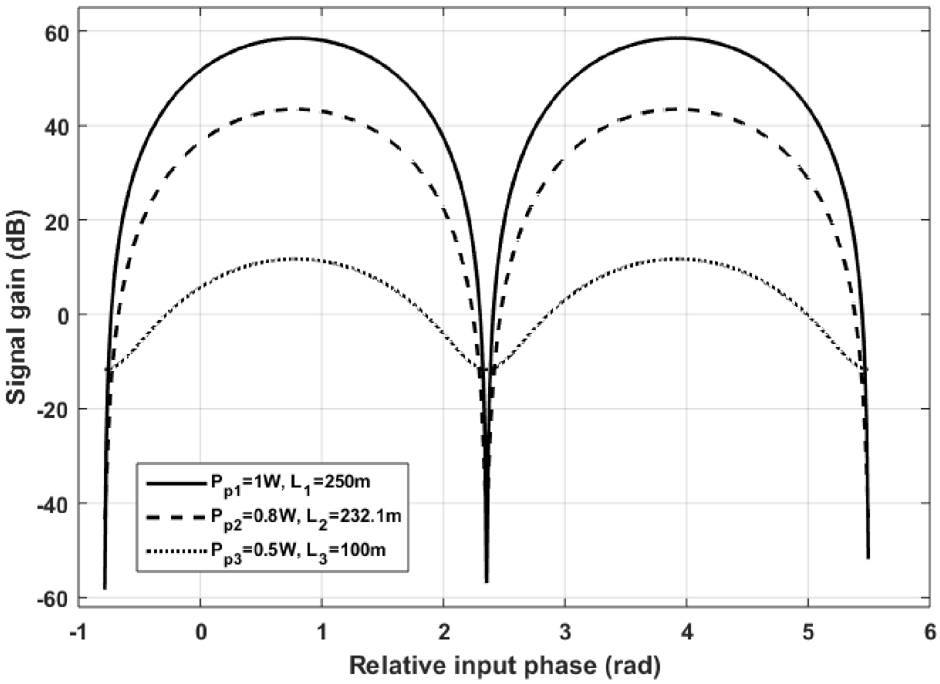

Figure 2.13: Phase sensitive gain for different $\gamma P_p L$ values in exponential gain regime.

reinstated in the quadratic gain regime. The analysis has been carried out for a pump and signal waves with wavelengths $1560.7nm$ and $1584nm$ respectively. In this case, L-band wavelengths have been considered, because parametric amplifiers in general can be identified as broadband amplifiers which can be operated away from the conventional C-band [46]. Two polarization maintaining HNLFs (PM-HNLFs) which serve as the PIA and the PSA stages have been used as the gain media. The idler wave created along in the first PM-HNLF along with the signal and pump waves was fed into the second PM-HNLF which has a dispersion slope of $0.03ps/nm^2km$, a nonlinear coefficient of $11W^{-1}km^{-1}$ and a ZDW of $1559nm$. Initially, the gain performance at exponential gain regime was analyzed and then, signal wavelength was set to $1560.7nm$ to analyze the gain performance at quadratic gain regime. Initially, PSA gain was obtained for three different pump powers of $0.8W, 3W$ and $5W$ while fiber length is kept at $100m$.

Figure 2.15 is a magnified overlook on the maximum attenuation points corresponding to the PSA gain curves for pump powers of $0.8W, 3W$ and $5W$ for a fiber length of $100m$. There are three main observations that can be made.

- The higher the pump powers are, the narrower the tips corresponding to maximum attenuation become.

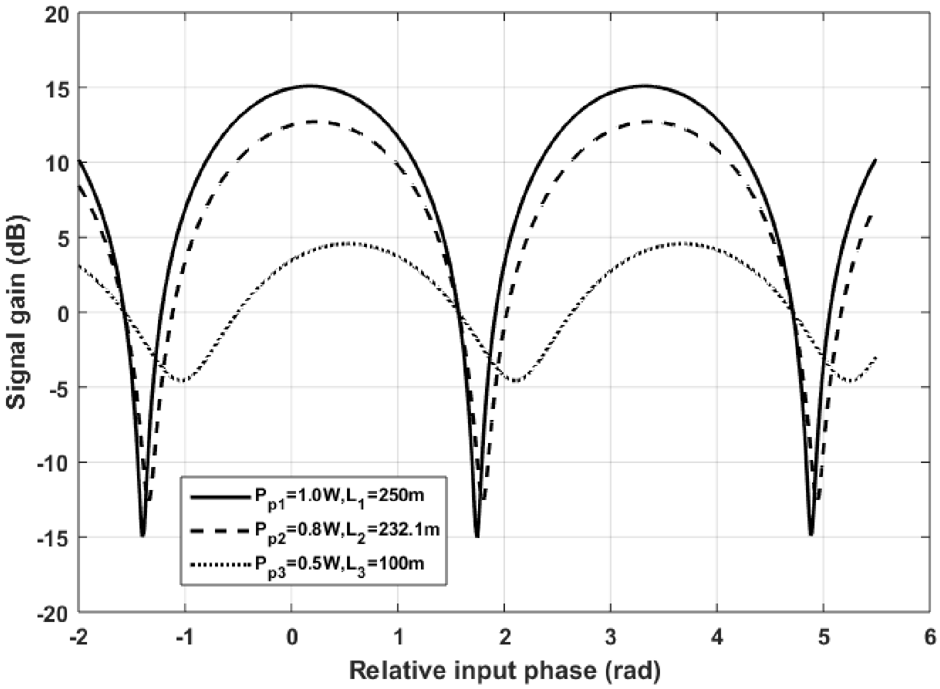

Figure 2.14: Phase sensitive gain for different $\gamma P_p L$ values in quadratic gain regime.

- The value of maximum attenuation is maximum for the highest pump power value as maximum attenuation is a function of parametric gain i.e., for exponential gain regime, maximum attenuation is given by $exp(-2gL)$ where g is a function of pump power.
- The shift in the input relative phase, θ_{rel} for different pump powers. The shift is significant for lower pump powers.

Therefore, it can be concluded that, the gain performance of PSA in the quadratic gain regime is not strictly phase stabilized. This can be an issue when in a WDM environment where multiple wavelengths are phase regenerated in a PSA and one or more wavelengths lie in the vicinity of pump wavelength.

In this work, we have identified that by carefully selecting the values for pump power and fiber length, phase stabilized gain can be achieved with a negligible shift in the relative input phase [47]. Initially, the variation of shift in the relative input phase is observed with the increasing of pump powers for a fiber length of $500m$.

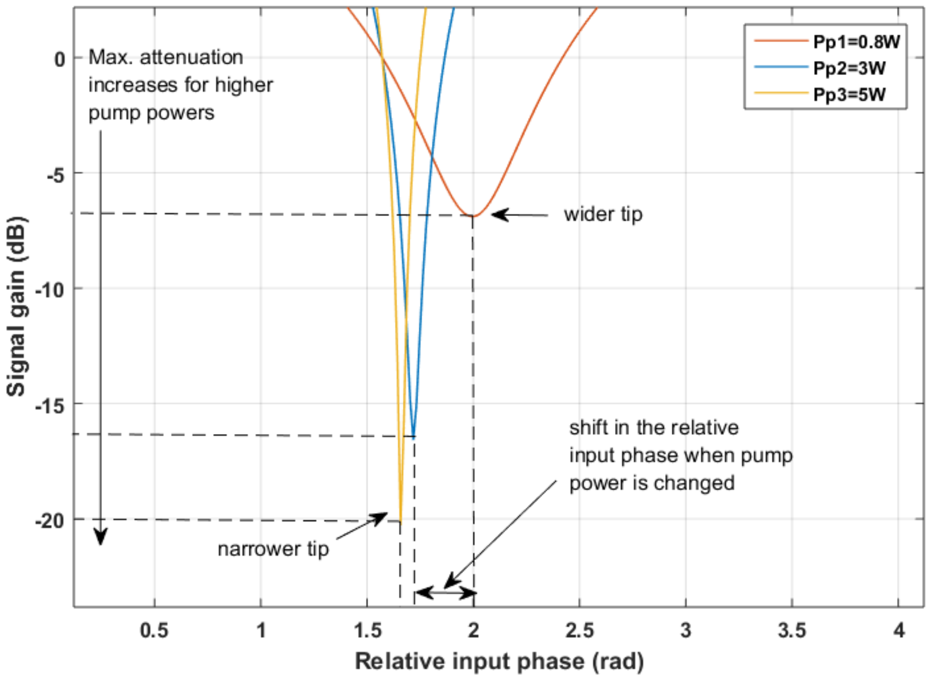

Figure 2.15: Variations of the sharpness of the tip, value of maximum attenuation, shift in the relative input phase for different pump powers.

According to figure 2.16, the pump power has been increased from $0.5W$ to $15W$ in 0.5 intervals and the relative input phase (θ_{rel}) corresponding to maximum attenuation points in the gain curve has been illustrated against the maximum obtainable PSA gain for that particular pump power. As can be seen, higher pump powers have led to lower shifts in θ_{rel}. Therefore, it is evident that, phase stabilization of gain can be achieved when higher pump power values are utilized in the quadratic gain regime.

Figures 2.17 and 2.18 represent the effect of fiber length on phase stabilization of gain for different values of pump power. In figure 2.17, fiber length has been increased to $500m$ while in figure 2.18 fiber length is at $5km$. As can be seen, more phase stabilization of gain can be achieved for higher fiber lengths.

Figure 2.19 represent the amount of shift in input relative phase for different pump powers and fiber lengths. As can be seen, the fiber length of 50m experiences a shift in θ_{rel} of around 0.1 radians ($\approx 6^0$) for lowest pump powers and reduces upto 0.007 radians for pump powers which are higher than $7W$. The shift is 0 radians or almost 0 radians for all the pump powers when fiber length is at $5000m$. Hence, phase stabilization of gain in the quadratic gain regime is achieved

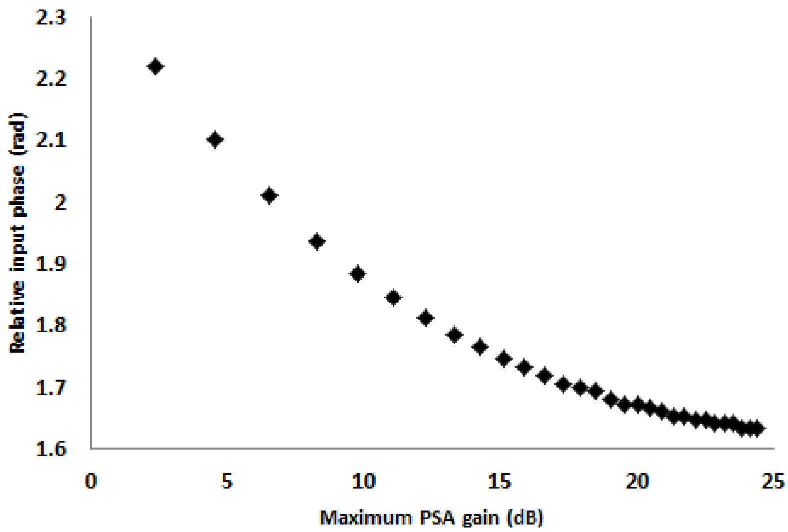

Figure 2.16: Variation of relative input phase with signal gain for different pump powers when fiber length is at $50m$

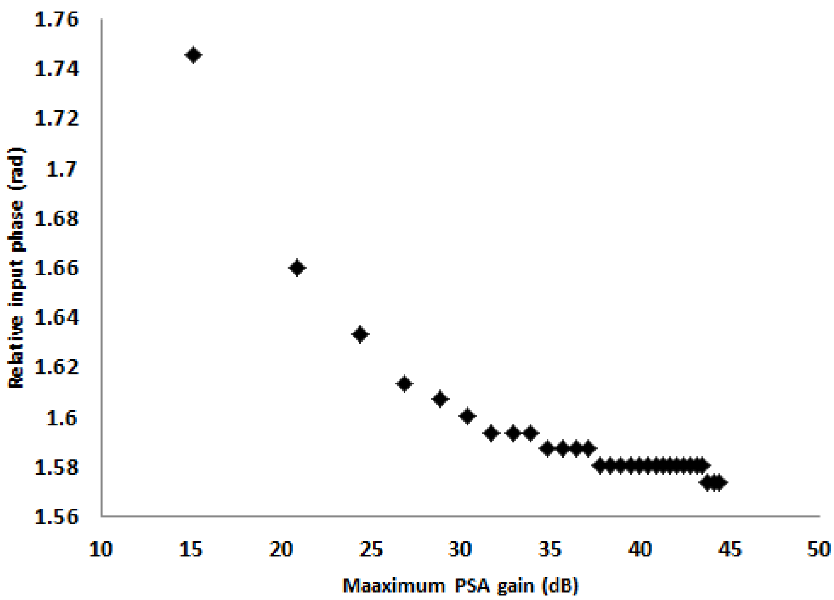

Figure 2.17: Variation of relative input phase with signal gain for different pump powers when fiber length is at $500m$

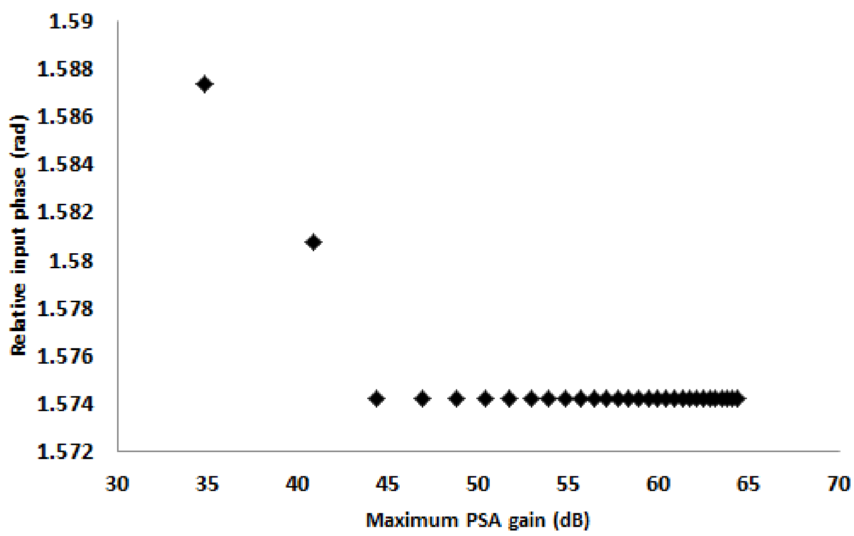

Figure 2.18: Variation of relative input phase with signal gain for different pump powers when fiber length is at 5000m

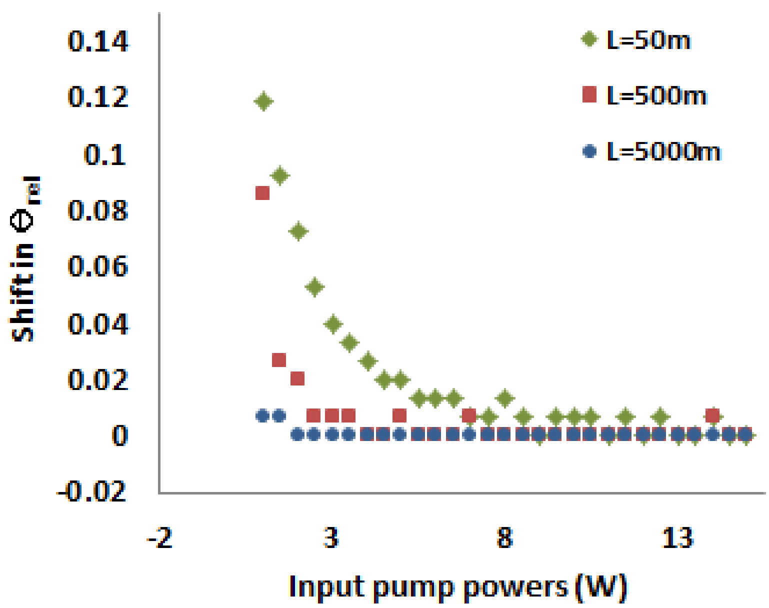

Figure 2.19: Variation of shift in θ_{rel} with input pump powers for different fiber lengths

for higher pump power and fiber length products. But there are a few concerns when choosing higher pump power values and fiber lengths. Higher pump powers trigger the SBS [36] and therefore, successful SBS suppression techniques have to be utilized [48]. Longer fiber lengths cause for the irregularities in fiber core to be significant and result in ZDW fluctuations. Also it is important to implement the PSA in a manner where polarization rotations are well taken care of.

2.6 Conclusion

Fiber optic parametric amplification gives an uneven gain spectrum in which, different gain regimes can be defined based on the phase matching conditions such as perfectly phase matched and nearly phase matched depending on the interplay between the wave vector mismatch based phase shift and fiber nonlinearity based phase shift attained by the propagating waves. The gain spectrum of FOPA can vary depending on different operating parameters such as pump power, fiber length, ZDW ect. Some parameters will only alter the gain value while other parameters will affect both gain and gain bandwidth of FOPA. When developing a baseline for PSA, the operating gain regimes of the FOPA should be considered. If the PSA is operating in the exponential gain regime where phase is perfectly matched, the PSA gives a maximum gain with phase stabilized output. On the other hand, when PSA is operating in the quadratic gain regime, the maximum attainable gain is lower and the gain is not phase stabilized. Phase stabilization of gain is affected by the pump power, fiber length and nonlinear coefficient of the fiber. In a fiber where nonlinear coefficient is fixed, higher pump powers and/or fiber lengths can be used to stabilize the phase in quadratic gain regime. In addition, the overall PSA gain will be subjected to increase.

Chapter 3

POLARIZATION DIVERSITY LOOP

3.1 Introduction

The context of polarization independent frequency conversion has been studied extensively in the past two decades. The polarization diversity loop has been identified as a successful technique which is capable of providing polarization insensitivity to the transmission systems using frequency modulated, phase modulated and polarization modulated signals. Hence, a thorough literature survey has been carried out to address the deployment of polarization diversity loop and to identify the issues concerned with this technique. Possible approaches to eliminate these issues and their feasibility if implemented in the diversity loop has been assessed by this literature survey.

3.2 Polarization Independent FOPA Schemes

Polarization independence in FOPA and PSA is analyzed extensively for single pump or dual pump FOPAs as well as PSAs and the approach is to split the signal SOP into its x and y orthogonal polarization states and amplified in a HNLF separately. The wave propagation happens in a fiber loop in bi-directional manner as orthogonal SOPs travel at opposite directions in the fiber [16]. This principle is same for both single pump as well as dual pump FOPAs and PSAs but the utilization of pump(s) for the amplification is different in single and dual pump schemes. It divides the existing polarization schemes for FOPAs and PSAs into two categories as vector scheme and polarization diversity scheme.

3.2.1 Vector Scheme for Dual-Pump FOPA

Vector polarization insensitive scheme is used for dual pump FOPA and PSA schemes where two pumps of same wavelength are in opposite orthogonal polarization states i.e., if $pump_1$ is x-polarized, $pump_2$ is y-polarized [49]. The random SOP of the signal is also split into two orthogonal polarization states. This way signal is exposed to same pump power despite of its SOP. The splitting into

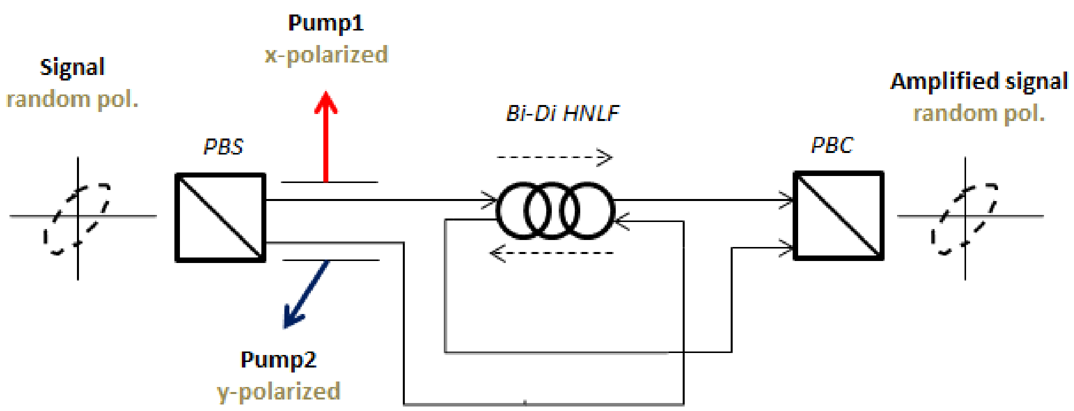

Figure 3.1: Vector polarization insensitive loop for dual-pump FOPA with two orthogonally polarized pumps of same wavelength.

orthogonal polarizations is done by polarization beam splitter (PBS) and the combination of split SOPs is done at the end of the gain medium with a polarization beam combiner (PBC). An advantage of this method is that it exhibits a flatter gain spectrum compared to single pump case but the effect of SBS is significant. Figure 3.1 illustrates the overview of the implementation of vector polarization insensitive scheme for dual-pump FOPA.

3.2.2 Polarization Diversity Loop Scheme for Single-Pump FOPA

In single pump FOPA, the polarization insensitivity is achieved using polarization diversity loop where the pump polarization state is equally split into two orthogonal x and y components [24]. The gain medium is a bidirectional HNLF where signal is getting amplified regardless of its input SOP. Figure 3.2 represents the schematic of polarization diversity loop. At the input, signal and pump are split into orthogonal polarization states using a polarization beam splitter and the orthogonal polarization states are re-combined at the output by a polarization beam combiner. In this thesis, the polarization diversity loop is being utilized since single pump FOPA is considered.

3.3 State of the Art Implementation of Diversity Loop Scheme

The first demonstration of the diversity loop for polarization independent FWM has been carried out by T.Hasegawa in 1993 [22]. Frequency conversion over a $1THz$ range has been carried out for a frequency modulated signal with a modulation speed of $622Mbps$ and a frequency deviation of 2 GHz. The feasibility of the polarization diversity technique has been assessed by the BER performance

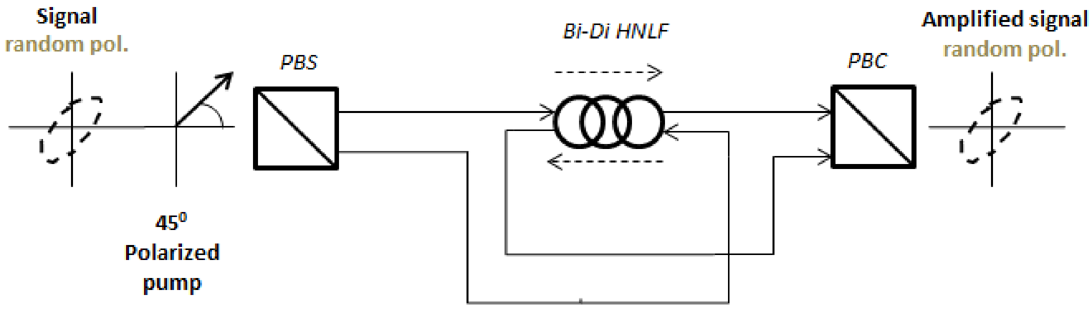

Figure 3.2: Polarization diversity loop for single-pump FOPA

at the receiver and by considering the gain deviation for different SOPs. The fiber used in the loop is a $10km$ long dispersion shifted fiber (DSF) with polarization controllers (PCs) attached to it. The reason behind this is to maintain the SOPs unchanged within the loop. But PCs must be adjusted continuously because SOPs of the waves travelling in the loop may change with time. They have suggested that instead of using PCs, it is possible to use polarization maintaining fibers which perform the same task although polarization maintaining fibers exhibit some disadvantages like comparatively high losses and high cost. A pump wave at $1550.70nm$ with a power of $11.32dBm$ and a FSK signal wave at $1555.93nm$ with a power of $8.5dBm$ have been participated in the FWM process within the DSF. The pump wavelength has been chosen such that it is slightly outward from the ZDW of the fiber for maximum conversion efficiency in the FWM process. In the loop, the reciprocity is conserved because the pump powers in clockwise and counter-clockwise directions are same. The polarization insensitivity of this technique is proved by the fact that the deviation of gain achieved by FWM process for different signal SOPs was around $0.2dB$ which is comparatively small as of when diversity loop is not employed. Additionally, the performance of this technique in frequency conversion for two pump linewidths has been assessed by considering BER curves. It could be seen that the SOP variation has not affected the frequency conversion by FWM when this diversity loop is used. But there is a deviation of BER performance for higher pump linewidth of $8.5MHz$. According to the authors, this is probably because of the spectrum broadening of the converted signal for such a higher pump linewidth. Spectrum broadening can occur as a result of effects like SPM, XPM and SBS. SBS induced spectrum broadening can be mitigated by using phase modulation of pump but this causes the broadening of pump spectrum which in turn broaden the signal and idler spectra. To avoid this, methods like phase conjugated pump dithering can be used [50]. Another important factor to be noted is that if the same SOP is maintained throughout the fiber, spectral broadening is not affected by the SOP, but if the SOP along the fiber varies randomly, spectral broadening becomes polarization dependent. The authors have also emphasized the importance of controlling the SOPs precisely within the loop or otherwise it may violate the very purpose of utilizing the diversity loop in frequency conversion using FWM. They also have pointed out that although this method brings out satisfactory results, the disadvantage of this approach is that the conversion efficiency by FWM process tends to be reduced by 6 dB compared to the non-looped configuration.

The first demonstration of the incorporation of diversity loop technique in a single pump FOPA has been done by authors in [24]. A visual analysis of this implementation has been represented in figure 2.1. They have implemented a phase insensitive FOPA or a PIA and modified it for polarization insensitivity. The diversity loop has been implemented by using a $1km$ long dispersion shifted HNLF (HNL-DSF) with PCs attached to it. Here, dispersion shifted HNLF has been used instead of dispersion flattened HNLF to acquire low dispersion slope and low loss based on the requirement of the experimental setup. The nonlinear coefficient (γ) of the fiber is around 17 $W^{-1}km^{-1}$ with a dispersion slope of $0.03ps/nm^2km$. A pump wave at $1564.6nm$ which is slightly above the ZDW wavelength of the HNL-DSF which is $1562.5nm$ has been used with a input power level of $25dBm$. The pump wave has been phase modulated to suppress the effect of SBS. The signal which is modulated at 10 Gbps with a pseudo random bit sequence (PRBS) is at $1571.54nm$ and the the polarization independence of the setup has been assessed for two more signal wavelengths at $1569.13nm$ and $1567.5nm$. The signal gain at different wavelength is different from each other due to the uneven gain spectrum of the PIA but when polarization diversity was deployed, significant polarization insensitivity could be seen regardless of the signal wavelength. When the polarization angle of the signal is varied from 0 to 90^0, for all these three signal wavelengths, there was only $0.41dB$ deviation in gain for all the SOPs. Authors have made a valuable comparison based on the fact that diversity loop is deployed or not in the PIA for these three wavelengths. A drastic gain deviation of around $10dB$ could be observed when in the case where diversity loop is not implemented. The BER of the amplified signal was quantified to assess the power penalty. They have demonstrated that there is a power penalty of around $0.9dB$ between the BER curves when diversity loop

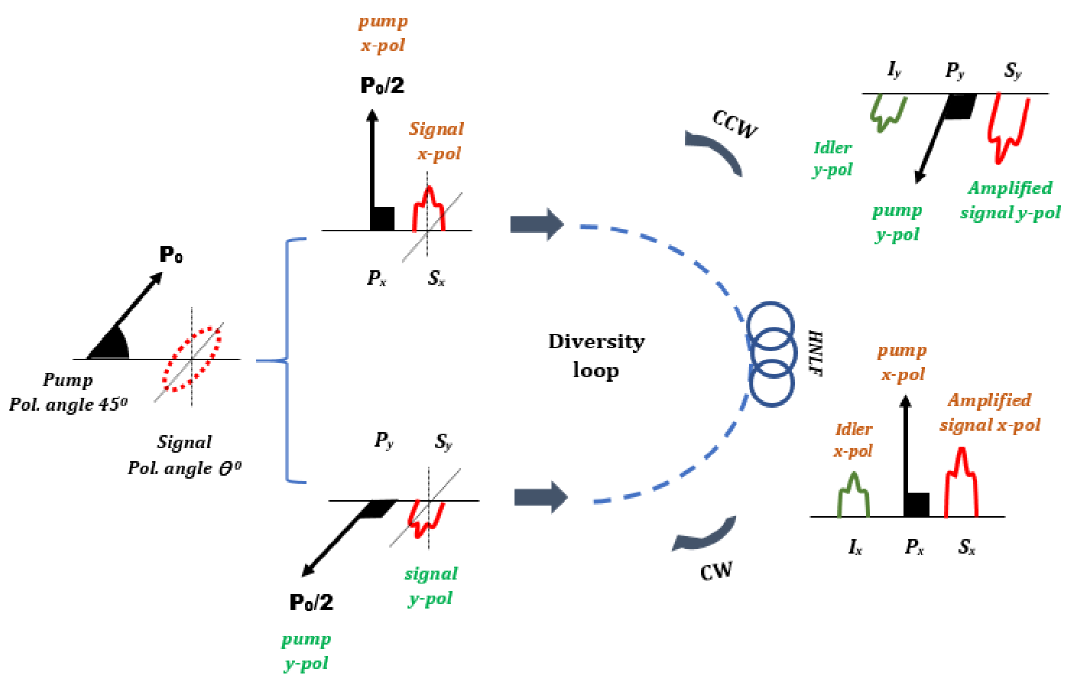

Figure 3.3: Implementation of polarization diversity loop in single pump FOPA.

is used and not used. Hence, received power of the signal at the receiver is high when polarization diversity loop is used in the PIA set up. The authors have stated that this power penalty is due to the inadequate SBS suppression although phase modulated pump wave is used. According to the authors, the performance degradation of the diversity loop is caused by three main reasons. One is due to the losses introduced by the components such as beam splitters used in the loop. Second is the crosstalk arise between counter-propagating waves due to Cross Phase Modulation and third is the Raileigh scattering. They have also emphasized the vast reduction of gain when diversity loop is implemented when compared to its no-loop, unidirectional counterpart just like was the case in [22]. According to the authors, the reason behind this is because of the fact that when the polarization of pump wave is split between two orthogonal polarization states at the beginning of the loop, the available pump power at a single propagation direction is also split into half. This reduction in the available pump power leads to the reduction in signal gain achieved by FWM process. Therefore, it could be seen that, although diversity loop mitigates the gain variations for different input SOPs, the maximum overall gain achievable by the FOPA is compromised.

As described earlier, polarization controlling in the HNLF within the diversity loop is a major concern. It should also be capable of maintaining the SOPs of propagating waves unchanged. Polarization controllers are usually assigned for this task but at times, the continuous adjustment of PCs may become troublesome. Therefore, as suggested by above authors, instead of using a HNLF as a gain medium with PCs attached to it, PM-HNLFs can be used instead. The feasibility of this approach has been discussed in [51]. They have been able to achieve a polarization dependence of only $0.7dB$ with a signal ON-OFF gain which is the signal power difference when pump is ON and OFF which is of about $19.2dB$. This work demonstrates the possibility of using a PM-HNLF instead of HNLF in the diversity loop according to the requirement.

3.4 Issues in the Existing Configuration

Several issues that can be identified during the implementation of diversity loop in a realistic scenario can be listed as follows.

- The HNLF should be highly polarization maintaining which means that precise polarization controlling within the HNLF is strictly necessary. This issue has been addressed in two ways. One is by using a PM-HNLF [52] and the other is using PCs [53]. Although these methods were used, there is a possibility for the PDG to occur due to non-reciprocal gain in the counter propagating directions. This can arise due to various scattering effects such as SBS that take place inside the HNLF as stated by authors in [54].

- The bidirectional propagation of waves within the HNLF leads to the arise of crosstalk between propagating waves as a result of XPM and SPM. The other form of crosstalk occurs due to reflections. These reflections may occur from the components used in the setup and reflected waves can interact with propagating waves adversely. Scattering is also another form of unwanted effect occurring as a result of bidirectionality. Both Rayleigh as well as Brillouin scattering can occur within the diversity loop. Scattered waves originated from SBS create crosstalk with counter propagating waves in such a way that it finally leads to the origin of PDG as stated above.

- The unavailability of total pump power in either propagation direction is the other major issue to be addressed. The input pump is split into two orthogonal polarization states in such a way that each direction is available with only half of the total pump power. That means the FWM based parametric amplification utilizes only half of pump power in each direction.

> Since the parametric gain coefficient is proportional to the product of available pump power, nonlinear coefficient and the fiber length, it is inevitable that the gain will be reduced by a greater extent when diversity loop is deployed when compared to its non-diversity loop counterpart.

Therefore, it is worth to address these issues to obtain the expected outcomes when a diversity loop is incorporated to a PSA configuration. Among many objectives, the primary purpose of an amplifier in a system is to boost the signal power to a higher value. Therefore, amplifier gain, which is the ratio between output to input signal powers is an invaluable measure which determines the performance of an amplifier. By using diversity loop, the reduction or the fluctuation of gain due to the variation of polarization state of the signal has been mitigated which is a great achievement. But, this strategy also influences the maximum achievable gain of the amplifier in a negative manner as the maximum attainable gain is reduced due to the inability of utilizing the total available pump power for the FWM process that takes place inside the diversity loop. By an extensive study of the existing literature, it was found that the current state-of-the-art implementations do not provide a suitable solution for this issue. Therefore, it is necessary to analyze the methods used in the literature related to gain enhancement techniques of the FWM based amplifiers and assess these methods to identify the most suitable to be incorporated in the diversity loop configuration.

3.5 FOPA Gain Enhancement Techniques

In the literature, there are several gain enhancement techniques that are being used in FWM based parametric amplification such as gain enhancement by introducing phase shifted fiber Bragg grating for phase matching, Raman enhanced FWM gain and cascaded fiber structure based gain enhancement utilizing conventional fiber arrangement as well as using quasi phase matched (QPM) fiber arrangement. Some of these techniques are tested on phase insensitive FOPAs and some are directly on PSAs. Existing gain enhancement techniques in FOPAs have to be investigated in addition to PSAs because they can also be deployed directly on PSA configurations.

3.5.1 Fiber Bragg Grating Based Gain Enhancement

Fiber Bragg grating based gain enhancement uses a phase shifted Bragg grating (PS-FBG) installed in between two HNL-DSFs [55]. The power of the idler

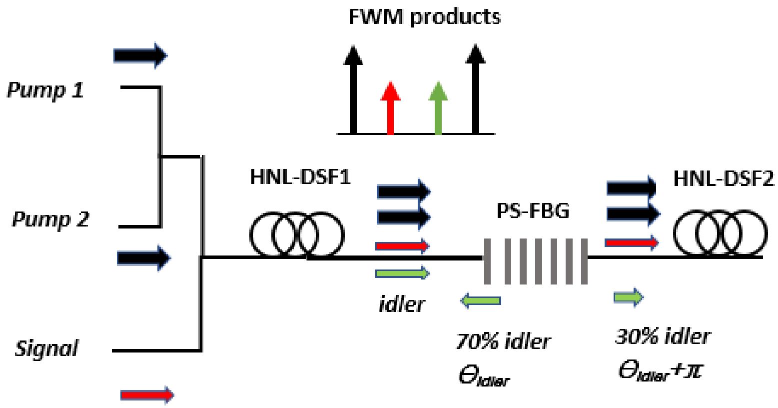

Figure 3.4: FOPA gain enhancement using fiber Bragg grating.

wave generated by the FWM process at the first HNL-DSF is reduced by the PS-FBG due to partial reflection and a phase shift is introduced to the idler wave. Other waves involved in the FWM process which are two pump waves and the signal wave will be transmitted through the PS-FBG as it is, without introducing any changes. Hence, PS-FBG can be identified as a frequency selective wavelength filter which also acts as a phase shifter in between the two HNL-DSFs. The configuration is illustrated in figure 3.4. FBG based gain enhancement and equalization are also deployed for WDM systems as type hybrid amplifiers for both C and L band wavelengths [56].

This method proposes a way to restore the relative phase value between the two pumps, signal and idler by introducing an additional phase shift to the idler wave that has been generated by HNL-DSF1. As can be seen in figure 3.4, PS-FBG transparent to the pump and signal waves while 70% of the idler wave is reflected back by the Bragg grating by introducing a phase change to the idler. The phase shift introduced by the grating can be varied by changing the grating length. According to the results of the experiment, a 4.3 dB enhancement in the signal gain could be achieved. By fine-tuning the parameters of the Bragg grating, the reflectivity and phase shift can be changed thus leading to an enhancement of gain and the maximum gain of the FOPA. Another advantage of this method is that, it can be used even for pump wavelengths which are far from ZDW of the fiber. But, the applicability of this method in the diversity loop configuration is less because the diversity loop relies on the bidirectional propagation of the waves.

3.5.2 Gain Enhancement Using Raman Pump

Gain enhancement in PSA with the assistance of SRS has been carried out in [57]. Figure 3.5 represents Raman pump assisted FOPA gain enhancement. Backward Raman amplification has been used to increase the phase insensitive phase insensitive gain which causes to improve the phase sensitive gain as a result. A $955mW$ Raman pump has been used to increase the gain extinction ratio (GER) by $9.2dB$ which has resulted in the the increasing of maximum PSA gain by $18.7dB$. The weak pump wave contributing to the FWM process is amplified by the Raman pump and as a result, the signal gain by the FWM process is increased. Idler is generated from the Raman enhanced phase insensitive process at the first HNLF. Once a second HNLF is introduced and signal, generated idler and Raman enhanced pump is passed through it, the process becomes phase sensitive and gain enhancement is still preserved. According to the authors, the applicability of this method is most suitable in cases where the available pump wave is weak and broadband Raman amplification is available. Although this method supports bidirectional gain enhancement, the configuration can become more complex when deployed in the diversity loop where two orthogonal polarization states exist and the possibility of the occurrence of SBS is also high.

3.5.3 Gain Enhancement Using Cascaded Fiber Architecture

Fiber pieces can be casacaded together in order to obtain a wide band, higher gain parametric amplification. There are several methods to cascade the fiber pieces together both of which focus on improving the phase matching such as periodic dispersion compensation based, quasi-phase matching based and by using genetic algorithms to determine the parameter values of fiber pieces to be cascaded together to obtain higher gains.

3.5.3.1 Periodic Dispersion Compensation

M.E. Marhic proposed a method to enhance the gain and gain-bandwidth of a single pump FOPA by cascading several fiber pieces together with same lengths and parameter values by inserting short pieces of dispersion compensating fiber pieces in between [58]. The theory was built up based on the fact that, in computer modelling of an optical fiber when fiber is divided into smaller sections where nonlinear and dispersive properties of the fiber are exhibited in alternating steps which is also the basis of split-step Fourier method (SSFM) [59]. In this paper, authors assume that, the dispersion acquired by the waves propagating

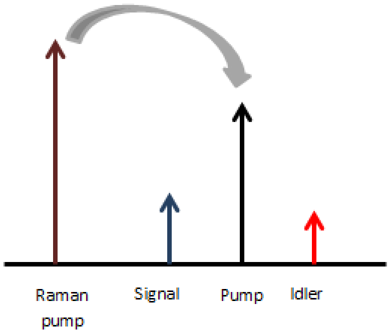

Figure 3.5: FOPA gain enhancement using Raman pump.

in a nonlinear fiber piece will be compensated by adding a dispersion compensating fiber (DCF) consecutively and this way, phase matching can be achieved efficiently before propagating the waves along the second piece of nonlinear fiber. The fiber arrangement in periodic dispersion compensation technique has been illustrated in figure 3.6. The experimental demonstration has shown that by this method, a considerable gain enhancement of around $5dB$ could be obtained along with a increased gain bandwidth from $7nm$ to $28nm$ even for pump wavelengths farther away from zero dispersion wavelength. Cascaded nonlinear fibers used are $40m$ long. These results have been obtained by considering the practical splicing losses that may encounter when fiber pieces are cascaded together.

3.5.3.2 Quasi-Phase Matching Technique

QPM based gain enhancement utilizes a cascaded fiber arrangement with optimized parameters to obtain a maximum gain by establishing a proper phase relationship between the interacting waves [60]. Instead of increasing the length of the HNLF to enhance the gain, cascaded arrangement of HNLF pieces has been used because a long, continuous fiber may induce phase mismatch as well as undesirable effects from ZDW fluctuations. Here, at the maximum gain point of the parametric amplification process, an additional phase shift will be introduced to restore the phase relationship so that the maximum gain will be further enhanced. QPM technique requires the knowledge of the amount of phase shift to be introduced as well as the point at which the phase shift is introduced. Based on the results in [60], more than $12dB$ gain enhancement has been achieved with a three stage dispersion shifted fiber optic parametric amplifier having a wavelength separation of $11nm$ between the pump wavelength and the ZDW. The limitations of this method, tend to arise after three concatenated segments due to the splicing loss, polarization effects and the technical difficulty of setting the

Figure 3.6: FOPA gain enhancement using periodic dispersion compensation

polarization relations between pumps and signal waves. Applicability of QPM technique in the polarization diversity loop with bidirectional transmission has been demonstrated in with an alteration to the conventional diversity loop arrangement [61]. That is by modifying it as a half passed loop (HPL) where x-polarized and y-polarized wave components will be amplified separately using two series of QPM based fiber arrangements where x and y polarized pumps will be removed after traversing half way across the loop. This method has been used to mitigate the effect of SBS due to counter-propagating pump waves and by introducing QPM at each gain section, the HPL-FOPA setup has been able to obtain a higher gain [61], [62]. The QPM has been applied by concatenating two HNLFs together in each x and y HNLFs in order to obtain a higher gain by restoring the phase relationship between the waves. By carefully choosing the parameter values of the concatenating fiber sections, the SBS thresholds have been increased as well.

Figure 3.7 shows the HPL-FOPA implementation where $HNLF_x$ is the gain medium for x-polarized signal components where x-polarized pump will be used in the parametric amplification process. When QPM is applied in this configuration, $HNLF_x$ is composed of two fiber segments with concatenated together. Similarly, $HNLF_y$ serves as the gain medium for y-polarized components where QPM is applied by concatenating two other fiber segments together. This way, x and y polarized components of the waves will be subjected to parametric amplification in different gain media and their corresponding pump components will be filtered out immediately afterwards. Therefore, this configuration avoids the counter-propagating pump components so that the effect of SBS will be suppressed while enhanced gain will be achieved by QPM technique. Although the flexibility of this configuration in terms of adding, removing and altering the parameters of gain medium is high and the SBS is mitigated effectively, the gain medium of x and y components of the signal are physically different. This may lead to issues like mismatching of ZDWs as well as the mismatching of other fiber parameters.

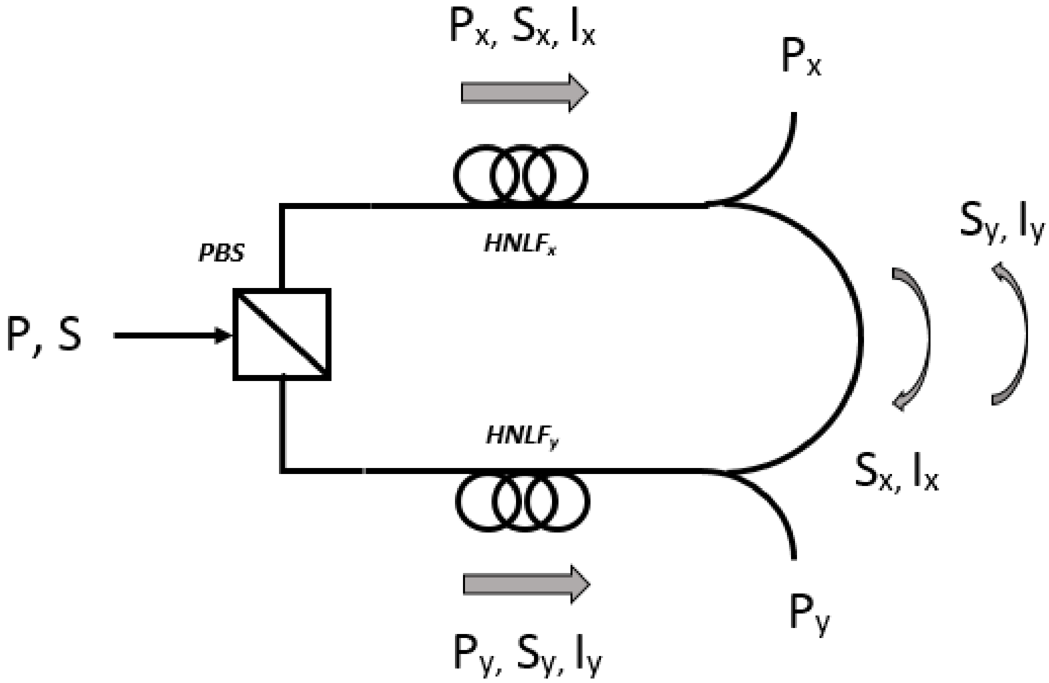

Figure 3.7: Half passed loop FOPA using QPM technique.

It can in turn affect the reciprocity of FOPA gain spectra in counter-directions of the diversity loop. Therefore, the requirements of a strategy which enhances the gain in a conventional diversity loop by conserving reciprocity is still a challenge.

3.5.3.3 Utilizing Genetic Algorithm

In addition to the gain enhancement using QPM technique in the cascaded fiber configuration, a genetic algorithm based gain enhancement and optimization has been introduced in a cascaded fiber architecture [63], [64]. In [63], authors have introduced a FOPA with multi-section fiber arrangement deploying two pump waves. A GA has been utilized to optimize the parameters of the two fiber segments to obtain a broadband and a gain enhanced FOPA.

3.6 Conclusion

Polarization variations in the interacting waves in the FWM process greatly affect the FWM efficiency and in turn varies the parametric gain. Therefore, strategies should be developed in both phase sensitive and phase insensitive fiber optic parametric amplifiers in order to make the gain independent of polarization state variations. Among different polarization independent strategies, vector scheme and polarization diversity loop based schemes stand out. When one-pump phase insensitive and phase sensitive parametric amplifiers are considered, polarization diversity loop is deployed to achieve polarization insensitivity. But, the overall gain of PSA tends to decrease in this arrangement due to the unavailability of total pump power for parametric amplification. Therefore, a requirement for gain enhancement technique arises in the diversity loop configuration. One such method is by using a cascaded fiber arrangement where overall gain can be improved but the parameters on which the performance of such an arrangement has to be identified and their impact should be quantified.

Chapter 4

MODIFIED POLARIZATION DIVERSITY LOOP FOR PSA

4.1 Introduction

The polarization diversity loop can be modified by including a cascaded fiber structure whereby, concatenating multiple nonlinear fiber segments together to enhance the gain of the FOPA. Such implementations in the existing literature have been done for FOPAs which are phase insensitive [58]. Here, the effect of such a cascaded configuration on the gain of the phase sensitive FOPA or PSA when it is operating in the bidirectional configuration is discussed. In this work, the gain enhancement of polarization diversity loop based PSA is discussed by a mathematical framework and numerical simulation when cascaded fiber configuration is introduced. Furthermore, polarization insensitivity of the overall structure will be assessed along with the gain enhancement.

4.2 Modified Diversity Loop Scheme

According to equation 2.35, PSA gain is a function of the product of pump power (P_p), nonlinear coefficient (γ) and fiber length (L). Therefore, PSA gain increases with fiber length. But in realistic environment, when fiber length is increased, the effect of ZDW fluctuations becomes prominent and the fiber attenuation becomes significant owing to the fluctuations and reduction of overall PSA gain [39]. Therefore, increasing the length of the gain medium by cascading discrete fiber pieces together which are shorter in length so that the effect of ZDW fluctuations and fiber attenuation can be ignored, significant enhancement of PSA gain can be expected. In this work, such an arrangement has been incorporated in the polarization diversity based PSA where polarization independent phase sensitive amplification is achieved in a bidirectional fiber.

Figure 4.1 illustrates the basic arrangement of the polarization diversity loop implementation using the concatenated fiber architecture. In this work, a po-

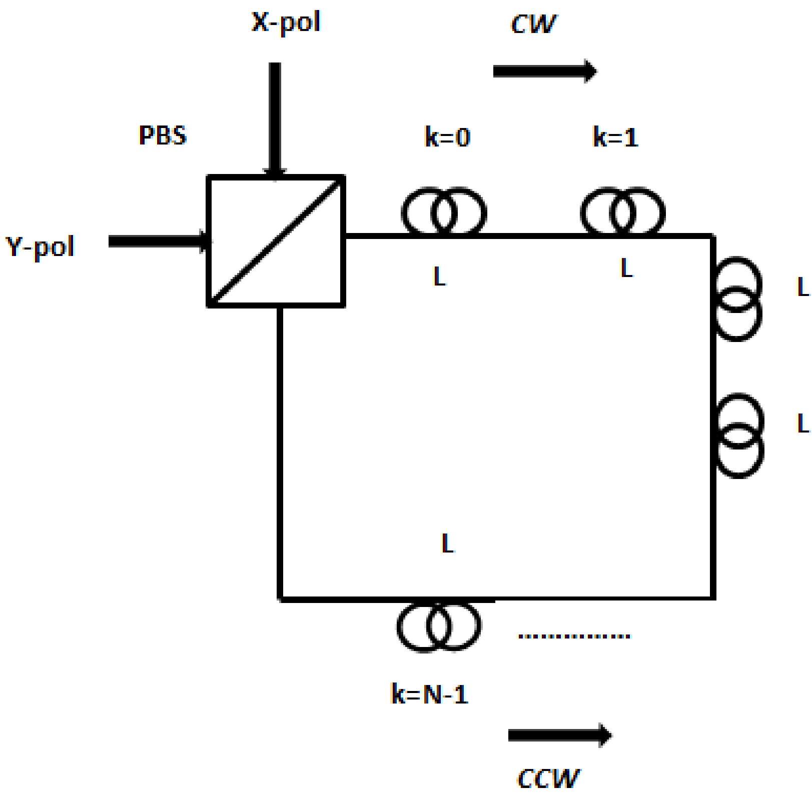

Figure 4.1: Proposed modified diversity loop; k is the k^{th} fiber, L is the length of one fiber segment, N is the number of fiber segments, CW is the clockwise direction, CCW is the counter-clockwise direction, PBS is the polarization beam splitter.

larization diversity loop arrangement where N number of HNLF fiber pieces each with length L have been concatenated together as the nonlinear amplifying medium is considered. It is assumed that these fiber pieces are identical in nature. A polarization beam splitter is deployed at the beginning in order to split the incoming pump, signal and idler waves into orthogonal polarizations. The x-polarized wave components are propagated in the clockwise directions while the y-polarized components are propagated in the counter-clockwise direction. It is to be noted that the SOPs of the waves once they enter the loop via polarization beam splitter are kept constant throughout.

4.2.1 Mathematical Analysis

The basis for the mathematical interpretation of the PSA gain in cascaded fiber architecture is the input-output transfer matrix of a FOPA expressed in equation 2.29. In this section, the transfer matrix is expressed using different notations for matrix elements as follows.

$$T = \begin{bmatrix} m_{11} & m_{12} \\ m_{21} & m_{22} \end{bmatrix} \tag{4.1}$$

where, m_{11}, m_{12} are the matrix coefficients that are given in equations 2.31 and 2.32 in section 2.5.1, which are re-written as follows.

$$m_{11} = \mu = cosh(gL) + \frac{ik}{2g} sinh(gL) \tag{4.2a}$$

$$m_{12} = v = \frac{i\gamma P_p}{g} sinh(gL) \tag{4.2b}$$

$$m_{21} = m_{12}^*, m_{22} = m_{11}^* \tag{4.2c}$$

where, k, g, L, γ, P_p represent the net phase mismatch, parametric gain coefficient, fiber length, nonlinearity coefficient of the fiber and pump power respectively.

The phase sensitive signal gain is calculated by using the first row first column and first row second column matrix coefficients which represents the coherent superposition of signal and idler fields in analogous to equation 2.30.

$$A_s(L) = \mu A_s(0) + v A_i^*(0) \tag{4.3}$$

where, $A_s(0), A_s(L)$ and $A_i^*(0)$ represents the complex amplitude of signal field at the beginning of the fiber, the complex amplitude of signal field at the beginning of the fiber and the complex conjugate of idler field at the beginning of the fiber.

In a concatenated series of fiber segments of equal lengths, the parameters at the k^{th} fiber section can be expressed as follows and hence the matrix coefficients can be written as [58],

$$\mu_k = cosh(g_k L) + \frac{ik_k}{g_k} sinh(g_k L) \tag{4.4}$$

$$v_k = \frac{i\gamma P_{pk}}{g_k} e^{i\Phi_k} sinh(g_k L) \tag{4.5}$$

The gain coefficient of the k^{th} fiber segment is,

$$g_k^2 = (\gamma P_{pk})^2 - (\frac{k_k}{2})^2 \tag{4.6}$$

where, the net phase mismatch can be written as,

$$k_k = \Delta\beta + 2\gamma P_{pk} \tag{4.7}$$

It is to be noted that, the symbols used in equations 4.4, 4.5 and 4.6 are corresponding to the k^{th} value of corresponding symbols interpreted by equations 2.22, 2.25, 2.31 and 2.32. The pump power is reduced from segment to segment due to the splicing and connector losses. Therefore, the available pump power at the k^{th} segment is [58],

$$P_{pk} = P_0\alpha^k \tag{4.8}$$

where, α is the transmittance through the splices given by, $\alpha = 10^{-0.2L_s}$ where, L_s is the power loss in dB and P_0 is the input pump power. The total phase shift accumulated in the pump due to SPM is given by,

$$\Phi_{SPM}^{(k)} = 2\gamma P_0 L\Big(\frac{1-\alpha^k}{1-\alpha}\Big) \tag{4.9}$$

Initially, if we assume that the transmittance through splices is 100% (which implies that, $\alpha = 1$), then, $P_{pk} = P_0$, $g_k = g_0 = g$, $k_k = k_0 = k$ and $\Phi_k = k\Phi_1$. The N^{th} power of the transfer matrix is given by [58],

The N^{th} power of the transfer matrix given in equation 4.1 can be written as,

$$(T)^N = \begin{bmatrix} m_{11} & m_{12} \\ m_{21} & m_{22} \end{bmatrix}^N = \prod_{k=0}^{N-1} T_k \tag{4.10}$$

where, T_k is the transfer matrix of the k^{th} fiber segment.
Hence the characteristic matrix T is a unimodular matrix where the determinant of the matrix reduces to +1, the N^{th} power of such a unimodular matrix can be approximated as follows using Chebyshev polynomials [65].

$$T^N = \begin{bmatrix} m_{11}U_{N-1}(a) - U_{N-2}(a) & m_{12}U_{N-1}(a) \\ m_{21}U_{N-1}(a) & m_{22}U_{N-1}(a) - U_{N-2}(a) \end{bmatrix} \tag{4.11}$$

where, U_N are the Chebyshev polynomials of 2^{nd} kind given by,

$$U_N(a) = \frac{sin[(N+1)cos^{-1}(a)]}{\sqrt{1-a^2}} \tag{4.12}$$

and $'a'$ in equation 4.3 is given by,

$$a = \frac{1}{2}(m_{11} + m_{22}) \tag{4.13}$$

which can further be simplified as, $a = Re\{m_{11}\} = cosh(gL)$. The overall gain of the cascaded fiber structure is the product of the individual gains of each subsequent pieces.

The coefficients present at the end of the N^{th} concatenated fiber piece is given by the first row first element and the first row second element of the matrix T^N in equation 4.11 and can be re-written as,

$$\mu_N = m_{11}U_{N-1}(a) - U_{N-2}(a) \tag{4.14}$$

$$v_N = m_{12}U_{N-1}(a) \tag{4.15}$$

which can further be simplified as,

$$\begin{aligned} \mu_N = \frac{1}{\sqrt{1-a^2}} &\{cosh(gL)sin(Ncos^{-1}(a)) - sin[(N-1)cos^{-1}(a)] \\ &+ \frac{ik}{2g} sinh(gL)sin(Ncos^{-1}(a))\} \end{aligned} \tag{4.16}$$

$$v_N = \frac{i\gamma P_p}{g} sinh(gL)\Big\{\frac{sin[Ncos^{-1}(a)]}{\sqrt{1-a^2}}\Big\} \tag{4.17}$$

4.2.1.1 PSA Gain of the Modified Diversity Loop

Although in case of phase insensitive FOPA, only μ_N is sufficient to calculate the gain of the amplifier, when phase sensitive case is considered, according to equation 4.3, both μ_N and v_N have to be taken into consideration. Therefore,

$$G^N_{PSA} = \mid \mu_N \mid^2 + \mid v_N \mid^2 + 2 \mid \mu_N \mid\mid v_N \mid \cos(\theta_{rel}) \tag{4.18}$$

With the substitution, $Ncos^{-1}(a) = x$, $\mid \mu_N \mid^2$ and $\mid v_N \mid^2$ can be written as,

$$\begin{aligned} \mid \mu_N \mid^2 = \frac{1}{(1-a^2)} \Big\{ &cosh^2(gL)sin^2(x)[1 + \frac{k^2}{4g^2}] - sin^2(x) + sin^2[x - cos^{-1}(a)] - \\ &2cosh(gL)sin(x)sin[x - cos^{-1}(a)] \Big\} \end{aligned} \tag{4.19}$$

$$| v_N |^2 = \frac{1}{(1-a^2)}\Big\{\Big(\frac{\gamma P_p}{g}\Big)^2 sinh^2(gL)sin^2(x)\Big\} \tag{4.20}$$

Therefore, by using equation 4.18, the phase sensitive gain at the end of the concatenated series of N fiber segments can be calculated.

When the signal and idler conversion efficiency, η is considered, the signal gain can be written as,

$$G^N_{PSA} = | \mu_N |^2 + | v_N |^2\eta^2 + 2| \mu_N || v_N |\eta cos(\theta_{rel}) \tag{4.21}$$

where, $\eta = \sqrt{\frac{P_i(0)}{P_s(0)}}$, which is the function of the power ratio between input signal and idler powers given by $P_i(0)$ and $P_s(0)$.

4.3 Simulation Setup

The polarization diversity PSA was implemented using $VPI - Transmission\ Maker^{TM}$ simulation environment. Initial simulation setup was developed to simulate and characterize a single-pump FOPA to demonstrate the fiber optic parametric amplification using FWM. The simulation setup is depicted in figure 4.2 A pump wave at $1560.7nm$ with an output power of $1W$ has been used with a QPSK modulated signal operating at $1580nm$ with an output power of $0.02mW$. The pump wave has been phase modulated with 4 RF tones at $100MHz, 300MHz, 900MHz$ and $2700MHz$, in order to suppress the effect of SBS during parametric amplification. Optical signal to noise ratio (OSNR) of the input QPSK signal is improved and combined with the phase modulated pump wave using a $N : 1$ combiner and directed to the $HNLF_1$ which acts as the phase insensitive FOPA (i.e.PIA) where input QPSK signal is amplified and an idler wave will be formed through the parametric FWM process. The $HNLF_1$ is a $250m$ long fiber with an attenuation of $0.2dB/km$. The ZDW, dispersion slope, nonlinear coefficient and fiber core area are $1559nm, 0.03ps/nm^2km, 11W^{-1}km^{-1}$ and $12\mu m^2$ respectively. After phase insensitive amplification in $HNLF_1$ stage, the 10% of the optical power available at $HNLF_1$ output will be directed to a OSA where output spectrum can be analyzed. Remaining 90% of power is directed towards the PSA stage. Polarization of the waves are controlled through the polarization controller (PC_1) and pump wave from initial PIA stage will be filtered out using an OBSF. Second amplifying fiber stage i.e., PSA stage is a bidirectional highly nonlinear fiber $HNLF_2$ where polarization diversity loop is

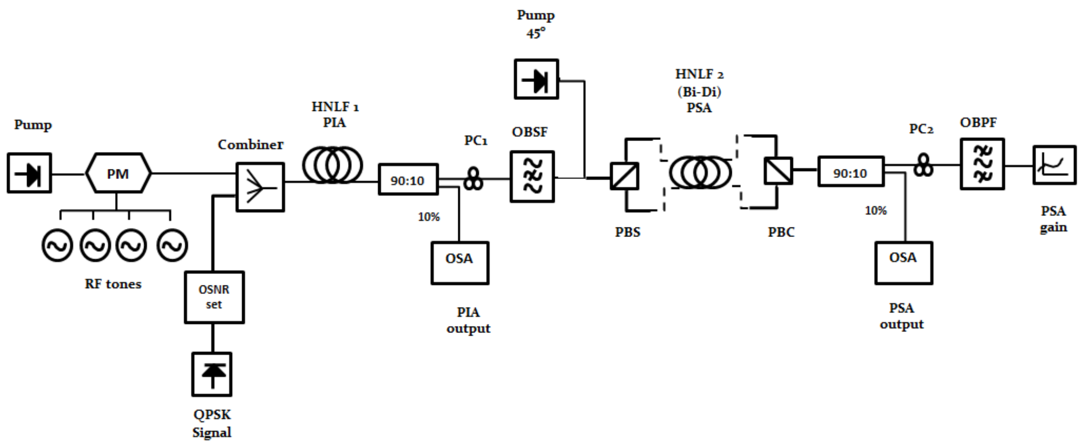

Figure 4.2: Simulation setup of polarization diversity loop based PSA; PM: phase modulator, HNLF: highly nonlinear fiber, PC: polarization controller, OSA: optical spectrum analyzer, OBSF: optical band stop filter, PBS: polarization beam splitter, PBC: polarization beam combiner, OBPF: optical band pass filter.

deployed.

It is a $750m$ long HNLF with a ZDW, fiber attenuation, dispersion slope, nonlinear coefficient and core area of $0.7dB/km$, $0.03ps/nm^2km$, $13.43W^{-1}km^{-1}$, and $12\mu m^2$ respectively. It should be noted that, in the implementation of cascaded fiber configuration proposed in this research, the length of one fiber piece can be changed while other parameters are same and length of $HNLF_2$ which is $750m$ is in compliance with the analysis of PSA gain and its polarization dependence only. A locally generated 45^0 linearly polarized pump wave with wavelength $1560.7nm$ and an output power of $1W$ is input to the diversity loop along with the QPSK signal and newly generated idler wave which is phase and frequency correlated to the QPSK signal. The PBS in the diversity loop splits the input SOPs of the incoming signals into orthogonal components as x and y polarizations. The PBC at the end of the loop combines the orthogonal SOPs of the incoming signal back to their original SOPs. As was described in section 3.2.2, the purpose of the polarization diversity loop is to provide polarization insensitive gain to the input signal irrespective of its SOP variations at the beginning of the $HNLF_2$ stage.10% of the output optical power after polarization diversity loop is tapped to analyze the output spectrum using OSA. The remaining optical power is polarization controlled and passed through a OBPF which allows only QPSK signal wave to pass through to analyze the PSA gain using a 2D analyzer. The concatenated fiber based polarization diversity loop proposed in this section depicted by figure 4.1 is an extension of the existing diversity loop depicted in figure 3.6 where multiple short fiber pieces are concatenated together instead of using a long continuous fiber in order to increase the signal gain as signal gain is a function of fiber length. Using a long fiber is not feasible due to ZDW fluctuations and due to difficulty in maintaining the SOP constant throughout the fiber length.

4.4 Results and Discussion

The results and discussion of the implementation of the PIA, PSA, polarization diversity loop based PSA and polarization diversity loop based PSA with cascaded fiber configuration will be presented in this section.

4.4.1 PI-FOPA gain spectrum

Initially, the process of phase insensitive fiber optic parametric amplification in $HNLF_1$ which is the PIA stage was demonstrated using the developed setup in figure 4.1 and the output spectrum at the output of $HNLF_1$ was analyzed using the first OSA in the setup. In figure 4.3, the optical output spectrum before PIA (in grey color) and after PIA (in maroon color) is demonstrated. It can be seen that the QPSK signal at $189.87THz$ is amplified and an idler which is a copy of the QPSK signal is generated at $194.57THz$ with the phase and frequency relationship to the QPSK signal as a result of the parametric amplification by FWM taking place inside $HNLF_1$. It can be seen that, the initial optical spectrum with pump, QPSK signal and noise floor have been amplified parametrically mimicking the shape of the FOPA gain spectrum given in figure 2.5. The measured signal gain of PIA is $7.1dB$ for the fiber parameter values for $HNLF_1$ specified in section 4.3. It is to be noted that, in figure 4.3, an OSNR degradation can be observed since the signal as well as the noise is amplified in the PI-FOPA as it is operating in the phase insensitive mode.

It is worthwhile to analyze the input polarization variations of the input QPSK signal after passing through the PIA stage. The Poincare sphere is the best representation that can be used to represent all the available SOPs with varying azimuth and ellipticity angles using Stoke's parameters $(S1, S2, S3)$ in which all the linear polarization states lie on the equator of the sphere, all the right and left circular polarization states lie on north and south poles of the sphere and all elliptical polarization states lie on the remaining surface of the sphere [66].

Figure 4.4 represents the Poincare sphere representation of the SOP at the input of PIA stage (figure 4.4(a)) and the SOP at the output of PIA stage (figure 4.4(b)). It can be observed that, the input SOP is a linear horizontal polarization. But after passing through PIA, i.e., $HNLF_1$, the single linear polarization

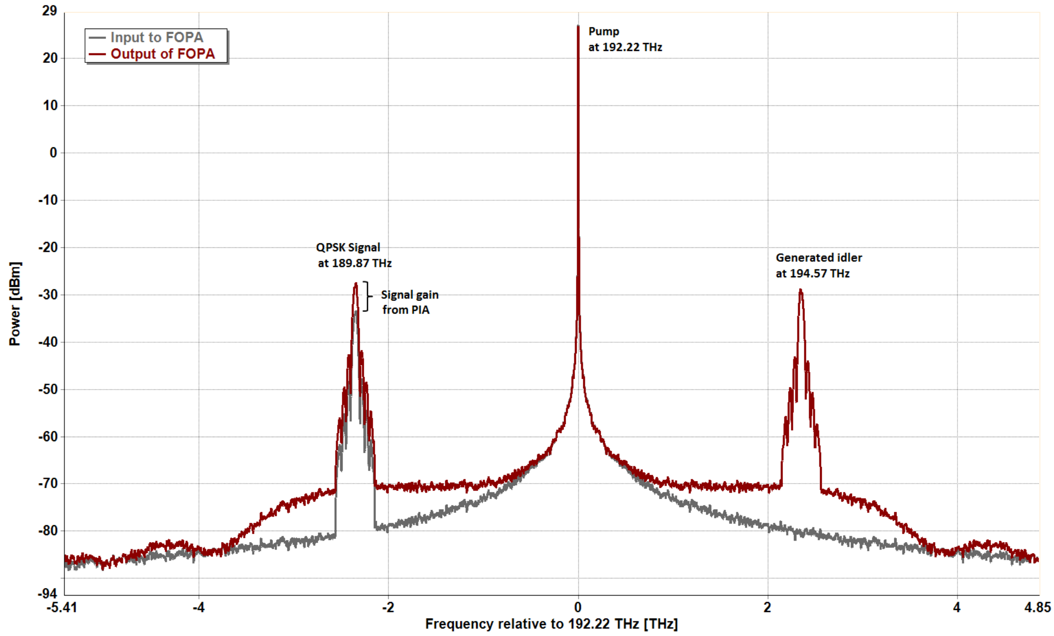

Figure 4.3: $HNLF_1$ input and output spectra: PI-FOPA output

state of the frequency spectrum of the QPSK signal has spread throughout the Poincare sphere and different SOPs are available at the PIA output. Therefore, since gain from the FWM process is highly polarization state dependent, if different frequency components of the BPSK signal exhibit different SOPs, the gain attained by the signal at the next amplifying stage which is the PSA, varies throughout the spectrum. The tracking of SOP variations is not practically viable and hence mitigating or controlling the input SOPs is not possible. Therefore, it is extremely important to implement the polarization diversity loop at the PSA stage in order to make the BPSK signal gain insensitive to its SOP variations.

4.4.2 PSA gain spectrum

The output from PIA stage, i.e., $HNLF_1$ is input to the PSA stage, i.e., $HNLF_2$ to amplify the QPSK signal phase sensitively. The output from PSA stage was monitored by the second OSA in the simulation setup of figure 4.2 by tapping 10% of the output optical power. PSA gain spectrum should be analyzed to observe the further parametric amplification of the QPSK signal along with the idler wave generated at PIA stage. Figure 4.5 represents the output optical spectra available at the input of PSA (in green color) and the output of PSA (in blue color). Note that, similar to figure 4.3, the parametric amplification of the noise floor of the spectrum at PSA input is mimicking the FOPS gain spectrum

(a) SOP at PI-FOPA input

(b) SOP at PI-FOPA output

Figure 4.4: Poincare sphere representation of the input SOP variation at the output of PIA

given in figure 2.5. The PSA gain observed was approximately $10.5dB$. Note that the PSA gain was initially taken in the absence of polarization diversity loop where a unidirectional $HNLF_2$ is used without PBS or PBC. Hence, the PSA gain of $10.5dB$ is relevant to a unidirectional $HNLF_2$ which has the same parameter values for the $HNLF_2$ described in section 4.3. In figure 4.5, it can be seen that both BPSK signal and idler wave have been amplified and in addition, two higher order idler waves are formed as a result of the parametric interaction of the three input waves i.e., QPSK signal, pump and idler. The theoretical aspect of the formation of higher order idlers is discussed in section 2.3.3. However, it should be noted that the formation and influence of higher order idler waves are not considered in the discussion carried out in this thesis.

4.4.3 Polarization independence of PSA gain with polarization diversity loop

The PSA gain is sensitive to polarization variations of the input signal. Since polarization variations is inevitable in realistic environments where fiber optic communication systems are deployed, techniques like polarization diversity which makes the PSA gain insensitive to the input polarization state variations should be implemented. Figure 4.6 represents the polarization dependence of PSA gain when polarization angle has been changed from -45^0 to $+45^0$ for a single signal wavelength. The green curve in figure 4.6 represents the PSA implementation in the absence of immunity to polarization variations. It can be clearly observed that, the highest PSA gain is observed when relative polarization angle is zero (i.e. polarization angle relative to pump and idler waves) which means that, all the three waves involved in the parametric amplification process are in the same state of polarization. On the other hand, blue curve in the figure 4.6 represents the implementation of polarization diversity loop in the PSA where PSA gain

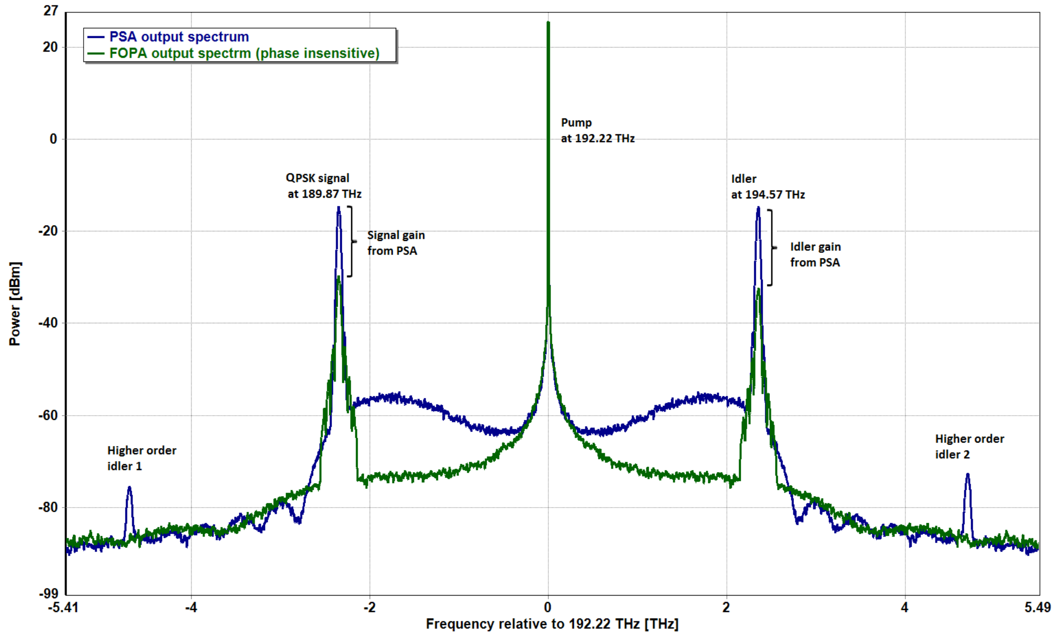

Figure 4.5: $HNLF_2$ (PSA) input and output spectra

is immune to polarization state variations. Although polarization diversity loop implementation of PSA provides considerable immunity to PSA gain for polarization state variations, the maximum achievable PSA gain is compromised. It can be seen that, the diversity loop based PSA gain is significantly lower than that of the polarization sensitive PSA gain. Therefore, it is important to introduce a strategy which will increase the overall PSA gain when diversity loop is implemented. In the upcoming sections, the gain enhancement by introducing a cascaded fiber architecture to the existing diversity loop configuration will be presented.

4.4.4 Characterization of gain enhancement in the cascaded fiber polarization diversity loop based PSA

Based on the mathematical analysis in section 4.2.1.1, simulation was carried out in order to analyze the effect of the number of fiber pieces cascaded together for the overall gain of the polarization diversity loop based PSA for an arbitrary signal wavelength of 1580nm. The pump power input to PSA is 1.06W and is kept constant during the simulation. It should be noted that although input pump power is 1.06W at the beginning of the polarization diversity loop, since pump is 45^0 linearly polarized, the PBS of the diversity loop splits the pump power into two orthogonal linearly polarized components. Clockwise and counter-clockwise

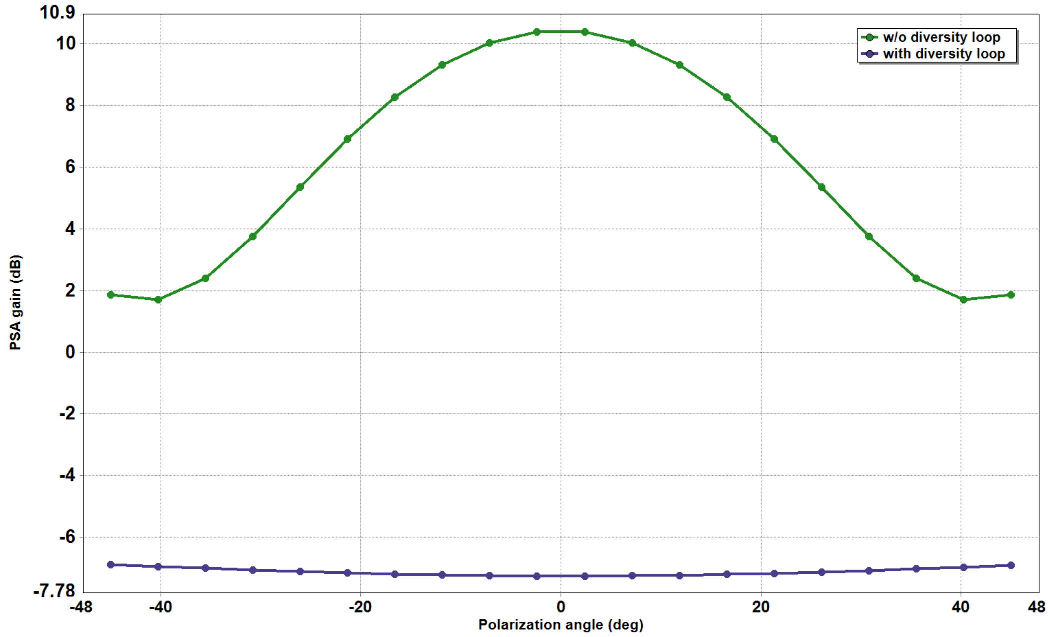

Figure 4.6: Polarization dependence of PSA gain and polarization insensitivity of PSA when polarization diversity loop is deployed

propagation directions inside the fiber will experience a pump power of 0.75W each and this amount will be available for parametric amplification of the QPSK signal in one particular direction inside the loop. Hence, although polarization diversity loop makes the parametric amplification insensitive to the input SOP variations, the total pump power is not utilized in the amplification process. Therefore, diversity loop based PSA gain is significantly lower than that of a non-loop PSA configuration. Therefore, a successful method for gain improvement is necessary in the diversity loop based PSA configuration. This section assesses the feasibility of using cascaded fiber configuration for this purpose which has initially been theoretically analyzed in section 4.2.1.1.

According to figure 4.7, with the increasing number of fiber pieces, a significant improvement in the polarization diversity based PSA can be observed. Initially, the PSA gain is increased and reaches to a maximum as the number of cascaded fiber pieces are increased. Then, with further increasing of the number of cascaded fiber pieces, the maximum PSA gain fluctuates and reaches to a stable constant value which has a negligible gain variation.

Since this variation is valid for the QPSK wavelength of 1580nm, it is important to analyze whether the variation is wavelength dependent in the gain spectrum.

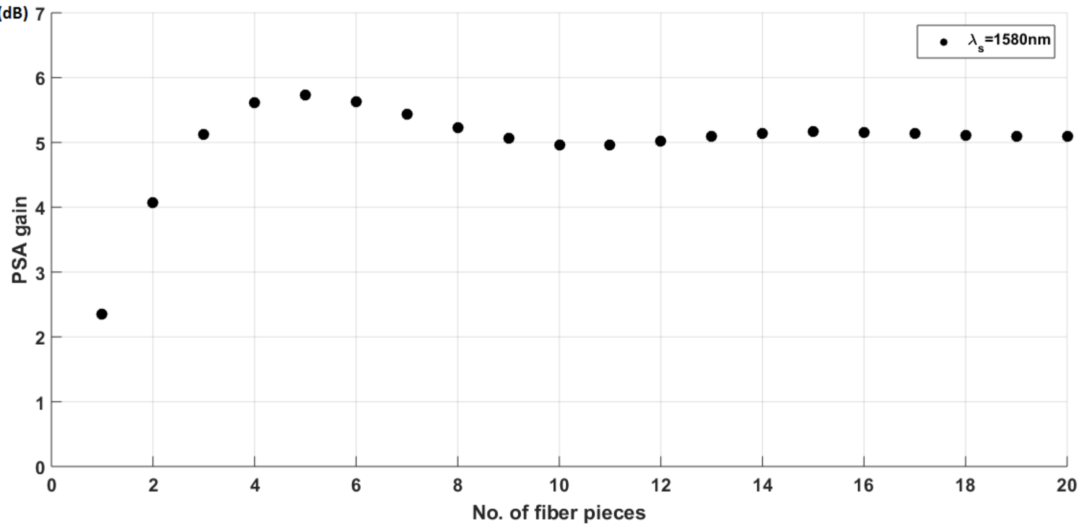

Figure 4.7: PSA gain with increasing number of cascaded fiber pieces

Another important analysis is the dependence of PSA gain in cascaded fiber configuration on different pump powers for a given signal wavelength. In addition, the theoretical aspects behind aforementioned variations should be discussed in detail.

4.4.4.1 Dependence of PSA gain on signal wavelength and fiber length in cascaded fiber diversity loop configuration

Figure 4.7 represents the PSA gain variation with increasing number of cascaded fiber pieces for a single wavelength. According to parametric gain spectrum represented in figure 2.5 in section 2.4.3 and discussion in section 2.4.2, the fiber optic parametric amplifier gain is not uniform throughout the gain bandwidth. In other words, different signal frequencies experience different gains although same pump power values and fiber parameters are used. The reason behind this is the fiber dispersion dependence on the signal wavelength which affects the parametric gain coefficient which in turn causes the PIA gain or PSA gain vary with signal wavelength. Therefore, it is worthwhile to analyze the signal wavelength depended gain for the proposed cascaded fiber architecture implementation of the polarization diversity loop based PSA designed for the phase sensitive gain enhancement of the signal.

Analysis was carried out for different signal wavelengths which belong to different gain regions of FOPA gain spectrum which is given below in figure 4.8. The corresponding FOPA gain spectrum has been obtained by considering the non-

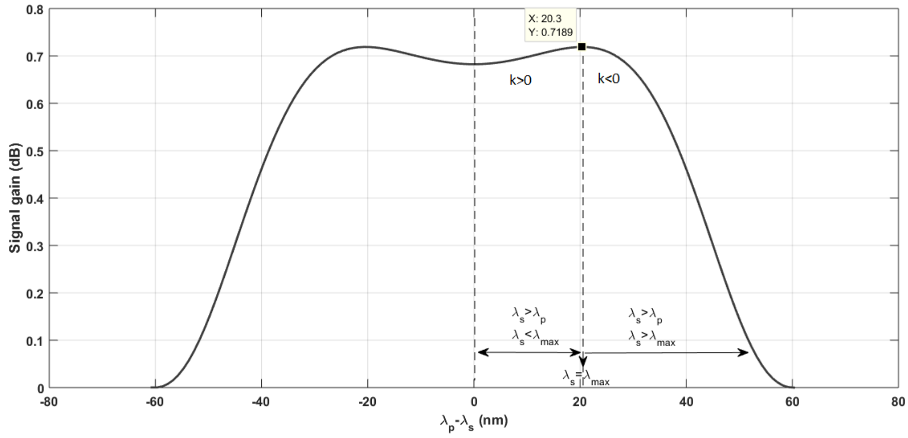

Figure 4.8: Signal gain regions in FOPA gain spectrum corresponding to cascaded fiber based PSA gain analysis

linear coefficient, dispersion slope, zero dispersion wavelength and fiber length as $11W^{-1}km^{-1}, 0.03ps/nm^2km, 1559nm$ and $50m$ respectively. The pump was at $1560.7nm$ and the input pump power was $0.75W$. For this analysis, only the positive lobe of the gain spectrum was considered (signal wavelengths which are greater than pump wavelength) due to the symmetric nature of the gain spectrum. According to figure 4.8, two gain regions can be identified corresponding to the positioning of signal wavelength (λ_s) with respect to the pump wavelength (λ_p). Gain region 1 is where signal wavelengths are less than the peak gain wavelength (λ_{max}) and where net phase mismatch, k, given by equation 2.22 is a positive value. For the given parameter values, λ_{max} is $1581nm$ which is $20.3nm$ away from pump wavelength with a gain of $0.72dB$. In gain region 1, it can be observed that, the signal gain increases with the signal wavelength detuning from pump wavelength i.e, $\lambda_p - \lambda_s$. The peak gain at λ_{max} is corresponding to the exponential gain regime of FOPA gain spectrum which was elaborately discussed in section 2.4.3.1. Gain region 2 of the spectrum can be identified as the gain region corresponding to the signal wavelengths which are greater than the λ_{max} in which the net phase mismatch, k, is negative. In this region, it can be observed that the signal gain decreases with the signal wavelength detuning from pump wavelength i.e, $\lambda_p - \lambda_s$. The following discussion is based on the analysis of the gain dependency of polarization diversity loop based PSA with cascaded fiber architecture on the signal wavelength where both gain regions which belong to different phase matching conditions discussed in 2.4.3.1 are taken into consideration .

Gain variation for $\lambda_s < \lambda_{max}$

In this section, the variation of cascaded fiber based PSA gain is analyzed for the gain region 1 where $k > 0$. In figure 4.9, the polarization diversity loop based PSA gain with increasing number of cascaded fiber pieces has been demonstrated for ten different signal wavelengths. According to figure 4.9, a strong signal wavelength dependence can be observed in polarization diversity cascaded fiber architecture based PSA. The simulation has been carried out for 20 fiber pieces of an arbitrary length of $50m$ that are concatenated together. Since parametric gain is a function of fiber length, the PSA gain is expected to be increased with the increasing of accumulated fiber length as the number of cascaded fiber pieces increases. For example, we can expect the PSA gain after concatenating 10 fiber pieces together to be greater than the PSA gain that can be obtained after 5 fiber pieces concatenating together. But according to figure 4.9 this simple argument fails. It can be seen that, for certain signal wavelengths, the overall gain is decreasing with increasing number of cascaded fiber segments and for certain others the gain is increasing in general but not uniformly. According to figure 4.9, for signal wavelengths which are closer to the pump wavelength demonstrate a decrease in the PSA gain with the increasing number of concatenated fiber pieces. Hence, although the goal is to increase the gain of the diversity loop based PSA with increasing number of fiber pieces, careful attention should be paid on the operating frequency of the signal that is being amplified by the diversity loop based PSA. Since the variation shown in figure 4.9 is only valid for $50m$ long fiber pieces, it is important to analyze the changes in this variation for fiber segments with different lengths, i.e., shorter fibers, moderately long fibers, longer fibers. It is to be noted that this analysis is valid for signal wavelengths which are less than peak gain wavelength i.e., $\lambda_s < \lambda_{max}$.

Figure 4.10 shows the dependence of variation illustrated in figure 4.9 for different lengths of concatenating fiber segments. The simulation has been carried out for the length of one fiber segment that is being concatenated together as, $1m, 10m, 20m, 30m, 50m, 100m, 200m, 300m$ by considering 9 signal wavelengths from $1563nm$ to $1579nm$. By analyzing the variations in figure 4.10 from (a) through (h), it is clear that the signal wavelength dependence of cascaded PSA gain is significantly different for different fiber lengths. For a fiber length of $1m$, which is a very shorter value, the signal gain of all the wavelengths follow a similar variation where PSA gain is increased with increasing number of concatenated

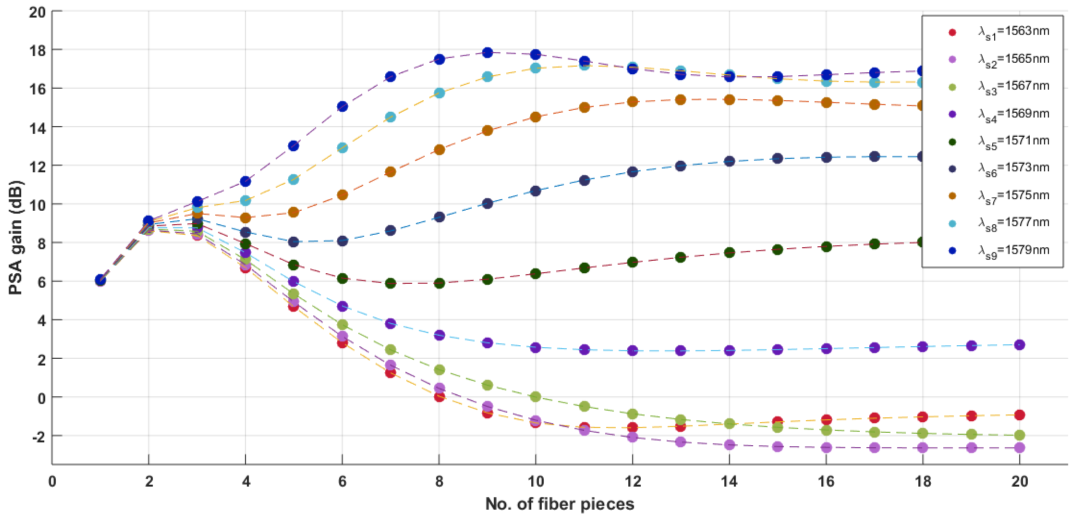

Figure 4.9: Signal wavelength dependence of polarization diverse PSA based on cascaded fiber architecture for $\lambda_s < \lambda_{max}$ for $L = 50m$

fiber pieces. Although this type of a variation is ideal as all signal wavelengths respond equally and gain shows an enhancement irrespective of the signal wavelength used, the issue is the maximum gain that is attainable. As the accumulated fiber length is very less i.e., in this case, the maximum accumulated fiber length at the end of polarization diversity loop is only $20m$. Therefore, fiber length contribution to the parametric gain coefficient given in equation 2.35 is less which in turn reduces the overall PSA gain of the signal. On the other hand, as the fiber length increases, different wavelengths respond differently to the increasing number of fiber pieces. Initially, the signal wavelengths which are closer to the pump wavelength ($1560.7nm$) i.e., $1563nm$ tend to reduce the overall PSA gain with the increasing number of fiber segments. But the signal wavelengths which are away from the pump wavelength and are closer to the peak gain wavelength (λ_{max}) i.e., $1579nm$ demonstrate an increase in the overall PSA gain. At shorter fiber lengths, the gain enhancement is uniform while for moderately long fiber lengths, fluctuations in gain can be observed. However, these fluctuations in gain are reduced when length per one fiber piece is increased further. For example, for fiber lengths $20m, 30m$ and $50m$, approximately uniform gain enhancements can be observed while for the lengths of $100m$, $200m$ per fiber piece, there are significant gain fluctuations. In contrast, fiber length of $300m$ shows reduced gain fluctuations compared to that of $100m$ and $200m$. It should also be noted from figures 4.9 and 4.10 that, after reaching for a certain value of accumulated fiber length, the gain remains at a constant value irrespective of the increasing number

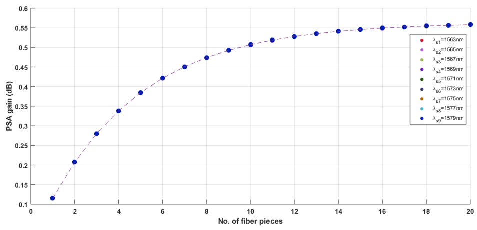

(a) L=1m

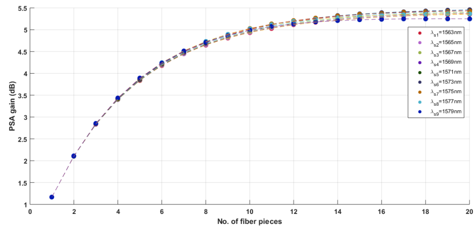

(b) L=10m

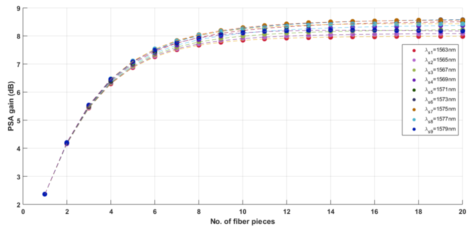

(c) L=20m

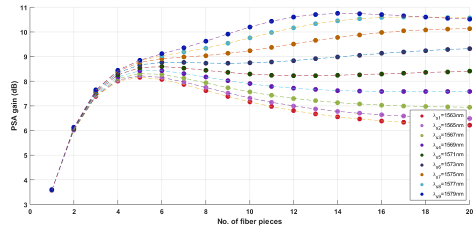

(d) L=30m

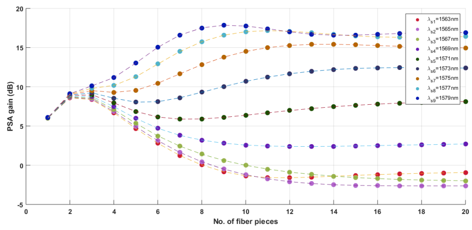

(e) L=50m

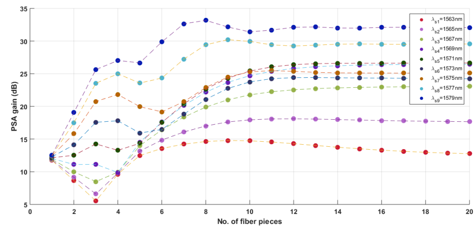

(f) L=100m

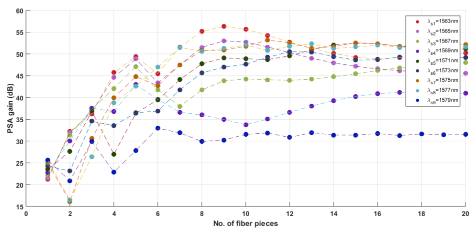

(g) L=200m

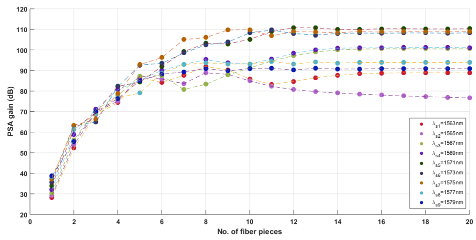

(h) L=300m

Figure 4.10: Signal wavelength dependence cascaded fiber PSA gain for different lengths of fiber pieces for $\lambda_s < \lambda_{max}$

of concatenated fiber pieces. The threshold number of fiber segments that should be cascaded together to reach this constant gain value is different for different fiber lengths.

Gain variation for $\lambda_s > \lambda_{max}$

In this section, PSA gain variation corresponding to region 2 in section 4.4.4.1 where signal wavelengths are greater than the peak gain wavelength is discussed. According to figure 4.8, in this wavelength region, the overall signal gain subjects to reduce for higher wavelengths. According to figure 4.11, it can be observed that for shorter fiber lengths, the gain improvement in different wavelengths is similar. But as the fiber length increases, the lowest gain improvement can be observed for signal wavelengths which are far away from the peak gain wavelength. For all the fiber lengths, the highest gain improvement is observed for the wavelengths which are closer to the peak gain wavelength. In addition, significant gain fluctuations can be observed for moderately long fiber lengths. For example, it is evident that the fluctuation in gain is negligible for shorter fiber lengths, i.e., $1m, 10m$ and much higher fiber lengths, i.e., $200m$, $300m$ while they are significant for fiber lengths like $50m$ and $100m$. Another important observation that can be made is the threshold number of fiber pieces that should be concatenated together to reach the constant gain region of PSA. As the length of one fiber piece increases, the threshold number of fiber pieces that should be exceeded for constant gain seems to decrease. In other words, it requires less number of fiber pieces to be connected together to achieve the highest possible gain improvement for fiber pieces of higher lengths.

4.4.4.2 Dependence of PSA gain on input pump power in cascaded fiber diversity loop configuration

Another important parameter that should be considered in the implementation of a PSA is the input pump power. Since PSA gain is dependent on input pump power, the characterization of the gain variation of cascaded fiber diversity loop based PSA is important. Hence, the variation of PSA gain with increasing number of concatenated fiber segments is characterised for different pump power values by considering the $1581nm$ signal wavelength and by taking the length of one fiber piece as $50m$. According to figure 4.12, it can be observed that PSA gain tends to increase as the pump power increases from $0.05W$ to $2.2W$. This variation agrees with the theory as PSA gain is a function of pump power and increase in pump power tends to the increasing of PSA gain. This has been discussed in

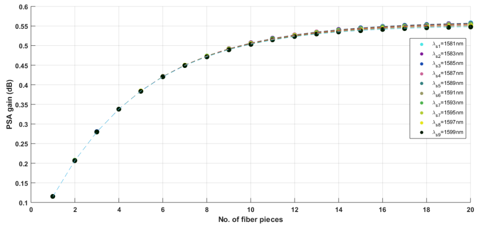

(a) L=1m

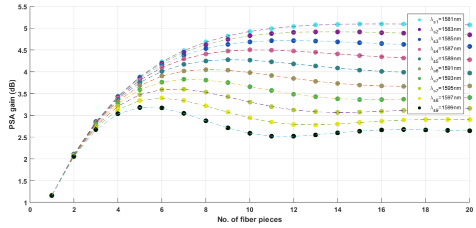

(b) L=10m

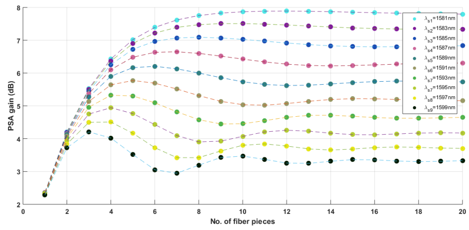

(c) L=20m

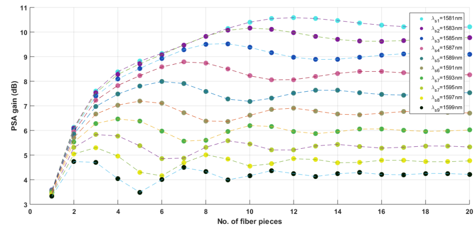

(d) L=30m

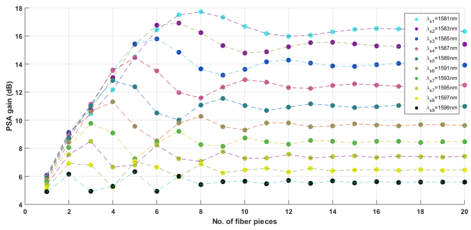

(e) L=50m

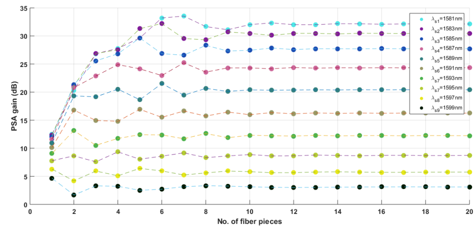

(f) L=100m

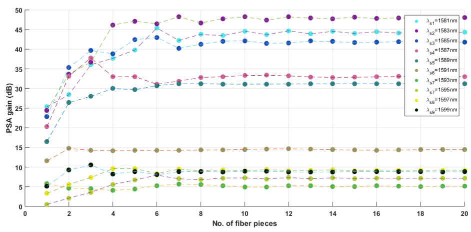

(g) L=200m

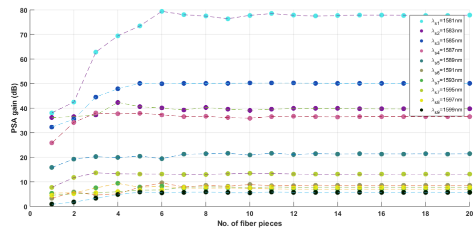

(h) L=300m

Figure 4.11: Signal wavelength dependence cascaded fiber PSA gain for different lengths of fiber pieces for $\lambda_s > \lambda_{max}$

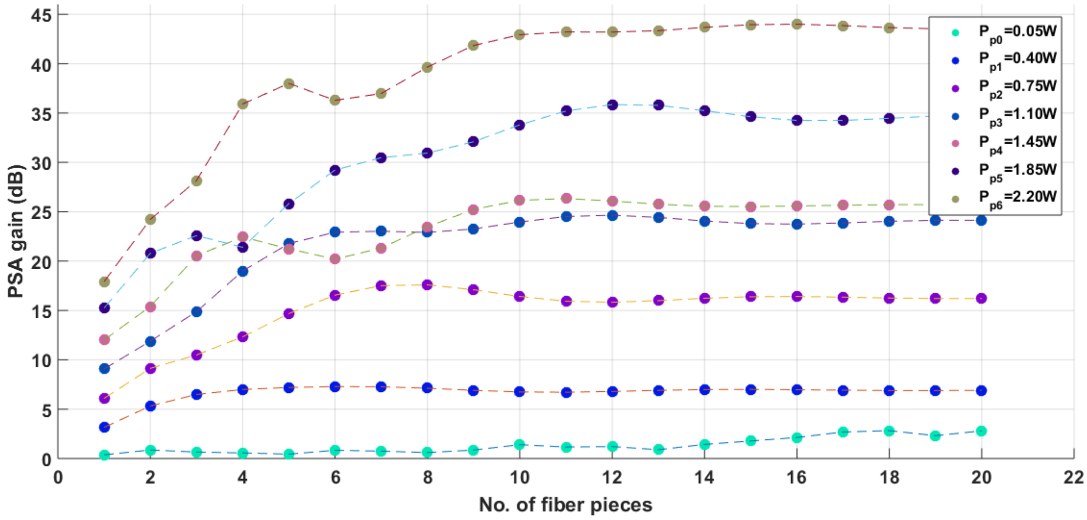

Figure 4.12: PSA gain variation with number of concatenated fiber pieces for different input pump powers, $L = 50m$, $\lambda_s = 1581nm$.

detail in section 2.5.2.1. However, although the gain increases initially, it becomes constant after passing through a certain number of fiber pieces. In addition, for higher pump powers, the signal gain becomes constant after passing through more number of fiber segments in comparison to that of lower pump powers.

The wavelength and fiber length dependence of signal gain in the cascaded fiber based PSA in both regions 1 and 2 of the gain spectrum (in figure 4.8) and also the dependence on pump power can be explained by taking several factors into consideration. One is the contribution of fiber length on the increasing of parametric gain as $\gamma P_p L$ product is a determining factor of the gain coefficient of FWM process. Another is the wavelength dependence of parametric gain as gain is not uniform throughout the gain bandwidth. The operating signal wavelength determines the conversion efficiency of the FWM process owing to the phase matching conditions of the interacting waves. These two factors alone fail to explain the variations exhibited by the cascaded fiber structure because these factors are limited to the cases where pump power is assumed to be constant throughout the parametric interaction. Therefore, it is important to consider the operation of PSA in the region where pump depletion is no longer negligible. An in depth analysis will be carried out in the discussion in which the effect of the direction of power flow of the FWM process will be used to explain the gain characteristics of cascaded fiber based polarization diversity PSA.

4.4.5 Discussion

This section discusses the theoretical aspects behind the variations illustrated in sections 4.4.4.1 and 4.4.4.2. First, a brief introduction to the theory will be given by using the concepts that have already been discussed in previous sections and then, explanations for the gain characteristics in cascaded fiber configuration will be presented based on the theory.

Four wave mixing is a frequency conversion process where its spatial evolution subjects a stronger pump wave to grow sidebands by conserving the momentum. The time domain interpretation of four wave mixing is known as modulational instability which gives rise to complex optical phenomena such as supercontinuum generation [67]. MI occurs as a result of the interplay between optical nonlinearity and the dispersive effects on the optical fiber and is originated in the presence of a weak input signal and a pump or in the presence of just the pump and input seed noise. The MI describes the creation of train of pulses out of a continuous wave propagating inside an optical fiber due to the spatial instability between dispersive effect and the nonlinear response. MI occurs in the anomalous dispersion regime (section:2.4.3.1) where wave vector mismatch, $\Delta\beta < 0$ [68].

When both MI and FWM is considered, the signal and pump is input to the fiber with a relative phase of $\pi/2$ between them in order to achieve maximum conversion efficiency (described by the power flow equations, 2.12-2.15). As was discussed in section 2.3.3.2, when waves start propagating along the fiber, dispersion can result in adding an extra phase shift to the waves. The sign of this phase shift depends on the dispersion regime in which the fiber is operating. In anomalous dispersion regime, the sign is negative. Due to the fiber nonlinearity, SPM induced nonlinear phase shift that will be acquired by the waves is positive. Therefore, net phase mismatch, k, is an interplay between the dispersion induced phase shift and nonlinear phase shift. Since dispersion induced phase shift is a function of operating wavelength of the signal, there exist a signal wavelength where net phase mismatch becomes zero which gives rise to exponential gain regime (discussed in section 2.4.3.1). Therefore, it can be concluded that, net phase mismatch determines the FWM efficiency and hence the gain acquired by the signal in this amplification process, assuming that the fiber loss is negligible.

In the case of perfect phase matching, initially, the signal is amplified exponentially along the fiber length. Here, it is assumed that the reduction in pump power is negligible and hence, pump depletion is not taken into account. This is called the *unsaturated gain region* or the small-signal region of the amplifier. In this region, signal experiences a wavelength dependent gain. But further parametric interaction along the fiber length causes pump depletion to be significant and a considerable amount of pump power to be converted into the side-bands (signal and idler). As a result, the nonlinear phase mismatch term, $\gamma P_p L$, is altered as P_p is no longer constant and therefore net phase mismatch, k, is affected. Hence, FWM efficiency will be reduced and signal gain will decrease. After a significant amount of pump power is converted into sidebands (for considerable pump conversion, large interaction fiber lengths are required), the sign of the relative phase mismatch changes and direction of power flow reverses (further explained by CMEs). As a result, signal gain reduces and pump starts growing. Depending on the initial relative input phase between the waves (in this case, $\pi/2$) and with further propagation along the fiber length, the power flows in a periodic fashion back and forth between pump and sidebands. Consequently, the signal gain evolves periodically along the fiber length. This can be used to explain the fluctuations in the signal gain with the increasing number of fiber pieces. In addition, this periodic power evolution has discretized the pump wave which was initially a continuous wave. This is an analogy to a phenomenon called Fermi-Pasta-Ulam (FPU) recurrence in the presence of spatial instability in nonlinear systems [69], [70], [71]. Using FPU, it is possible to explain that, a system tends to come back to its inital state by reversing the flow of energy to the opposite direction in a periodic manner. The periodicity of FPU can be broken due to the influence of noise as well as higher order MI. The characteristics of FPU recurrence can be observed in the responsiveness of signal gain variation with signal wavelength, pump power and fiber length in the proposed cascaded fiber based diversity loop.

Signal wavelength and fiber length dependence of gain in cascaded fiber polarization diversity PSA

When the wavelength region 1 described in figure 4.8 is considered where net phase mismatch 'k' is positive, different wavelengths respond differently with the increasing number of fiber segments (figure 4.10) and it can be observed that this wavelength dependence of gain varies drastically when length of a concatenating fiber piece is varied. The analysis can be carried out in three-folds to explain how the fiber length per one fiber piece is affecting the wavelength dependent gain.

- Case 1: *Signal wavelength dependence of gain characteristics for fiber pieces with very short lengths.*
  According to figure 4.10a, with $1m$ as the fiber length per piece, the wavelength dependence of gain is almost negligible. This can be described by referring to the FOPA gain variation with fiber length which is illustrated in figure 2.7. The gain spectrum becomes flatter for very low fiber lengths and the gain becomes almost independent of the operating wavelength. As a result, all the signal wavelengths follow the same gain characteristics and exhibit almost equal gain values. In addition, as expected, initially, there is an increase in signal gain with increasing number of cascaded fiber pieces because FWM efficiency increases with accumulated fiber length. But after passing through a certain number of fiber pieces, the increase in signal gain reduces and reaches a constant value. The reason behind this is the interplay between system losses and FWM efficiency which finally comes to a balance by conserving the total energy. No fluctuations in signal gain can be observed because since the FWM interaction length of one fiber is very less, the fiber length is not enough for a considerable pump conversion to take place. Same explanation is applied for the fiber lengths of $10m$ and $20m$ in figures 4.10b and 4.10c although the wavelength dependence of gain is more significant for $20m$ than for $10m$.

- Case 2: *Signal wavelength dependence of gain characteristics for fiber pieces of moderate lengths.*
  This is with respect to the variations illustrated in figures 4.10d and 4.10e. Here, the wavelength dependence of gain has become significant and in addition, drastic reduction in gain is observed for λ_s closer to λ_p (ex: 1563 nm). The system neither bounces back to the initial state by reversing the direction of power flow nor exhibits a periodicity in changing power flow direction because the conversion efficiencies are significantly low. This is due to poorly phase matched conditions and not long enough fiber lengths. For λ_s closer to λ_{max} (ex: 1579 nm), with the increasing number of fiber pieces, an initial increase in gain due to significant phase matching (higher FWM efficiency) proceeded by a slight decrease in signal gain due to the pump depletion to a certain extent (i.e., as P_p reduces, gain reduces in return since gain is a function of $\gamma P_p L$ product) can be observed.

- Case 2: *Signal wavelength dependence of gain characteristics for fiber pieces of higher lengths.*
  In this case, the variations illustrated in figures 4.10f, 4.10g and 4.10h are considered. It can be seen that fluctuations in gain appear for all the wavelengths because the length per one fiber piece is longer enough for periodic back and forth power flow to occur and the system to bounce back to the initial state. As fiber lengths increase further, the fluctuations gradually vanish for all the wavelengths. The reason is, with higher fiber lengths, the contribution of signal induced pump depletion is dominated by the contribution of noise induced pump depletion. This has been further discussed and illustrated in [69] where it states that for higher interaction lengths, the vacuum noise amplification and signal interaction becomes prominent. Therefore, pump depletion driven by the signal-idler generation can be neglected. Therefore, signal gain has not been affected by pump depletion. In addition, higher fiber lengths have contributed for higher signal gains.

For the wavelength region 2 illustrated in figure 4.8, and its variation with the increasing fiber length values depicted in figure 4.11, it can be seen that, signal wavelengths which are far away from the peak gain wavelength show the reduction of gain sooner which is in agreement with the theory. For example, in figure 4.11g, the signal wavelength $1559nm$ reduces the gain after passing through a lesser number of fiber pieces as opposed to the wavelength, $1581nm$. This is due to the poor phase matching for far away wavelengths which reduces the FWM efficiency significantly. It can be observed that for very low and very high fiber lengths, the fluctuations of the signal gain is not prominent due to the same reasons discussed for region 1 wavelengths (i.e.,case 1 and case 3).

Figure 4.13 represents the variation of PSA gain with signal wavelength for different fiber length values. According to figure 4.13a, as the length of one fiber piece increases, higher gains can be observed which is in agreement with the theory. But the question is, "is the variation similar at the output after every concatenated fiber segment for shorter length fiber segments and for higher length fiber segments?" We can presume that, generally, this should be true for all fiber segments irrespective of their lengths per one fiber piece as increasing the number of fiber segments means increased accumulated length and therefore, increased gain. For example, if we take the length of one fiber piece to be $50m$, we can predict that, the gain will increase after passing through 1^{st} fiber piece,

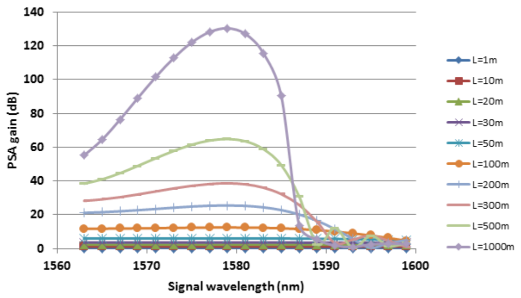

(a) Output at 1^{st} fiber

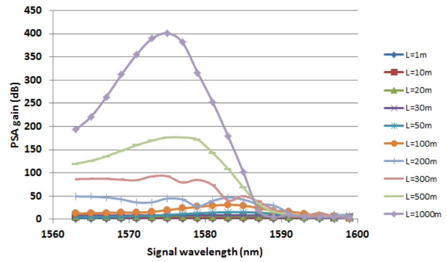

(b) Output at 5^{th} fiber

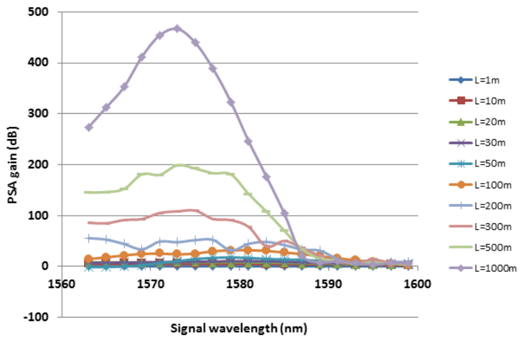

(c) Output at 10^{th} fiber

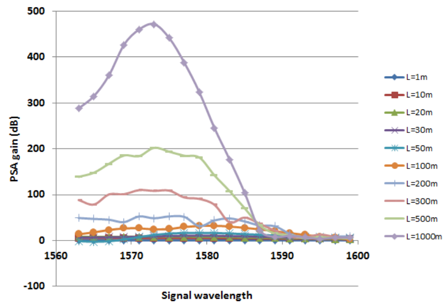

(d) Output at 15^{th} fiber

Figure 4.13: PSA gain variation available at the $1^{st}, 5^{th}, 10^{th}, 15^{th}$ fiber output with signal wavelength for different fiber lengths

2^{nd} fiber piece and so on. To clarify, observations have been made at the end of 1^{st} fiber segment (4.13a), 5^{th} fiber segment (4.13b), 10^{th} fiber segment (4.13c) and 15^{th} fiber segment (4.13d). It can be observed from figures 4.13a, 4.13b and 4.13c that this theory follows and gain has increased with increased number of cascaded fiber pieces. But when the output from 10^{th} (4.13c) and 15^{th} (4.13d) pieces is compared, the theory collapses where significant increase in gain cannot be observed although accumulated length is very high at the end of 15^{th} fiber piece. In addition, ripples in gain curve are observed. The explanation for this behavior is the back and forth power flow, where after passing through certain number of fiber pieces, the power flows from signal to pump instead of pump to signal.

Figure 4.14 represents the PSA gain available at the output of increasing number of fiber pieces for a fiber length of $50m$. As can be seen, initially, as the number of fiber pieces increase, the PSA gain is increased for all signal wavelengths except for the wavelengths which are at the lower end. The gain reduction for lesser wavelengths can be explained by the fiber loss dominating the parametric gain as phase matching in this area is poor. As the number of fiber segments increase, the gain increases and rippling effect can be observed as we go higher.

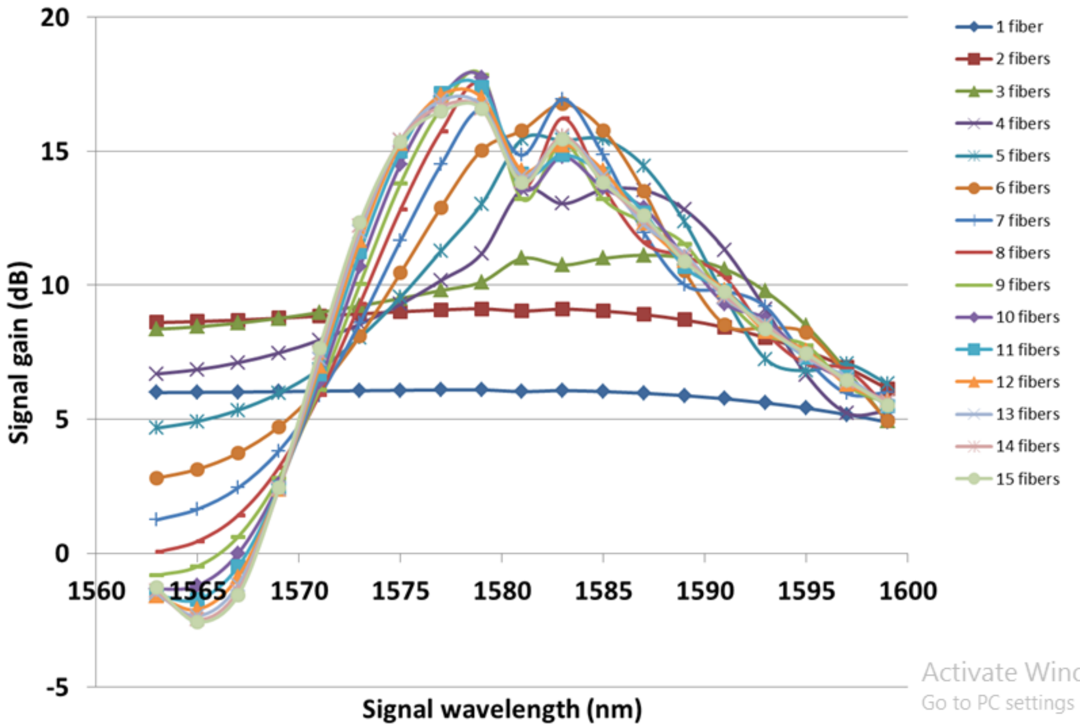

Figure 4.14: PSA gain at the output of each fiber segment from 1 to 15 for a length of one fiber piece at $50m$

The ripples in gain spectrum are caused by the periodic power flow introduced as a result of pump depletion which further proves the theory. It should also be noted that, for higher number of fiber pieces, there is no significant gain improvement because the back and forth power flow between pump, signal and idler waves attains a stability with no significant FWM between the waves. Therefore, it can be concluded that, concatenating higher number of fiber pieces together do not serve the purpose of this research as the focus is to attain a significant gain enhancement in the process.

Pump power dependence of gain in cascaded fiber polarization diversity PSA

Pump power is a determining factor for PSA gain. Figure 4.12 represents the variation of PSA gain with increasing number of fiber pieces for different pump powers. In general, PSA gain increases with pump power and the PSA gain saturates after certain number of concatenated fiber pieces.

Figure 4.15 further elaborates the variation given in figure 4.12 for $1581nm$ signal wavelength. In figures 4.15a and 4.15b, the signal gain tends to reduce after passing through lesser number of fiber pieces. A fluctuation in gain can be observed but with the further increasing of number of fiber pieces, the fluctuations

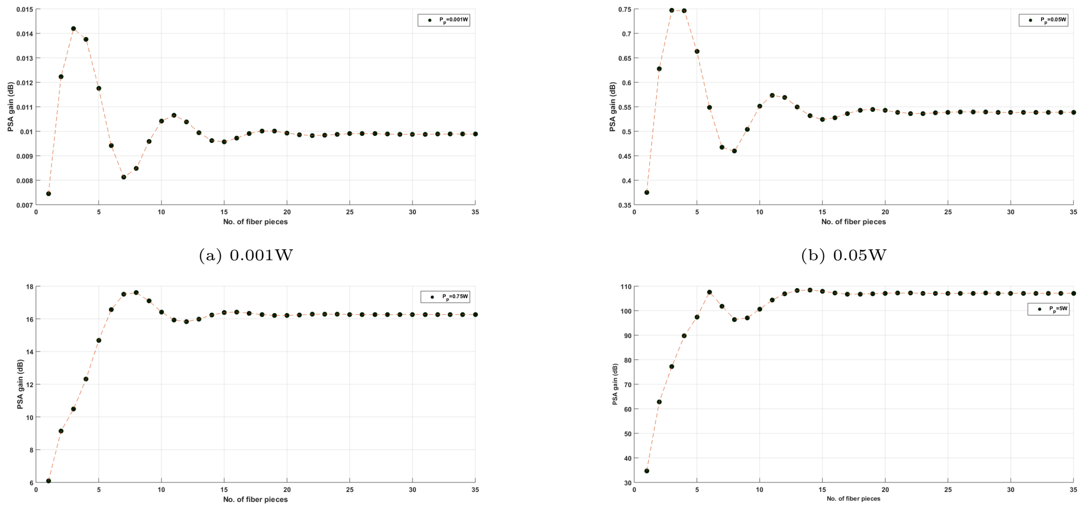

(a) 0.001W (b) 0.05W

(c) 0.75W (d) 5W

Figure 4.15: Changes in PSA gain with increasing number of cascaded fiber pieces for different pump powers (signal wavelength is $1581nm$, fiber length is $50m$)

tend to reduce and a constant gain can be achieved. Here, the parametric gain from FWM and fiber losses interplay to maintain a constant gain after passing through a certain number of fiber segments. In figures 4.15c and 4.15d, the fluctuations gradually vanish as the pump power increases. The reason behind this is, the depletion in a high power pump is not as significant compared to a low power pump and hence a high power pump is capable of providing gain to the signal for a longer time until signal power becomes comparable to pump power.

Performance comparison of PSA, diversity loop based PSA and modified diverdsity loop based PSA

Finally, the performance of the system for different amplifier types is discussed by keeping the system parameters unchanged and it is shown that a gain enhancement can be achieved by the proposed system. The simulations were carried out for the parameter values for nonlinear coefficient, dispersion slope, ZDW, fiber length, pump wavelength, pump power as $11W^{-1}km^{-1}, 0.03ps/nm^2km$, $1559nm, 50m, 1560.7nm, 0.75W$ respectively. Three signal wavelengths have been considered, $\lambda_{s1} = 1565nm, \lambda_{s2} = \lambda_{max} = 1581nm, \lambda_{s3} = 1597nm$ which represents two gain regions depicted in figure 4.8. Table 4.1 represents the different PSA gains with and without the polarization diversity loop. Firstly, a reduction in PSA gain can be observed for all the three wavelengths when polarization diversity loop is deployed. The reason is that the total available pump power is halved for parametric amplification within the diversity loop. Then an improvement in the gain can be seen when cascaded fiber architecture is used where three

Table 4.1: Comparison of signal gains for PSA, diversity loop based PSA and modified diversity loop based PSA (for 3 concatenated fiber pieces).

λ_s	PSA gain (without loop)	Diversity loop PSA gain	Modified diversity loop PSA gain (N=3)
1565nm	5.99dB	2.97dB	6.55dB
1581nm	6.09dB	2.95dB	6.17dB
1597nm	5.17dB	2.36dB	1.11dB

concatenated $50m$ long fiber segments are cascaded together. It can be seen that for the signal wavelength which is less than the maximum gain wavelength, by deploying the modified cascaded fiber based configuration, the PSA gain with the diversity loop can be improved but for the signal wavelength greater than maximum gain wavelength fails to do so. Therefore, it is important to consider the operating wavelength region along with the other parameters such as pump power and length of one fiber segment, in order to obtain an expected gain enhancement when modified cascaded fiber loop architecture is incorporated in the PSA.

4.5 Conclusion

Gain enhancement of polarization diversity loop using cascaded fiber configuration depends on variety of factors. It should be noted that, gain is not always enhanced and depends on the operating parameters like pump power, fiber length and the signal wavelength. When fiber pieces are cascaded together, pump depletion based power transfer as well as losses introduced by fiber attenuation and splicing should also be taken into consideration. With the increasing number of fiber pieces, the influence of these variety of parameters dominate each other interchangeably. Therefore, when fiber pieces are cascaded together, the collective effect of all these parameters should be taken into careful consideration in order to attain a desired gain enhancement in the polarization diversity loop.

Chapter 5

CONCLUSION AND FUTURE WORK

5.1 Introduction

Optical fiber nonlinearity based fiber optic parametric amplification has gained momentum in the past decade due to their capability of outperforming the popular commercially available amplifiers such as EDFAs and Raman amplifiers due to their remarkable noise performance, higher gains, higher gain bandwidths as well as the phase sensitive amplification. Although FOPAs that can be categorized as PIAs and PSAs have these attractive attributes, they have not been able to replace the EDFAs and other popular amplifier types due to the performance inhibiting factors that can cause significant performance degradation when implemented in an realistic communication system. One of the main factors that influence the attainable gain in FOPAs is their sensitivity to SOP variations of interacting waves in the gain medium i.e., highly nonlinear fiber. The gain experienced by the signal to be amplified is significantly lowered by input SOP variations or the changes in relative SOP between the interacting waves. SOP variations introduced to signals are mainly due to external environmental factors like temperature and internal factors such as fiber birefringence, stress and strain etc. majority of which can neither be tracked nor mitigated fully. Therefore it was extremely important to make the FOPA gains independent of input SOP variations. Among many strategies that have been used over the years, the polarization diversity loop is one of the successful techniques that has made the PIA and PSA gains insensitive to input signal SOP variations. There is a drawback in the polarization diversity loop technique which caused by the reduction of total available pump power that is used in the parametric amplification process which happens due to the requirement of splitting the pump power into two orthogonal polarization states at the beginning of the diversity loop. Since parametric gain coefficient increases with increasing of input pump power, the unavailability of total pump power tends to reduce the parametric gain drastically. Therefore, although diversity loop technique has made the FOPA gain insensitive in input

SOP variations, the attainable gain is reduced by a huge amount. Instead of using a single pump to split into orthogonal polarization states, two separate pumps which are orthogonally polarized can be used but any uncorrelated noise components present in the two separate pump may lead to different gain efficiencies in the signal. In recent years, researchers have been trying to address this issue by adopting different gain enhancement techniques that can be incorporated in a diversity loop based FOPA. Cascaded fiber architecture where several fiber segments are concatenated together to enhance the overall gain is on such approach. But this approach has been used by considering different conceptual aspects like Quasi-phase matching technique. The research on incorporating cascaded fiber architecture in a polarization diversity loop based PSA and its gain characterization with varying parameters has not been investigated before. Therefore, the main objective of this thesis was to analyze the gain enhancement technique associated with cascaded fiber architecture implementation in polarization diversity loop based PSA. Apart from addressing the polarization insensitivity of PSA, further characterization has been carried out in order to analyze the gain performance of PSA in different gain regimes.

5.2 Conclusion

Four wave mixing process is capable of providing a considerable amount of parametric gain to the signal. The efficiency of the FWM is determined by the interplay between linear phase mismatch that occurs due to the difference of wave vectors of the interacting waves and the nonlinear phase mismatch that occurs due to the operating pump power, fiber length and nonlinear coefficient when a high power pump wave is assumed. Depending on the phase matching conditions, the FWM gain can be represented using fiber optic parametric amplifier gain spectrum. The FOPA gain is wavelength dependent which means that, the wavelengths falling on different operating regimes owing to different phase matching conditions, show different parametric gain values for same nonlinear coefficient, pump power and fiber length. Since PSA gain is derived from the FOPA gain spectrum, a baseline for a PSA should be developed by considering the different gain regimes of FOPA gain spectrum such as exponential gain regime and quadratic gain regime. The importance is that, while in exponential gain regime, the signal gain increases with pump power, fiber nonlinearity and fiber length exponentially, in quadratic gain regime, the PSA gain shows a quadratic relationship to the increase of these parameters. In addition, the operating gain regimes affect the phase stabilization of gain where shifts in relative input phase is observed when pump power, fiber length and fiber nonlinearity is varied when PSA is operating in the quadratic gain regime. This does not occur in exponential gain regime where phase is perfectly matched. In this work, it was found that this phase instability of gain in the quadratic gain regime of PSA can be improved when higher pump powers, fiber lengths and fiber nonlinearities are used. Although when deciding the values of these parameters, care must be taken to avoid scattering effects due to high pump powers or fluctuations of ZDW due to longer fiber lengths.

The parametric gain dependence on the variations of relative state of polarization of the interacting waves should be addressed in order to attain the optimum performance of PSAs. For single pump PSAs, the strategy is to use a polarization diversity loop where the polarization states of input signals are split into orthogonal polarizations and are amplified separately using a fiber loop in which bidirectional propagation of the orthogonally polarized waves take place. But as the pump power is split into two orthogonal polarizations, the pump power available for parametric amplification in both directions is fraction of the initial pump power. Since parametric gain is a function of pump power and is increase with the increasing pump power, in te diversity loop configuration, although PSA gain is made independent of random polarization state variations, the maximum gain cannot be achieved due to reduced pump power. Parametric gain can be enhanced using different methods such as incorporating fiber Bragg gratings, quasi-phase matching, cascaded fiber architecture, etc. By thorough analysis and by considering the bidirectional nature of the implemented diversity loop structure, it was identified that the best gain enhancement technique was to use the cascaded fiber architecture where multiple fiber segments will be cascaded together to improve the overall gain of the PSA.

As was expected, the cascaded fiber architecture is capable of improving the overall PSA gain to a greater extent. But care must be taken when choosing the operating parameters like pump power, fiber length as well as the signal wavelength because the gain improvement of the cascaded fiber architecture is highly dependent on these parameter values. It was found out that, for certain signal wavelengths, the FWM power flow affects the overall gain negatively and results in a reduction of the overall gain to a greater extent only after passing through a few fiber pieces. Therefore, there is no gain improvement that can be observed afterwards. For certain signal wavelengths, the gain enhancement is significantly improved as the number of cascaded fibers increase. Length of one fiber piece also plays an important role when deciding the degree of gain enhancement. There is an interplay between gain improvement with increasing fiber length and the losses introduced by the increasing fiber length on the overall gain of the PSA. Pump power also has a similar influence where it determines the number of fiber pieces that show a significant gain improvement. Nonetheless, increasing the number of cascaded fiber pieces excessively neither increases nor decreases the gain and therefore, it is extremely necessary to identify the operating characteristics of the PSA gain for a given set of parameter values. The analysis carried out in this work contributes to deciding the operating parameter values of the polarization diversity loop based PSA which gives an improved gain. However, it is to be noted that, as presented in the results, the power flow in the FWM process can be reversed after a certain fiber length i.e., after a certain number of concatenated fiber pieces, in which amplified signal may contribute to the growth of idlers and residual pump which cause the signal to be depleted. Hence fiber lengths should be selected carefully by considering the operating parameters like signal wavelength, nonlinear index and pump power in order to avoid the FWM process to affect negatively on the overall gain of the polarization diversity loop.

5.3 Future work

In this thesis, as extensive characterization has been carried out on the gain enhancement of a polarization diversity loop based PSA using cascaded fiber architecture. In this work, only the concatenation of identical fiber pieces of equal length with non-varying zero dispersion wavelengths is considered. Although ZDW variations are considered to be negligible for fibers with shorter fiber lengths, as longitudinal ZDW fluctuations are significant in longer fibers and are unavoidable in the presence of fiber irregularities, characterization is required to assess the influence of ZDW fluctuations on the gain enhancement in the cascaded fiber architecture.

As stated above, since analysis is limited to the concatenation of identical fiber pieces together, further studies can be carried out to analyze the PSA gain performance and enhancement when techniques like quasi-phase matching where non-identical fiber pieces are concatenated together and to analyze how such a technique can be utilized in polarization diversity loop. Although quasi-phase matching technique has been used for half passed loop configuration where pump is filtered out after passing through half the length of the diversity loop, further analysis has to be carried out in this regard to address the PSA gain variations.

Apart from quasi-phase matching technique for gain enhancement using cascaded fibers of varying parameter values, another feasible configuration is to use use a cascaded fiber architecture with identical fiber pieces but using two different fiber types. For example, HNLFs and DCFs can be used interchangeably to enhance the gain of the amplifier. It is important to assess the incorporation of such an arrangement in a polarization diversity loop based PSA along with a separate analysis to characterize the influence of SBS and other scattering effects on such an arrangement.

When bidirectional fiber configuration is used where interacting signals are propagating in both clockwise and counter-clockwise directions in the same fiber, although the crosstalk between the signals are limited due to the clockwise and counter-clockwise polarization states being orthogonal to each other, the scattering effects like SBS can be significant for when higher pump powers are used. In this work, the influence of such scattering effects on the PSA gain has not been addressed. Therefore, characterization for the PSA gain variations in cascaded fiber architecture should be performed when such an implementation is carried out in realistic environments.

PSAs are low-noise amplifiers and therefore, it is important to analyze the noise performance of the system when amplitude and phase noise is added. Characterizations can be carried out to emphasize the suppression of quadrature phase noise components and evaluate the regeneration capability of the system.

In addition, pump depletion leads towards the saturation of gain in the amplifier. Therefore, this analysis can be extended to incorporate gain saturation characteristics and to identify the different gain saturation regions such as moderate gain saturation and deep gain saturation. Mathematical quantification and extensive analysis can be carried out to incorporate the aspects of gain saturation to further validate the outcomes of this research. It is also important to analyze the interactions of the waves with the residual pump once the pump depletion becomes significantly higher.

Lastly, in realistic implementations, cascading a series of fiber pieces together requires extensive analysis on different losses that can be introduced to the system as well as the back reflections that are inevitable. In order to mitigate the effect of back reflections, optical isolators can be incorporated in between two spliced fiber segments but this is not a feasible solution in a diversity loop based architecture in which interacting signals are propagated bidirectionally. The main reason behind concatenating multiple fiber pieces together is to enhance the parametric gain by increasing the accumulated fiber length as in theory, increasing of fiber length leads to direct increase in gain. The reason for not using a longer continuous fiber instead of a cascaded arrangement is the possibility of fiber losses becoming significant and the ZDW variations becoming prominent as the fiber length is increased in a single fiber piece. In this work, only splicing losses that can be prominent in such a cascaded fiber arrangement are considered. Therefore, effect of such factors should be assessed extensively.

References

[1] J. Hansryd, P. A. Andrekson, and et al., "Fiber-based optical amplifiers and their applications," *IEEE Journal of Selected Topics in Quantum Electronics*, vol. 8, no. 3, pp. 506–520, May/June 2002.

[2] P. Malin and G. P. Agrawal, *Light Propagation in Gain Media: Optical Amplifiers.* Cambridge University Press, 2011.

[3] M. Connelly, *Semiconductor Optical Amplifiers.* Kluwer Academic Publishers, 2002.

[4] E. Desurvire, *Erbium-Doped Fiber Amplifiers: Principles and Applications.* John Wiley and Sons, Inc, 1994.

[5] C. B. Gaur, F. Ferreira, V. Gordienko, and et.al., "Experimental comparison of fiber optic parametric, raman and erbium amplifiers for burst traffic for extended reach pons," *Optics Express*, vol. 28, no. 13, pp. 19 362–19 373, June 2020.

[6] R. H. Stolen and J. E. Bjorkholm, "Parametric amplification and frequency conversion in optical fibers," *IEEE Journal of Quantum Electronics*, vol. 18, no. 07, pp. 1062–1072, July 1982.

[7] G. P. Agrawal, *Nonlinear Fiber Optics.* Elsevier Science, 2020.

[8] M. N. Islam, "Raman amplifiers for telecommunications," *IEEE Journal of Selected Topics in Quantum Electronics*, vol. 08, no. 03, pp. 548–559, May/June 2002.

[9] R. U. Weerasuriya, *Data Retiming for Multi-Wavelength Regeneration.* University College Cork, 2011.

[10] R. Weerasuriya, S. Sygletos, S. K. Ibrahim, and et al., "Generation of frequency symmetric signals from a BPSK input for phase sensitive amplification." OFC, 2010.

[11] T. Torounidis, P. A. Andrekson, and B. E. Olsson, "Fiber-optical parametric amplifier with 70-dB gain," *IEEE Photonics Technology Letters*, vol. 13, no. 10, pp. 1194–1196, May 2006.

[12] M. E. Marhic, "Wide-band tuning of the gain spectra of one-pump fiber optical parametric amplifiers," *IEEE Journal of Selected Topics in Quantum Electronics*, vol. 10, no. 5, pp. 1133–1141, September/October 2004.

[13] e. a. Boggio, "Parametric amplifier for mid-span phase conjugation with simultaneous compensation of fiber loss and chromatic dispersion at 10 Gb/s," *Microwave and Optical Technology Letters*, vol. 42, no. 6, pp. 503–505, September 2004.

[14] P. A. Andrekson and M. Karlsson, "Fiber-based phase-sensitive optical amplifiers and their applications," *Advances in Optics and Photonics*, vol. 12, no. 2, pp. 367–427, June 2020.

[15] M. Karlsson, "Transmission systems with low noise phase sensitive parametric amplifiers." ECOC, 2015.

[16] A. L. Riesgo, *Phase-Sensitive Parametric Signal Processing in Optical Communications.* Chalmers University of Technology, 2016.

[17] M. E. Marhic, P. A. Andrekson, and et al., "Fiber optical parametric amplifiers in optical communication systems," *Laser Photonics Rev.*, vol. 1, no. 25, pp. 1–25, 2014.

[18] Z. Tong, C. Lundstrome, A. Bogris, and et al., "Measurement of sub-1dB noise figure in a non-degenerate cascaded phase-sensitive fibre parametric amplifier." ECOC, 2009.

[19] Z. Tong and S. Radic, "Low-noise optical amplification and signal processing in parametric devices," *Advances in Optics and Photonics*, vol. 5, pp. 318–384, 2013.

[20] F. Yaman, Q. Lin, and G. P. Agrawal, "A novel design for polarization-independent single-pump fiber-optic parametric amplifiers," *IEEE Photonics Technology Letters*, vol. 18, no. 22, pp. 2335–2337, 2006.

[21] A. L. Riesgo, P. A. Andrekson, and M. Karlsson, "Polarization-independent phase-sensitive amplification," *Journal of Lightwave Technology*, vol. 34, no. 13, pp. 3171–3180, 2015.

[22] T. Hasegawa, K. Inoue, and K. Oda, "Polarization independent frequency conversion by fiber four-wave mixing with a polarization diversity technique," *IEEE Photonics Technology Letters*, vol. 5, no. 8, pp. 947–949, 1993.

[23] K. Inoue, "Polarization independent wavelength conversion using fiber four-wave mixing with two orthogonal pump lights of different frequencies," *Journal of Lightwave Technology*, vol. 12, no. 11, pp. 1916–1920, 1994.

[24] K. Y. Kenneth, M. E. Marhic, K. Ueseka, and L. G. Kazovsky, "Polarization-independent one-pump fiber-optical parametric amplifier orthogonal pump lights of different frequencies," *IEEE Photonics Technology Letters*, vol. 14, no. 11, pp. 1506–1508, 2002.

[25] A. L. Riesgo, F. Chiarello, and et al., "Experimental analysis of degenerate vector phase-sensitive amplification," *Optics Express*, vol. 22, no. 18, pp. 21 889–21 902, 2014.

[26] J. K. Kakande, *Phase Sensitive Parametric Amplifiers and Their Applications*. University of Southampton, 2012.

[27] M. E. Marhic, *Fiber Optical Parametric Amplifiers. Oscillators and Related Devices*. Cambridge University Press, 2008.

[28] K. Kato, "Second-harmonic and sum-frequency generation in ZnGeP2," *Applied Optics*, vol. 38, no. 12, pp. 2508–2510, 1997.

[29] R. H. Stolen and C. Lin, "Self-phase-modulation in Silica optical fibers," *Physical Review A*, vol. 17, no. 4, pp. 1448–1453, 1978.

[30] M. N. Islam, L. F. Mollenauer, and R. H. Stolen, "Cross-phase modulation optical fibers," *Optics Letters*, vol. 12, no. 8, pp. 625–627, 1987.

[31] S. L. I. Olsson, *Optical Transmission Systems Based on Phase-Sensitive Amplifiers*. Chalmers University of Technology, 2015.

[32] C. Lundstrome, B. Corcoran, and M. e. a. Karlsson, *Phase and Amplitude Transfer Functions of a Saturated Phase-Sensitive Parametric Amplifier*. Chalmers University of Technology, 2015.

[33] O. M. Kharraz and et al., "Four-wave mixing analyses for future ultrafast wavelength conversion at 0.64 Tbps in a semiconductor optical amplifier," *Optical Engineering*, vol. 53, no. 11, pp. 116 111–1–116 111–8, 2014.

[34] R. Tang, P. S. Devgan, V. S. Grigoryan, and et al., "In-line phase-sensitive amplification of multichannel CW signals based on frequency nondegenerate four-wave-mixing in fiber," *Optics Express*, vol. 16, no. 12, pp. 9046–9053, June 2008.

[35] R. H. Stolen, "Phase matched stimulated four photon mixing in silica fiber waveguides," *IEEE Journal of Quantum Electronics*, vol. 11, no. 3, pp. 100–103, March 1975.

[36] M. Jazayerifar, I. Sackey, R. Elschner, and et al., "Impact of brillouin backscattering on signal distortions in single-fiber diversity loop based polarization-insensitive FOPAs," *Journal of Lightwave Technology*, vol. 35, no. 19, pp. 4137–4144, October 2017.

[37] K. Inoue and T. Mukai, "Signal wavelength dependence of gain saturation in a fiber optical parametric amplifier," *Optics Letters*, vol. 26, no. 1, pp. 10–12, January 2001.

[38] C. J. McKinstrie, S. Radic, and A. R. Chraplyvy, "Parametric amplifiers driven by two pump waves," *IEEE Journal of Selected Topics in Quantum Electronics*, vol. 8, no. 3, pp. 538–547, May/June 2002.

[39] M. Karlsson, "Four-wave mixing in fibers with randomly varying zero-dispersion wavelength," *J. Opt. Soc. Am. B*, vol. 15, no. 8, pp. 2269–2275, August 1998.

[40] M. E. Marhic and C. H. Hsia, "Optical amplification and squeezed-light generation in fiber interferometers performing degenerate four wave mixing," *Quantum Opt.*, pp. 341–355, 1991.

[41] S. E. Alahakoon, D. R. Munasinghe, G. S. Samarakkody, and R. Weerasuriya, "OSNR and dispersion tolerance of FWM based optical carrier recovery scheme," *Journal of Physics Communication*, vol. 4, no. 9, pp. 1–9, September 2020.

[42] G. S. Samarakkody, D. R. Munasinghe, S. E. Alahakoon, and et al., "The behavioral study of an optical injection-locked semiconductor laser under the influence of intensity and phase noise." ICWT, 2019.

[43] K. Balakier, L. Ponnampalam, J. F. Martyn, and et al., "Integrated semiconductor laser optical phase lock loops," *IEEE Journal of Selected Topics in Quantum Electronics*, vol. 24, no. 1, p. 1500112, January/February 2018.

[44] D. Levandovsky, M. Vasilyev, and P. Kumar, "Amplitude squeezing of light by means of a phase-sensitive fiber parametric amplifier," *Optics Letters*, vol. 24, no. 14, pp. 984–986, July 1999.

[45] C. Lundstrome, B. Corcoran, Z. Tong, and et al., "Phase and amplitude transfer functions of a saturated phase-sensitive parametric amplifier." ECOC, 2011.

[46] R. Malik, A. Kumpera, M. Karlson, and P. Andrekson, "Demonstration of ultra wideband phase-sensitive fiber optical parametric amplifier," *IEEE Photonics Technology Letters*, vol. 28, no. 02, pp. 175–177, January 2016.

[47] D. R. Munasinghe, G. S. Samarakkody, S. Alahakoon, and R. Weerasuriya, "Gain performance of single-pump phase sensitive amplifier in the quadratic gain regime." MERCon, 2020.

[48] X. Tian, X. Zhao, M. Wang, and Z. Wang, "Suppression of stimulated Brillouin scattering in optical fibers by tilted fiber Bragg gratings," *Optics Letters*, vol. 45, no. 17, pp. 4802–4805, 2020.

[49] M. E. Marhic, "Polarization independence and phase-sensitive parametric amplification," *J. Opt. Soc. Am. B*, vol. 28, no. 11, pp. 2685–2689, November 2011.

[50] K. Wong, M. Marhic, and L. Kazovsky, "Phase-conjugate pump dithering for high-quality idler generation in a fiber optical paramatric amplifier," *IEEE Photonics Technology Letters*, vol. 15, no. 01, pp. 33–35, January 2003.

[51] I. Sackey, T. Richter, C. Meuer, and et al., "Characterization of polarization insensitive FOPA using a polarization-maintaining highly non-linear fiber." OFC, 2013.

[52] L. G. Nielson, "Polarization maintaining highly nonlinear fibers and their applications," 2009.

[53] V. Gordienko, F. Ferreira, C. Laperle, and et al., "Polarisation-insensitive fibre optic parametric amplifiers for applications in modern communication networks." ICTON, 2020.

[54] I. Sackey, M. Jazayerifar, R. Elschner, and et al., "Non-reciprocal gain due to counter-propagating pumps in a polarization-independent FOPA with diversity loop." ECOC, 2015.

[55] H. Zhu, B. Luo, W. Pan, and et al., "Gain enhancement of fiber optical parametric amplifier via introducing phase-shifted fiber Bragg grating for phase matching," *J. Opt. Soc. Am. B*, vol. 29, no. 6, pp. 1497–1502, June 2012.

[56] S. K. Liaw and Y. Huang, "C+l-band hybrid amplifier using fbgs for dispersion compensation and power equalisation," *Electronics Letters*, vol. 44, no. 14, July 2008.

[57] X. Fu, X. Guo, and C. Shu, "Raman-enhanced phase-sensitive fibre optical parametric amplifier," *Scientific Reports*, 2016.

[58] M. E. Marhic, F. S. Yang, M. C. Ho, and et al., "High-nonlinearity fiber optical parametric amplifier with periodic dispersion compensation," *Journal of Lightwave Technology*, vol. 17, no. 2, pp. 210–215, February 1999.

[59] P. U. Suarez, "An introduction to the split step fourier method using MATLAB," January 2013.

[60] J. Kim, O. Boyraz, J. H. Lim, and et al., "Gain enhancement in cascaded fiber parametric amplifier with quasi-phase matching: Theory and experiment," *Journal of Lightwave Technology*, vol. 19, no. 2, pp. 247–251, February 2001.

[61] S. Takasaka and R. Sugizaki, "Polarization insensitive fiber optical parametric amplifier using a SBS suppressed diversity loop." OFC, 2016.

[62] M. F. C. Stephens, V. Gordienko, and N. J. Doran, "20dB net-gain fiber optical parametric amplification of 18x120Gbps polarization-multiplexed signals." OFC, 2017.

[63] M. Gao, C. Jiang, W. Hu, and J. Wang, "Optimized design of two-pump fiber optical parametric amplifier with two-section nonlinear fibers using genetic algorithm," *Optics Express*, vol. 12, no. 23, pp. 5603–5613, September 2004.

[64] Z. Zhu, J. Zhang, H. Sui, and et al., "Optimized gain of one-pump fiber optical parametric amplifier by using genetic algorithm with pump depletion." Asia Communications and Photonics Conference, 2019.

[65] M. Born and E. Wolf, *Principles of Optics*. Pergamon Press, 1980.

[66] E. Collett, *Filed Guide to Polarization*. SPIE Press, Bellingham, WA, 2005.

[67] J. Dudley and R. Taylor, *Supercontinuum Generation in Optical Fibers*. Cambridge University Press, 2010.

[68] K. Tai, A. Hasegawa, and A. Tomita, "Observation of modulational instability in optical fibers," *Physical Review Letters*, vol. 56, no. 2, pp. 135–138, January 1986.

[69] R. R. Nissim and S. Radic, "Response enhancement of deeply saturated fiber optic parametric amplifier via inhomogeneous fiber," *Optics Express*, vol. 22, no. 23, pp. 27 784–27 796, November 2014.

[70] A. Mussot, A. Kudlinski, and M. e. a. Droques, "Fermi-Pasta-Ulam recurrence in nonlinear fiber optics: The role of reversible and irreversible losses," *Pysical Review X*, pp. 011 054–1–011 054–9, 2014.

[71] G. Capellini and S. Trillo, "Third-order three wave mixing in single mode fibers: exact solutions and spatial instability effects," *J. Opt. Soc. Am. B*, vol. 8, no. 4, pp. 824–838, April 1991.